YGVA III

Brno • Czech Republic
12–14th July 2017

FACULTAS MEDICINAE VETERINARIAE

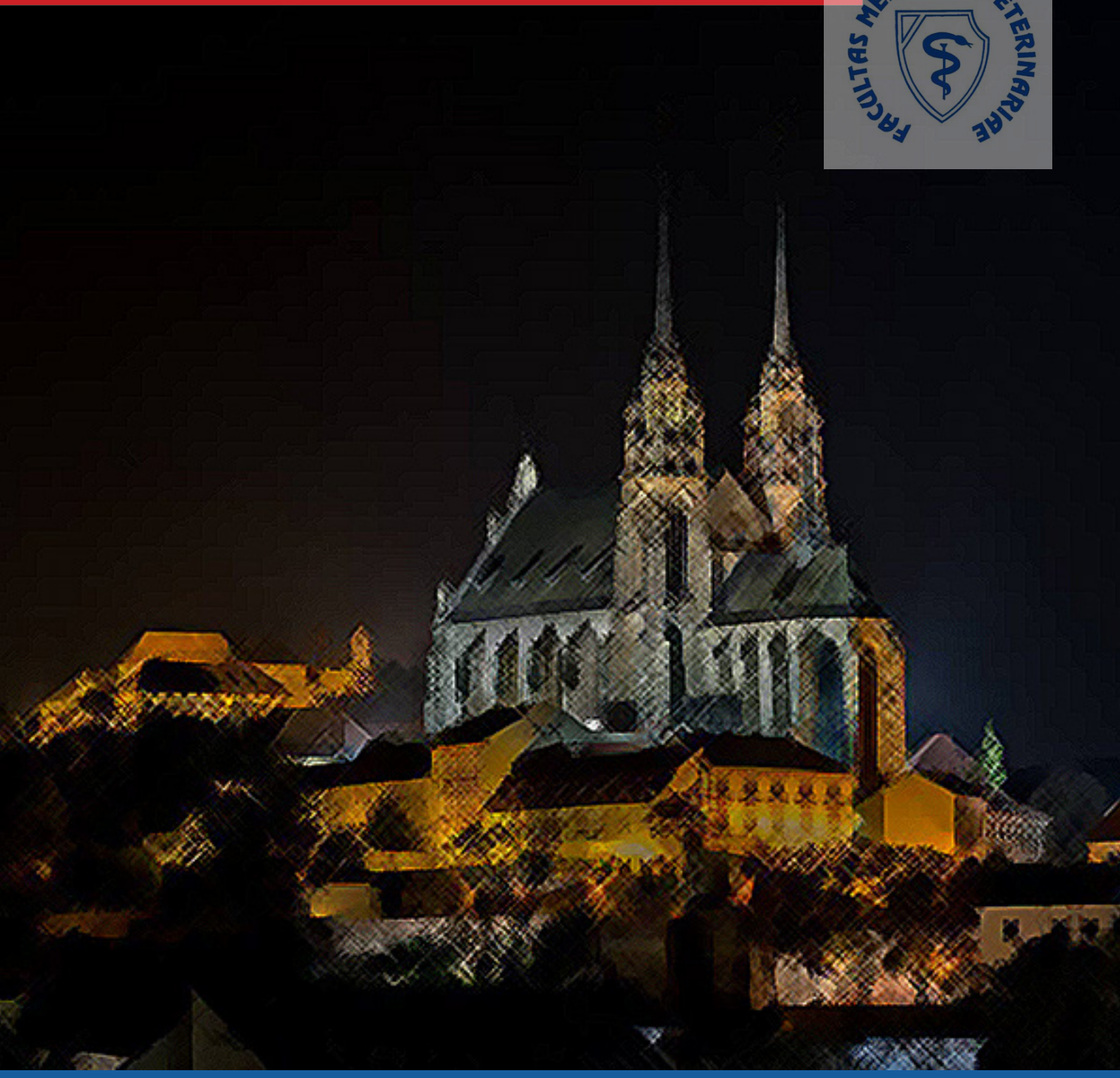

PROCEEDINGS

OF

THE 9TH MEETING OF THE YOUNG GENERATION OF VETERINARY ANATOMISTS

9th Meeting of Young Generation of Veterinary Anatomists

July 12th - 14th 2017

Brno, Czech Republic

PROCEEDINGS

Department of Anatomy, Histology and Embryology

Faculty of Veterinary Medicine

University of Veterinary and Pharmaceutical Sciences

Brno, Czech Republic

Editors

M.Kyllar

P. Čížek

Previous YGVA Meetings

2001 Vienna, Austria
2003 Giessen, Germany
2005 Ghent, Belgium
2007 Ljublana, Slovenia
2009 Utrecht, Netherlands
2011 Nottingham, United Kingdom
2013 Leipzig, Germany
2015 Poznan, Poland

The EAVA Board

C. Wolschrijn, Netherlands - President
C. Pfarrer, Germany - Vice-President
M. Kyllar, Czech Republic - Secretary General
A. Boos, Switzerland - Treasurer
C. Rutland, United Kingdom - YGVA Representative

The 2017 YGVA Meeting Committee

M. Kyllar
P. Čížek
F. Tichý
M. Buchtová
V. Páral

CONTENTS

CAMPUS MAP 7

PROGRAMME AT GLANCE 8

DETAILED PROGRAMME 9

ABSTRACTS OF ORAL PRESENTATIONS 13

ABSTRACTS OF POSTER PRESENTATIONS 55

UNIVERSITY CAMPUS MAP

34 - Registration at the Department of Anatomy, Histology and Embryology

24 - Opening Ceremony - Student's Information Centre

23 - University Diner - lunches during the conference

University Address:

University of Veterinary and Phamaceutical Sciences Brno
Faculty of Veterinary Medicine
Department of Anatomy, Histology and Embyology
Palackeho Trida 1
612 42 Brno
Czech Republic
Tel.: 00420541562201

SOCIAL PROGRAMME

WEDNESDAY 12th of July 2017

19:00 Opening ceremony at the Student Information Centre
(building no.: 24 on the map)

THURSDAY 13th of July 2017

15:30 Villa Tugendhat guided tour
(only pre-booked participants)

Villa Tugendhat
Černopolní 45
613 00 Brno

19:00 Dinner at Restaurant Pivovarska Starobrno

PIVOVARSKÁ STAROBRNO

Mendlovo náměstí č. 20
Brno 603 00

FRIDAY 14th of July 2017

16:00 Mendel Museum and Augustinian Abbey visit
Mendlovo Museum

Mendlovo namesti 1a

603 00 Brno

19:00 Dinner at Orea Resont Santon Hotel
Přístavní 38

635 00 Brno

PROGRAMME AT GLANCE

WEDNESDAY					12:00 - 19:00					19:00 - 20:30
					Registration at the hall of the Department of Anatomy, Histology and Embryology (building no. 34 on the campus map)					Opening Ceremony SIS (building no: 24 on the campus map)
THURSDAY	9:00 - 9:30	9:30 - 10:15	10:15 - 10:30	10:30 - 12:00	12:00 - 13:00	13:00 - 14:00	14:00 - 15:00	15:00 - 18:00	18:00 - 19:00	19:00
	Invited lecture	Poster Introduction	Coffee Break	Oral Session I. Anatomy Teaching	Lunch	Oral Session II. Histology	Poster Session & Coffee Break EAVA Board Meeting	WORKSHOP I. Osteoarcheology in practice WORKSHOP II. Embryology Villa Tugendhat visit	Individual programme	Dinner at Pivovarska Note 1.
FRIDAY	9:00 - 10:15		10:15 - 10:30	10:30 - 12:00	12:00 - 13:00	13:00 - 14:00	14:00 - 16:00	16:00 - 18:00		19:00 - 24:00
	Oral Session III. Histology		Coffee Break	Oral Session IV. Anatomy & Anatomy Teaching	Lunch	YGVA Matters & Discussion	Individual programme	Mendel museum & Augustinian Abbey visit Note 2.		Dinner at Santon Hotel Note 3.

NOTES

1. PIVOVARSKA STAROBRNO Address: Mendlovo náměstí č. 20 Brno 603 00 See MAP
2. MENDEL MUSEUM Address: Mendlovo nám. 1a 603 00 Brno See MAP
3. OREA RESORT SANTON Address: Přístavní 38, 635 00 Brno-Bystrc See MAP

DETAILED PROGRAMME

WEDNESDAY 12th of July, 2017

12:00 - 19:00 Registration at the Department of Anatomy, Histology and Embryology

19:00 Welcome reception at Student Information Centre (SIS)

THURSDAY 13th of July, 2017

9:00 - 9:30 Invited speaker

Role of FGF signaling in zeugopod development
Buchtová M

9:30 - 10:15 Poster introduction

10:15 - 10:30 Coffee Break

10:30 - 12:00 Oral Session I. Anatomy Teaching

10:30 - 10:45 **CHILDREN VOICES IN A SILENT DEPARTMENT: A DIFFERENT PERSPECTIVE ON ANATOMY DEPARTMENTS**
Ekim O, Akyol AA, Hazıroğlu RM, Akyol A, İnsal B, Aral N, Bakıcı I, Özdoğan Özbal E, Akgün RO

10:45 - 11:00 **USING OF 3D PRINTING DOG SKULL MODEL IN VETERINARY ANATOMY**
Oto C

11:00 - 11:15 **DOES SPATIAL ABILITY VARY BETWEEN VET STUDENTS?**
Dickson J, Rhind S, Gardiner A, Ritchie S, Baillie S, Richens I

11:15 - 11:30 **ANATOMY AND HISTOLOGY COURSES OF VETERINARY MEDICINE IN ENGLISH LANGUAGE AT UNIVERSITY OF ZAGREB**
Đuras M, Trbojević Vukičević T, Pavić M, Kužir S

11:30 - 12:00 **LET´S WORK TOGETHER! VET-SUSTAIN**
Rieger J, ... and YOU?*

12:00 - 13:00 Lunch

13:00 - 14:30 Oral Session II. Anatomy and Histology

13:00 - 13:15 **COMPARISON OF THREE BLOOD DERIVED PRODUCTS ON PROLIFERATION AND MIGRATION CAPACITY OF EQUINE CORNEAL CELLS**
Kammergruber E, Rushton JO, Tichy A, Egerbacher M, Nell B, Gabner S

13:15 - 13:30 **IN WHAT WAYS CAN WE CONSIDER THE TERM OF "HISTOSTRUCTURAL BIODIVERSITY" APPLICABLE TO ALL SIMPLE SQUAMOUS EPITHELIAL TISSUES?**
Cazimir I

13:30 - 13:45 **IDENTIFICATION OF TELOCYTES IN THE PORCINE HEART**
Tay H, Vandecasteele T, Van den Broeck W

13:45 - 14:00 **MRI ASPECTS OF THE CEREBELLUM IN ADULT CHINCHILLAS (CHINCHILLA LANIGERA)**
Irina Irimescu, Turcu F, Chiriac L, Fărcăşanu A, Ştefan R, Damian A

14:00 - 15:00 Poster Session (EAVA Board Meeting)

15:00 - 18:00 Workshop Session

Workshop I. Osteoarcheology in Practice - Dr. Martin Pyszko; Doc. Václav Páral

Workshop II. Embryology - Dr. Marcela Buchtova

Cultural workshop - Guided tour of Villa Tugendhat

19:00 - 24:00 Dinner at restaurant Pivovarska - Starobrno brewery

FRIDAY 14th of July, 2017

9:00 - 10:00 Oral Session III. Histology and Embrylogy

9:00 - 9:15 **PISCINE ORTHOREOVIRUS (PRV) MELANISED FOCI IN WHITE MUSCLE OF ATLANTIC SALMON (SALMO SALAR)**
Bjørgen H, Koppang EO

9:15 - 9:30 **DISTRIBUTION OF THE α- AND β-KERATIN IN EPITHELIUM OF THE TONGUE IN THE DOMESTIC GOOSE**
Skieresz-Szewczyk K, Jackowiak H, Buchwald T, Szybowicz M

9:30 - 9:45 **MECHANISM OF COMPLEX TOOTH SHAPE DEVELOPMENT IN REPTILES**
Landová M, Zahradníček O, Dosedělová H, Kavková M, Zikmund T, Buchtová M

9:45 - 10:00 **MORPHOGENESIS AND ANGIOARCHITECTURE OF THE UTERINE TUBE IN DOMESTIC CAT**
Prozorowska E, Jackowiak H

10:00 - 10:15 Coffee Break

10:15 - 12:00 Oral Session III. Anatomy and Anatomy Teaching

10:15 - 10:30 **MODIFYING TRADITIONAL CLAW TRIMMING - ARE THERE ANY BENEFITS?**
Munzel J, Oehme B, Geiger SM, Grund S, Röhrmann N, Weiß M, Mülling CKW

10:30 - 10:45 **COMPARISON OF THE GASTROINTESTINAL TRACT OF A DUAL-PURPOSE AND A BROILER CHICKEN LINE**
Alshamy Z, Hünigen H, Hafez H, Plendl J, Al Masri S

10:45 - 11:00 **SAFE CORRIDORS FOR EXTERNAL SKELETAL FIXATION PIN PLACEMENT IN CATS - PRELIMINARY STUDY.**
Pračková I, Kyllar M

11:00 - 11:15 **THE ORBITAL REGION OF THE SKULL OF THE GREY HERON (Ardea cinerea)**
Bavdek SV, Golob Z, Janžekovič F, Rutland C, Kubale V

11:15 - 11:30 **X-RAY OF TENDONS IN MOTION: INVESTIGATIONS ON STRAIN OF THE EQUINE SUPERFICIAL DIGITAL FLEXOR TENDON (SDFT) WITH BIPLANAR HIGH-SPEED FLUOROSCOPY**
Grandt FC, Reese S, Gerlach K, Gittel C, Böttcher P, Mülling CKW

11:30 - 11:45 **TESTING ANATOMY: DISSECTING SPATIAL AND NON-SPATIAL KNOWLEDGE IN AN MCQ ASSESSMENT**
Dickson J, Rhind S, Gardiner A, Ritchie S

12:00 - 13:00 Lunch

13:00 - 14:00 YGVA Matters & Discussion Forum

16:00 - 18:00 Mendel Museum and Augustinian Abbey visit

19:00 - 24:00 Dinner at Orea Resort Santon

ABSTRACTS
of
ORAL PRESENTATIONS

IN ALPHABETICAL ORDER
OF
PRESENTING SPEAKERS

ROLE OF FGF SIGNALING IN ZEUGOPOD DEVELOPMENT

Buchtova M, Cela P, Horáková D, Krejci P

[1] *Laboratory of Molecular Morphogenesis, Institute of Animal Physiology and Genetics AS CR; Institute of Experimental Biology, Faculty of Sciences, Masaryk University, Brno, Czech Republic*

[3]*Department of Biology, Faculty of Medicine, Masaryk University, Brno, Czech Republic*

INTRODUCTION

The fibroblast growth factor (FGF) signalling system regulates many developmental processes including skeletogenesis, brain patterning, branching morphogenesis or limb development (Mariani et al. 2008). The FGF ligands control cell proliferation and differentiation by activating four transmembrane tyrosine kinase receptors, the fibroblast growth factor receptors (FGFR1-4) (Mohammadi et al. 1997). In mammals, there are 22 known FGF ligands with at least five of them being expressed in the embryonic limb and seven during craniofacial development (Martin 1998). FGFs produced by AER contribute to the maintenance of proliferation in the limb mesenchyme, resulting in proximal-distal growth and patterning of limbs (Niswander et al. 1993; Tickle 2002). Later, FGF signalling is involved in chondrogenesis where it contributes to the regulation of cell survival and chondrocyte differentiation (Ornitz 2005).

As fibroblast growth factors (FGFs) are key players in the variable processes of chondrogenesis, we experimentally manipulated this pathway to test its effect on zeugopode modeling.

MATERIAL AND METHODS

Fertilized chicken eggs (ISA brown) were obtained from Integra farm (Zabcice, Czech Republic). Eggs were incubated in a humidified forced air incubator at 37.8°C, and embryos were staged according to Hamburger and Hamilton (1951). All procedures were conducted following a protocol approved by the Laboratory Animal Science Committee of the University of Veterinary and Pharmaceutical Sciences (Brno, Czech Republic).

FGF inhibitors were purchased from Tocris Biosciences (Bristol, UK). Inhibitors were applied into the chicken right wing bud at the stage HH20-22. Micromanipulator (Leica, Germany) and a microinjector (Eppendorf, Germany) were used to better target the selected area of application. Three injection sites (anterior, posterior, distal) were used to inhibit FGF signalling in the whole limb bud equally.

Affigel Blue beads (Bio-Rad Laboratories, Hercules, Canada) of 200-lm diameter were soaked in FGF proteins and implanted into the right wing bud at stage HH20–22. Embryos were collected after 10–12 days of incubation and stained with alizarin red/alcian blue solution.

RESULTS

We used loss-of-function approach, where FGFR inhibitor PD173074 was injected into chicken wings or limb. The inhibitor treatment caused shorter and thinner humerus as well as the partial or full absence of the radius while ulna remained without morphological changes. The phenotype of hindlimbs resembles the wing phenotype with a more severe effect on the anterior skeleton. The application of PD173074 caused significant changes in cell proliferation and mesenchymal condensation formation during early stages of chondrogenesis in vivo, which was also confirmed in vitro in the micromass cultures. We observed more significant inhibition of chondrogenesis in anterior micromass cultures in comparison to posterior ones.

Next, we used gain-of-function approach where recombinant FGF2 ligand was applied into the right chicken wing bud at stage HH20-22. FGF implantation resulted in skeletal malformations resembling aberrant activation of FGFR/ERK MAP kinase signaling in the growth plate cartilage. Further abnormalities included hypoplasia in both the humerus and ulna accompanied by ossification delay and ectopic cartilaginous outgrowths on the humerus or proximal antebrachium. Interestingly, humerus and ulna was shorted and thicker, while radius did not exhibit this phenotype.

DISCUSSION

Zeugopod area displays large variability in bone patterning. In some species such is horse, the radius is the main load-bearing bone of the forelimb and the ulna can be significantly reduced in size. On the other hand, in chicken or alligator, the ulna is much larger than the radius.

Here, we showed that the anterior cells are more sensitive to FGFR inhibitors. From the evolutionary point of view, it is interesting that a subtle modulation of a strength of FGF signal leads to a size changes of one of the antebrachial bones. The application of FGFR inhibitors can help in the future to solve the puzzle of limb bone reduction during evolution.

In conclusion, we found that gain-of-function as well as loss-of-function of FGF signaling affects the size and shape of zeugopog bones during limb development. Based on our results, we propose that similar alteration of FGF signaling could play a role during limb evolution in vertebrates where different degrees of zeugopodial bones reduction are seen.

ACKNOWLEDGEMENT

This project was supported by the Czech Science Foundation (grant 14-31540S) and by the Ministry of Education, Youth and Sports of the Czech Republic from the Operational Programme Research, Development and Education (CZ.02.1.01/0.0/0.0/15_003/0000460).

REFERENCE

Mariani, F. V., Ahn, C. P. & Martin, G. R. 2008. Genetic evidence that FGFs have an instructive role in limb proximal-distal patterning. Nature 453, 401–405.

Mohammadi, M., Mcmahon, G., Sun, L., Tang, C., Hirth, P., Yeh, B. K., Hubbard, S. R. & Schlessinger, J. 1997. Structures of the tyrosine kinase domain of fibroblast growth factor receptor in complex with inhibitors. Science 276, 955–960.

Martin, G. R. 1998. The roles of FGFs in the early development of vertebrate limbs. Genes Dev. 12, 1571–1586.

Tickle, C. 2002. Molecular basis of vertebrate limb patterning.Am. J. Med. Genet. 112, 250–255.

COMPARISON OF THE GASTROINTESTINAL TRACT OF A DUAL-PURPOSE AND A BROILER CHICKEN LINE

Alshamy Z[1]*, Hünigen H[1], Hafez H[2], Plendl J[1], Al Masri S[1]

[1] *Institute of Anatomy, Department of Veterinary Medicine, Freie Universität Berlin, Germany*
[2] *Institute of Poultry Diseases, Department of Veterinary Medicine, Freie Universität Berlin, Germany*

INTRODUCTION

Every year about 50 million one day old male chicks of egg-laying hens are killed in Germany because their growth rates are significantly less than that of meat-producing chicken breeds. Ethical and cost factors suggest that an alternative to the current cull is to use dual-purpose chickens. The aim of this study is to compare anatomical characteristics of the gastrointestinal tract of dual-purpose chickens (Lohmann Dual, LD) with broiler chickens (Ross 308) raised under conditions typical for meat production.

MATERIALS AND METHODS

Sixtysix (LD) and 54 (Ross) chickens were housed until 5 (Ross) or 9 (LD) weeks of age, under the same husbandry conditions. At roughly 7 day intervals 6 birds from each line were weighed and then euthanized by decapitation. The length of each intestinal segment, and the weight of the empty gizzard and intestinal segments were measured.

The jejunum was examined histologically and morphometrically. Villus and epithelial heights, crypt depth, and the tunica muscularis thicknesses were measured. Digitalized live pictures were analyzed using an image analysis program NIS-Elements AR (Nikon Instruments Inc., U.S.A.).

The allometric relationships between the organ masses and body mass were determined. Data was examined using the Mann–Whitney U test, by analysis of variance and multiple linear regression analysis. P values lower than 0.05 were considered statistically significant.

RESULTS

The Ross birds were about 2.6 times heavier than the LD birds by day 35. The normalized gizzard mass was greater in the LD than in the Ross. A multiple regression analysis showed that both the BW and the chicken line had an influence on the mass of the gizzard, $p \leq 0.001$.The length of the intestine of Ross birds increased faster than in the LD birds. The normalized intestinal mass showed that the two lines were similar, peaking at day 7 and decreasing to plateau between days 21-35. From day 35-63 the intestinal mass of LD birds dropped dramatically.

Multiple regression analysis showed that both the BW and the genetic line had an influence on the entire intestine length and mass. The light microscopic studies showed that villus height was higher in Ross than LD in the jejunum from day 7-35.

DISCUSSION

Whilst Lohmann Dual birds took 63 days to reach 2000 g BW, compared to the 35 days by Ross birds this is faster than found in other slow-growing lines.

The higher normalized organ masses reported here in LD suggest that a greater portion of nutrients are used for organ development than for BW. A larger gizzard in LD than in Ross corresponds to an increased food processing, which could influence intestinal morphometry. Smaller intestines and smaller jejunal villus surface areas in LD suggest a lesser area for digestion and absorption than in Ross. This could represent an adaptation of the lower portions of the digestive to the gizzard size.

PISCINE ORTHOREOVIRUS (PRV) MELANISED FOCI IN WHITE MUSCLE OF ATLANTIC SALMON (SALMO SALAR)

Bjørgen H[1*], Koppang EO[1]

[1]Department of Anatomy. Faculty of Veterinary Medicine, Norwegian University of Life Sciences

INTRODUCTION

In Atlantic salmon (Salmo salar), melano-macrophages, i.e. pigment producing leukocytes, are normally wide-spread in the stroma of haemopoietic organs (spleen and kidney). The cells form the extracutaneous pigment system, an important part of the innate immune system. The cells can respond to antigenic stimulants and pathogens and are present in several common inflammatory conditions, e.g. vaccine-induced peritonitis and chronic muscle changes.

Chronic, melanised muscle changes occur in every fifth salmon fillet produced. The fillets are considered as lower quality, causing large economic losses for the salmon producers. The changes have previously been investigated for the presence of bacteria, fungus and certain viruses, however the changes had not been tested for Piscine reovirus (PRV). PRV is a commonly occurring virus in farmed salmon, causing the disease Heart and Skeletal Muscle Inflammation (HSMI). Most fish get infected by the virus during the sea phase, however not all fish develop the disease.

MATERIALS AND METHODS

In our recent study, muscle changes from groups of farmed fish were ivestigated for the presence of virus by immunohistochemistry (IHC) and RT-qPCR. Control tissue was collected from non-affected muscle tissue next to the melanised changes in each individual. Five groups of farmed fish were included from different parts of the Norwegian coast, in addition to two groups of experimental fish kept in in-house tanks and a group of wild fish (used as a control group).

RESULTS

PRV was detected in all changes investigated (65 changes from 5 different populations), both by IHC and RT-qPCR. IHC positive macrophage-like cells were found in degenerated and necrotic myocytes. Melano-macrophages were occasionally PRV-positive. All muscle samples in the control group were devoid of virus.

DISCUSSION

In this study, we have shown that the common denominator in melanised focal changes is PRV. We conclude that PRV is associated with the focal pathological changes in the white muscle of farmed Atlantic salmon and is a premise for the development of focal melanised changes.

IN WHAT WAYS CAN WE CONSIDER THE TERM OF "HISTOSTRUCTURAL BIODIVERSITY" APPLICABLE TO ALL SIMPLE SQUAMOUS EPITHELIAL TISSUES?

Cazimir I*

Department of Preclinical Sciences, Faculty of Veterinary Medicine, University of Agronomic Science and Veterinary Medicine, Bucharest, Romania,

INTRODUCTION

Modern agriculture contributes to the progress of society but it more or less changes the ancient connections established between human and nature. The concept of anthropological agricultural ecotone arises, widely encountered in plain areas, where the man consciously and actively dictates bio-productivity. Most often, human's actions on the environment lead towards the appearance of pollutant factors and to the manifestation of ecological imbalances.

The main pollutant factors which affect the health state of an anthropological agricultural ecotone are chemical and biological. Potentially pollutant factors will try to reach any animal organism by breaching through the epithelial barriers. Facing this risk, the entire body must be prepared to reject the potentially harmful impact, which depends on the structure of the epithelia, as well as on their biochemical and structural particularities.

Generally referring to epithelial tissues, they can be described as complex groups of cells fixed to one another through cellular junctions. They lined, internally or externally, organs or components of organs, separating themselves from profound tissue through a basal lamina which also serves to strictly border them.

The most basic epithelial tissues are made of a single layer of more or less flattened epithelial cells, organised on a single row. Everything seems accessible, simplified. A territory covered with such cells can be imagined, cells with orderly structure forming a continuous, homogenous layer. But could this uniformity be real? Can we talk about the same type of cells in different organs or just in the same organ? Are these simple squamous epithelia identical, similar or different according to their localisation? Are there considerable differences between cell dimensions, even within the same epithelium no matter the organ studied? In the following research we wish to answer these questions, observing the differences that occur between epithelial tissues which appear if not similar then identical in optical-microscopic imagery.

MATERIALS AND METHODS

For this study a comparative histostructural analysis was performed on a series of simple epithelial tissues, encountered in different organs. The samples came from adult representatives, both male and female, of some species of mammals, birds and amphibians, integrated in a rural plain's ecotone: Equus ferus caballus; Bos taurus; Ovis aries; Sus scrofa domesticus; Canis lupus familiaris; Felis catus domestica; Oryctolagus cuniculus; Mus musculus; Nyctalus noctula; Gallus domesticus; Phasianus colchicus; Coturnix japonica; Pica pica; Pleobates fuscus.

The histological slides that were used in the research work were obtained through the paraffin wax technique, and the following methods were applied for their colouring: Hematoxylin-Eosin, Hematoxylin-Eosin with Metilene Blue, modified Mallory, Hematoxylin-Eosin with Light Green and Toluidine Blue. The examination of the histological slides was done using the Olympus CX42 optic microscope and the images were captured with an Olympus E-330 photo camera and the quick CAMERA PHOTO 2.3 software, which allowed digital editing of images and a morphometric appreciation of the analyzed structures. The visible surface of the different types of epithelial cells, sectioned transversally and rarely longitudinally was measured, registering the average values of their width and height. Within the study, in some cases, ultrastructural analysis was performed, using detailed images of the cells used through the Transmission Electronic Microscope Technique

(TEM). In order to view and photograph required images, the TEM Phillips EM 2008 Microscope was used, which was equipped with an editing software as well as a Veleta video camera.
The experimental protocol was in accordance with the legislation in use (of Annex 4, L. no.43/ 2014 and L. no.96/ 2015).

RESULTS

The simple squamous epithelial tissue is made of a single layer of flattened polygonal cells, attached on a thin underlying basal lamina. This tissue frequently lines internally the walls of blood vessels, or covers the serosa of cavitary viscera. Should we analyze the dimensions of the epithelial cells observed in the structure of the venous wall, in muscular veins studied in sections on the kidney, the average length of about 20μm would be encountered. The maximum height the cell reaches is of circa 3μm, and it is reached in the central area which is occupied by the nucleus. Towards the edges, the cells thin considerably, reaching approximately 1μm. The nuclei of these cells appear normo-chromatic, oval shaped, with a constant width/heigh rapport of about 11μm/3μm. The same measurements being done on the capillary wall in the same species but in different organs resulted in the same height of endothelial cells (3μm), but in a slight decrease in cell length, within 18μm and 20μm. The diameter of the capillary lumen is constant, at about 6μm.
Analysing the walls of a small-calibre vessel from the ureteral wall by the TEM technique, the flattened aspect of the epithelial cells can be noticed, as well as the cells attached to a thin basal lamina. In this case too, the plasmalemma presents folds on its luminal surface. The normochromatic, oval shaped, flattened nucleus has the heterochromatin organised towards the nuclear envelope, surrounding the peripheral area. The cytoplasm has mitochondria, tubules of the rough endoplasmic reticulum, microfilaments, and polyribosomes. An interesting aspect is the fact that numerous vesicles can be identified in the superficial plasmalemma area, especially in the basal domain, indicating an active cellular transport.
Squamous epithelial cells are also encountered in the structure of the serosa, where they reach a length of approximately 28-30μm. Mesothelial cells will also reach their maximum height in the area occupied by the nucleus, height of about 3-4 μm. In the case of oval-shaped nuclei, which are discreetly heterochromatic, a value of 14μm/3μm for the width/height rapport can be observed.
The squamous simple epithelium in the structure of interdigital membranes at Pleobates fuscus can be described on the same principle, where its cells appear polygonal in a sagittal section, with a diameter of 23,4μm, while the nucleus can reach around 8,5μm.
A particular type of squamous epithelium noticed in the structure of the parietal layer of the capsule of the renal corpuscle. Its cells appear very extended and flattened, reaching an average length of about 20 μm and a height of 1-2 μm. TEM images further confirms the establishment of strong junctional connections between neighbouring cells, constituting true protection barriers.
In the lung parenchyma, the alveolary area integrates a simple squamous epithelium at the blood vessels' level. Flattened epithelial cells also line the lung alveoli, participating along side of the endothelial cells in the formation of the blood-air barrier. Their average height is of about 2-3μm, while the average width of circa 15 μm. This identification does not seem to be concluding in optical-microscopic images, because the presence of numerous capillaries creates a lacy aspect to the alveolar walls, which does not allow the appreciation of the exact contour of the flattened type I pneumocytes. Their nucleus reaches dimensions of 3-8μm.
The squamous epithelial cells can have a scaly aspect in the case of the hair follicle. In this case, a dimensional uniformity can be observed. Their average height is of about 3 μm.
In the corneal wall, the cells of the posterior epithelium are at the limit between squamous and flattened cuboidal epithelium. The average width/height rapport is 15/5μm for the cell and 8/4μm for the nucleus. The basal lamina reaches a thickness of circa 8μm, making it the thickest basal lamina of all the epithelia.

DISCUSSION

When comparing the width, in the case of the endothelial cells which line internally the walls of veins

and the continuous wall of the capillaries, a difference of maximum 2 μm can be observed.

This reduced difference is not necessarily real, and can be attributed to meaningless errors that arose when the measurement of incredibly small circular structures, visible only through electronic microscopy on images that were zoomed in over 1200 times, was attempted. It should be noted that the endothelial cells in the capillary wall become frizzy, forming numerous folds, unlike their aspect in larger vessels. In the capillary area the endothelial cells participate in an active or very active communication with the neighbouring structure through the basal lamina. In the other blood vessels, endothelial cells appear elongated, which highlights their role in the protection of the vascular wall. However, the presence of numerous intracytoplasmic vesicles in TEM images offers the possibility of considering all cells, including the ones lining the venous walls, as active cells that are collaborating with all surrounding structures.

Should we compare the endothelium to the mesothelium, in representatives of the same species, a slight increase in the width of mesothelial cells will be observed, in contrast with the endothelial cells. Their nuclei appear more flattened, and slightly more distanced in the epithelium. This imagery, alongside morphometric data, leads towards a likely more wide aspect of mesothelial cells compared to the endothelial ones. In lack of an electronic microscopy analysis, significant differences cannot be observed; however, they can neither be considered identical epithelia, under the generic term of "simple squamous epithelia".

Of all the analysed cells, the maximum width is encountered in the cells of the parietal layer of the capsule of the renal corpuscle, followed by mesothelial cells and by those of the interdigital membrane in frogs. The minimal width is encountered in type I pneumocytes and in the cells which line the posterior corneal epithelium. Cells with a maximal width will have a significantly reduced height, with a general image of very wide, flattened cells. Endothelial cells have relatively constant dimensions no matter where they are localised. Following the approximation of cell sizes in the main types of simple squamous epithelia, the variability established through electronic-microscopy is also apparent in their dimensions.

The study of cells and tissues will complete the biological diversity within ecosystems with an individual structural diversity, accentuated microscopically, which configures the interdependence established between anatomy, histology, biochemistry and physiology.

The study of the animal organism with the optic microscope has the tendency to create images that shortly become standard, more often than not ignoring the existence of a real histostructural biodiversity.

REFERENCES

Bacha W.J., Bacha L. (2011) Color Atlas of Veterinary Histology, third edition. Ed. Wiley-Blackwell. ISBN: 978-0-470-95851-3.

Cazimir I., Cornilă N. (2011) Noţiuni practice de morfologie microscopică, vol.II., Editura Ceres, Bucureşti. ISBN: 978-973-40-0897-1.

Cazimir I. (2016) Aplicarea principiilor ecosanogenezei în domeniul educațional medical-veterinar prin studiul biodiversității histostructurale, lucrare de cercetare științifică pentru finalizarea programului postdoctoral, contract POSDRU/89/15/s/nr. 63258, Academia Română, București.

Mescher A. (2013) Junqueira - Basic Histology. Text & Atlas, 13-th edition. Lange Medical Books, Ed. By McGraw-Hill Medical. ISBN: 978-1-259-07232-1.

Nasri H., Baradaran A., Nasri P., Kafeshani M., Assari S., Rafieian-Kopaei M. (2016) From intestine to kidney; a narrative literature review. Acta Persica Pathophysiol. 1 (1): e03.

Ross M., Pawlina W. (2011) Histology: A Text and Atlas: with Corrlated Cell and Molecular Biology, sixth edition. Ed. By Lippincot Williams & Wilkins. ISBN: 978-1-45110-150-8.

Shaykhiev R., Bals R. (2007) Interactions between epithelial cells and leukocytes in immunity and tissue homeostasis. Journal of Leukocyte Biology, vol. 82 no. 1 1-15. doi:10.1189/jlb.0207096.

Zvorăşteanu R., Cornilă N., Cazimir I., Mănoiu S., Savin S., Constantinescu C., Draghici A., Petcu C. (2011) Ultrastructural aspects concerning the capillaries of the renal parenchyma in Phasianus colchicus, Scientific Works UASVM, Seria C, vol.LVII (3), pg.236-243, Bucharest. ISSN: 1222-5304.

Zvorăşteanu R.M. (2012). Studii histologice privind particularităţile structurale ale aparatului urinar la fazan (Phasianus species). Teză de doctorat. USAMV Bucureşti.

Terminologia Histologica: International Terms for Human Cytology and Histology (2008) Book/CD-ROM Bundle. Hagerstown, MD: Lippincott Williams & Wilkins, ISBN:0-7817-7537-X.

DOES SPATIAL ABILITY VARY BETWEEN VET STUDENTS?

Dickson J[1]*, Rhind S[1], Gardiner A[1], Ritchie S[2], Baillie S[3], Richens I[3]

[1]Royal (Dick) School of Veterinary Studies, The University of Edinburgh, Edinburgh, UK
[2] School of Philosophy, Psychology and Language Sciences, The University of Edinburgh, UK
[3]School of Veterinary Sciences, The University of Bristol, Bristol, UK

INTRODUCTION

Human spatial abilities can be defined as 'the ability to generate, retain, retrieve and transform or manipulate structural images to orientate and interpret the surrounding environment' (Wright et al. 2009). This ability to mentally manipulate objects is fundamental to many medical disciplines such as anatomy, surgery and radiography, yet this important cognitive ability is poorly understood in veterinary students. Several studies have tested the spatial ability of medical students and compared this to exam results on different types of anatomy assessment, as a means to evaluate if a relationship exists but there appears to be no research on how stable a trait this is between veterinary students across different universities. This research analyses the results of three cohorts of first year veterinary students, from two universities, on three well-validated tests of spatial ability. The tests used measure the spatial ability sub-categories of mental rotation and spatial visualisation. Participation was voluntary and human ethics approval was granted by the two institutions.

MATERIALS AND METHODS

Cohorts 1 and 2 were first year veterinary students from the University of Edinburgh academic years 2014/15 (n=108) and 2015/16 (n=98) respectively. Cohort 3 were first year veterinary students from the University of Bristol academic year 2016/17 (n=74). Demographic details of the students were obtained including age, gender, left/right handed and any previous degree studied by means of a questionnaire given prior to testing. Participants completed three timed paper and pencil tests on spatial ability: 1. Card rotation test (CRT), 2. 3D mental rotation test (MRT) and 3. Surface development test (SDT). The tests were given twice in the same order, once at the start (Pre) of academic teaching and then 15/16 weeks later (Post). Test instructions were read out to the students. No negative marking was used. Participants repeating studies, those who had a previous degree relating to anatomy and/or those who had incomplete exam results were excluded from the study.

RESULTS

Pre spatial ability test results were used for the statistical analysis to assess the baseline spatial ability of newly enrolled undergraduates on a veterinary degree programme. Kolmogorov-Smirnov statistical tests were used to compare whether there was a difference in the distributions between the three cohorts; all possible pair-wise combinations for each spatial ability test were analysed with no statistically significant differences found between the cohorts. This analysis was further divided by gender, with no statistically significant differences noted. Although the distribution of the SDT was left skewed, this was found for all three cohorts. To compare whether there were any differences in the student scores obtained for the three spatial ability tests between the cohorts a Kruskal-Wallis analysis was performed for each spatial ability test. Again, no statistically significant differences were found between the three veterinary student cohorts for each spatial ability test.

DISCUSSION

The results of the analysis show there are no statistically significant differences in the Pre results of the spatial ability tests between the three cohorts. This suggests that spatial ability, as measured

by the 3 instruments used, is a stable trait among undergraduate veterinary students in this study. Although sample sizes of each cohort are not large, this is difficult to control as participation is voluntary and institutions vary in the number of students accepted on to the veterinary degree programme. Further analysis involving the same institutions and other new institutions may help to continue to explore spatial ability among veterinary students. Additionally this research provides evidence of the utility of these well validated tests of spatial ability but within the context of veterinary student cohorts.

REFERENCES

Wright, R., Frier, B. & Deary, I., 2009. Effects of Acute Insulin-Induced Hypoglycemia on Spatial Abilities in Adults With Type 1 Diabetes. Diabetes Care, 32(8), 3–6.

TESTING ANATOMY: DISSECTING SPATIAL AND NON-SPATIAL KNOWLEDGE IN AN MCQ ASSESSMENT

Dickson J[1]*, Rhind S[1], Gardiner A[1], Ritchie S[2]

[1]Royal (Dick) School of Veterinary Studies, The University of Edinburgh, Edinburgh, UK
[2]School of Philosophy, Psychology and Language Sciences, The University of Edinburgh, UK

INTRODUCTION

In recent years much research has been conducted in the medical field on the relationship between spatial ability and anatomy learning. Although many studies have shown that spatial ability is linked to anatomy learning, others have shown no link (Lischka & Gittler 1997; Sweeney et al. 2014). Recently Langlois et al (2017) completed a systematic review of the literature on spatial abilities and the assessment of anatomy knowledge. They concluded that anatomy knowledge could be assessed both spatially and non-spatially, but that 'the relationship between spatial ability tests and anatomy knowledge assessment using spatial MCQs were unclear.' In the study reported here an anatomy MCQ test was designed to test the anatomy knowledge of first year veterinary students on the canine hindlimb, pelvis and the theory of ultrasonography. The test included both spatial ability (SA) and non-spatial ability (nSA) questions. Two cohorts of first year veterinary undergraduate students completed the MCQ as part of their in-course assessment. Cohort 1 (n=108) comprised students in academic year 2014/15 and cohort 2 (n=98) were in academic year 2015/16. The spatial ability of each cohort was assessed at the start of the academic year. Subsequently, each cohort received a different teaching method: cohort 1 were taught predominantly using 2D materials (T-2D), cohort 2 with 3D materials (T-3D).

MATERIALS AND METHODS

The MCQ test consisted of 30 MCQs with an equal 50:50 split of nSA and SA anatomy questions. nSA questions consisted of text only questions and the SA questions consisted of questions involving a combination of diagrams and/or photographs of anatomical cross-sections, bones and radiographs. The questions were piloted with 6 academic staff and refined. The assessment was administered as a 60-minute written examination. Demographic details including age, gender, left or right handedness and any previous degree were collected, along with results on three paper and pencil tests of spatial ability: 1. Card rotation test (CRT), 2. 3D mental rotation test (MRT) and 3. Surface development test (SDT). Participants repeating studies, those who had a previous degree relating to anatomy and/or those who had incomplete exam results were excluded from the study.

RESULTS

Correlations between the nSA questions and each of the three spatial ability tests showed no statistically significant correlation for each cohort (cohort 1: CRT $p=0.8768$, MRT $p= 0.2494$, SDT $p=0.6467$; cohort 2: CRT $p=0.9445$, MRT $p=0.9280$, SDT $p=0.0971$). Correlations were conducted for the SA questions and the spatial ability tests and in contrast, only the MRT for cohort 2015 was not statistically significantly correlated to the SA questions (cohort 1: CRT, MRT, SDT $p<0.01$; cohort 2: CRT $p<0.05$, MRT $p=0.1842$, SDT $p<0.05$). In addition, all three spatial ability tests significantly correlated with one another ($p<0.001$). The nSA questions and the SA questions for both cohorts were statistically significantly correlated to one another (cohort 1 $p<0.05$; cohort 2 $p<0.001$). To determine whether the correlation between each spatial ability test and the SA questions, and the spatial ability tests and the nSA questions, are significantly different from one another a dependent correlation comparison was conducted for each cohort. The nSA and SA questions were found to be statistically significantly different to one another for each spatial ability test (cohort 1: CRT $p<0.01$, MRT $p<0.01$, SDT $p<0.001$; cohort 2: CRT $p=0.01$ and SDT $p<0.001$) apart from the MRT for cohort

2015 ($p<0.16$). To determine whether the T-3D method affected performance on the MCQ, a 2x2 ANOVA was performed between teaching methods, score on the MCQ and nSA/SA questions. The ANOVA analysis showed there is a significantly higher score for the nSA questions ($p<0.001$).
Cohort 2 had a overall higher MCQ score when compared to cohort 1 but this was not significant ($p=0.852$). Cohort 1 had a higher MCQ score on the SA questions compared to cohort 1, and the nSA questions were not different between the two cohorts.

DISCUSSION

Initial findings from this MCQ study show that it is possible to design questions which appear to test anatomy spatially, as evidenced by correlations between spatial ability and test performance. This in turn may help to demonstrate whether students have gained a deeper learning on the topic of anatomy, as spatially demanding questions theoretically require acquired knowledge to answer plus problem solving spatial abilities. Furthermore the results of the ANOVA suggest that teaching with 3D materials can improve students' performance on this type of assessment and thus help guide students to a deeper level of learning. The SDT distribution is skewed to the left and this may not reflect an accurate comparison as a ceiling effect is being exhibited with all students performing well on this test making comparisons difficult. Further analysis needs to be conducted on this MCQ with other veterinary student cohorts and potentially other tests of spatial ability to further analyse and confirm the nSA and SA assessment of this MCQ.

REFERENCES

Langlois, J. et al., 2017. Spatial abilities and anatomy knowledge assessment: A systematic review. Anatomical sciences education, 10(3), 235–241.

Lischka, M. & Gittler, G., 1997. Spatial abilities and learning modes in anatomy beginners. In A. J. J. A. Scherpbier et al., eds. Advances in Medical Education. 166–169.

Sweeney, R., Hayes, J.. . & Chiavaroli, N., 2014. Does Spatial Ability Help the Learning of Anatomy in a Biomedical Science Course? Anatomical sciences education, 7(4), 289–94.

ANATOMY AND HISTOLOGY COURSES OF VETERINARY MEDICINE IN ENGLISH LANGUAGE AT UNIVERSITY OF ZAGREB

Đuras M, Trbojević Vukičević T, Pavić M, Kužir S

Department of Anatomy, Histology and Embryology, Faculty of Veterinary Medicine, University of Zagreb, Zagreb, Croatia

INTRODUCTION

In 2016 the Faculty of Veterinary Medicine, University of Zagreb enrolled students in the programme of veterinary medicine in English language for the first time. Seven students altogether from Canada, Israel (2 students), Hungary, France, Greece and Slovenia enrolled in the programme. Anatomy of Domestic Animals with Organogenesis I (ADAO I) is a first semester course and includes 18 hours of lectures and 64 hours of practicals. The topic of ADAO I includes the basics of the locomotor apparatus, angiology, nervous system and topographic anatomy of the thoracic and pelvic limb. Anatomy of Domestic Animals with Organogenesis II (ADAO II) starts in the second semester and includes 20 hours of lectures and 100 hours of practicals. The topic of ADAO II is the anatomy of the trunk. Histology with General Embryology (HGE) starts also in the second semester and includes 30 hours of lectures and 60 hours of practicals. It provides insight into the general embryonic development and the microscopical structure of tissues and organs of domestic animals. The students continue with Anatomy of Domestic Animals with Organogenesis III (ADAO III) in the second year where they study the anatomy of the head and neck of domestic animals and anatomy of poultry during 15 hours of lectures and 63 hours of practicals. The aim of our study was to analyse the success of the enrolled students during the first year courses (ADAO I & II, HGE) at the Department of Anatomy, Histology and Embryology at the Faculty of Veterinary Medicine, University of Zagreb. We also considered their impressions and suggestions for possible course improvements.

MATERIALS AND METHODS

Five women and two men enrolled in the programme of veterinary medicine in English language in the academic year 2016/2017 at the University of Zagreb. Their age ranged from 18 to 27 years. Previous education of these students was secondary school (57.1%) or 1-2 years of higher education (42.9%). According to their statements, the students were informed about the programme in English via internet (57.1%), recommendations of their professors (28.6%) or colleagues (14.3%). The reason for choosing the study in Zagreb was the proximity to their home country (14.3%), enrolment without admission exam (14.3%) and information about Croatia as an interesting and beautiful country to live in (28.6%). As a special advantage, they highlighted the affordable price of the study and the recognition of diplomas in the EU. Currently, they plan to complete their study in Zagreb (85.7%) or Ljubljana (14.3%). The first course they enrolled in the first semester at our Department was ADAO I lasting from October 2016 until the end of January 2017. ADAO II and HGE started in the second semester, in March and they will last until June 2017. Student work was graded and evaluated throughout the courses and separately for each course (ADAO I, ADAO II and HGE). The grading system of each course was set in the official course programme. The grade for each course was formed as the sum of points collected during the course. Following course elements were evaluated and graded with different number of points (100 points in total): lecture attendance (max. 6 points), practical session attendance (max. 12 points), active participation in the practical session (max. 10 points), written tests (max. 32 points) and oral exam (max. 40 points). At the end of each course the students evaluated teachers and the course content via an anonymous questionnaire.

RESULTS

At the time of abstract submission only ADAO I course was fully analysed. Students attended on

average 85.7% of lectures and 92.4% of practicals. Their active participation was evaluated through short oral tests during practicals on anatomical specimen and they achieved on average 91.9% of maximum points. Two written tests were included in grading of ADAO I. 71.4% of students passed the written test I in the first attempt, 14.3% of students passed the written test I in the second attempt and 14.3% of students passed the written test I in the third attempt. The success of the students in written test II was 71.4% in the first attempt, nobody passed in the second and 28.6% in the third attempt. On average students reached 78.6% of maximum points in the written test I and II. The oral exam was the last grading element of student work and the final grade was defined as the sum of collected points. 57.1% of students passed the oral exam in the first attempt and 42.9% in the second (1 to 4.5 months after the end of ADAO I). The most frequent grade achieved in ADAO I was 3 (good) (on a scale from 1 - insufficient to 5 - excellent). The analysis of the student questionnaire showed that the students graded the use of English language of teachers as very good (57.1%) and excellent (42.9%) (descriptive words: excellent, very good, good, insufficient were used in evaluation process). They evaluated their difficulties with Latin terms as relatively easy (71.4%) and easy (28.6%) (descriptive words: very difficult, difficult, relatively easy, easy were used in evaluation process). Most of the students (55.9%) mastered 50-70% of anatomical units already during lectures and during practicals and the rest of the material during self-learning hours. They mastered anatomical units (11 in total) with the help of textbooks and anatomical websites (62.7% of units) and spent additional self-learning hours on anatomical specimen at the department (54.5% of units). They asked for additional help during self-learning hours from colleagues (48.2% of units) and teachers (73.6% of units) and did not need any external professional help. In general, students were very satisfied (85.7%) and satisfied (14.3%) with ADAO I (descriptive words: very satisfied, satisfied, relatively satisfied, not satisfied were used in evaluation process), however, they suggested to redistribute the teaching hours. All students (100%) agreed that there is a need for the increase of hours for the study of vessels and nerves of the limbs. They also suggested to increase the number of hours for the study of the hoof (57.1%) and joints (42.9%).

DISCUSSION

Our analysis of student work during ADAO I gives insight into their success in the course. Their average points within course elements and grades could be used for comparison of the English and Croatian programme that have the same evaluation and grading system. The great difference between the number of enrolled students, 7 in the English and 150 in the Croatian programme, makes a comparison for the academic year 2016/2017 unreliable. However, the collected data will be archived for the future analysis. The enrolled students have continued with ADAO II and HGE in the second semester. The student work is being graded and evaluated throughout the courses in the same manner as explained above. At the end of the courses the students will evaluate ADAO II and HGE as they did ADAO I. The analysis of the rest of the collected material shall be prepared and presented at the 9th YGVA conference.

CHILDREN VOICES IN A SILENT DEPARTMENT: A DIFFERENT PERSPECTIVE ON ANATOMY DEPARTMENTS

Ekim O[1]*, Akyol AA[2], Hazıroğlu RM[1], Akyol A[3], İnsal B1, Aral N[3], Bakıcı C[1], Özdoğan Özbal E[4], Akgün RO[1]

[1] Department of Anatomy, Faculty of Veterinary Medicine, Ankara University, Ankara, Turkey
[2] Department of Conservation and Restoration of Cultural Assets, Faculty of Fine Arts, Gazi University, Ankara, Turkey
3 Child Development Department, Faculty of Health Sciences, Ankara University, Ankara, Turkey
[4] Department of Elementary Education, Faculty of Educational Sciences, Ankara University, Ankara, Turkey

INTRODUCTION

Due to the nature of our profession, anatomy departments have always been a quiet place when compared to various veterinary departments. Even though they have specified museums, anatomy departments are generally visited by the researchers and veterinary students. Despite all these mentioned above, it should not be forgotten that a well-designed and convenient anatomy museum can have a significant potential for the education of all community members, especially the children. Scientific museology activities in our anatomy department had been started by the establishment of the Anatomy Institute in 1933. However, most of the specimens prepared in these years could not be conserved due to the lack of accoutred facilities and services for preservation and demonstration. In the year 2009, a decision on establishment of an anatomy museum was made to protect these specimens most of which have not only scientific but also historical significance. Ankara Veterinary Anatomy Museum officially opened its doors to public in 2013. Since then, over ten thousand visitors have visited.

Our museum is not only an education centre for undergraduate students, but also a reference lab for post graduate students and researchers as well. More important than that, it became an interesting and attractive education area for all members of our society and especially for the children.

MATERIALS AND METHODS

After we realized the potential inside our department, we've decided to prepare a professional education program for the children visitors. Hereby, a national project, Ankara Veterinary Anatomy Museum Education Project (TÜBİTAK/ BT 4004, Project Number: 115B131) was born in 2015. All financial support has been provided by Science and Society Department of TÜBİTAK, The Scientific and Technological Research Council of Turkey. The active part of the project was implemented between April and June 2016.

The target group was elementary students aged 8-9 who had taken basic theoretical lectures in their schools about nature, animal species and the mechanism of the living body. The target group has been selected from every part of the society. In this selection process, great care has been taken to ensure that students especially from economically disadvantaged regions are included in the target group.

A multidisciplinary team prepared the curriculum in 3 main stages which were theoretical interactive lectures before museum visit, museum visit, drama, atelier and practice classes after museum visit respectively. Basic topics planned to be given within this program were as follows: Information about animal species, our cute friends animals, what's inside an animal's body/main anatomical differences between species, what a veterinarian does, extinct species, protect the nature and environment, microcosmos, what is museology. Furthermore, Veterinary Anatomy Museum was modified and updated in conformity with the psychological and cognitive needs of elementary children.

This 6-hour education program was completed in 1 day for each group. Classes, ateliers and the museum of our anatomy department were the essential training areas for this project. Besides, pre and post education tests prepared by child development and elementary education specialists were

applied to target group to evaluate the efficiency of education program. Detailed statistical analyses have been performed by comparing answers among the tests.

RESULTS

Between April 2016 and June 2016, 11 different elementary schools, totally 600 students, from various levels of our community attended to our program. Five specialists, 5 educators and 10 guides took part in this project. Besides, a student organization about veterinary museology education was established through this project and members of this organisation helped our team for preparation and preservation of specimens.

At the end of the activities all of the supplies such as the brochures, the artificial animals they examined, the play dough they made, the pictures, the objects they painted and also the notebooks, pencils, erasers etc. were given not only to students participated our program but also the children and all teachers in their schools who couldn't attend. In this way, it is ensured that the information will be remembered by the children for a long time and also spread the knowledge to a wide range. During the training, the visual content obtained by our visual communication team was transformed into a short film. This trailer and all the electronic education data as well were sent to the schools throughout the country to introduce the project content.

DISCUSSION

The feedbacks from students and teachers attended our program indicated that Ankara Veterinary Anatomy Museum Education Project achieved most of the planned goals. Not only the anatomic knowledge but also a lot of useful information about animals, veterinary profession, and the mechanism of the body can be given to our community by the help of a well-designed education program and a veterinary anatomy museum of course.

After this exciting and informative experience, we can clearly state that anatomy departments have a very important role on the interactive education of the society especially the children beside the anatomical researches and veterinary education. From now on anatomy departments should improve and modify their inner structure and facilities for being an interactive education centre for all individuals in their community.

REFERENCES

Bell P. (2009). Learning Science in Informal Environments: People, Places, and Pursuits, National Academies Press, Washington.

Blud M. L. (1990). Social interaction and learning among family groups visiting a museum, Museum Management and Curatorship 9, 43-51.

Dierking L., Falk J. (1994). Family Behavior and Learning in Informal Science Settings: A Review of the Research, Science Education 78, 57–72.

Falk JH & Dierking LD (1992) The museum experience; Whalesback Books, Washington, DC.

Falk JH & Dierking LD (2000) Learning from museums – visitor experiences and the making of meaning, published by Altamira Press, Walnut Creek, CA.

Falk JH, Scott C, Dierking L, Rennie L & Cohen-Jones M (2004) Interactives and visitor learning; Curator 47, 171-199.

Gerber B., Cavallo A., Marek E. (2001). Relationships among informal learning environments, teaching procedures and scientific reasoning ability. International Journal of Science Education 23, 535-549.

Kubota C. A. & Olstad R. (1991). Effects of novelty-reducing preparation on exploratory behavior and cognitive learning in a science museum setting, Journal of Research in Science Teaching 28, 225–234.

Pedretti E. (2004). Perspectives on Learning Through Research on Critical Issues-Based Science Center Exhibitions, Science Education 88, 34-47.

Rennie, L. J. and T. P.McClafferty. 1995. "Science Centers and Science Learning." Studies in Science Education 27, 53-98

Rudy L & Goodman G. (1991). Effects of participation on children's reports: Implications for children's testimony. Developmental Psychology 27, 527-538.

Tran, L. U. (2006). Teaching Science in Museums: The Pedagogy and Goals of Museum Educators, Science Education 91, 278-297.

Tunnicliffe S. (2000) Conversations of family and primary school groups at robotic dinosaur exhibits in a museum: what do they talk about?, International Journal of Science Education 22, 739-754.

X-RAY OF TENDONS IN MOTION: INVESTIGATIONS ON STRAIN OF THE EQUINE SUPERFICIAL DIGITAL FLEXOR TENDON (SDFT) WITH BIPLANAR HIGH-SPEED FLUOROSCOPY

Grandt FC[1,2,*], Reese S[3], Gerlach K[4], Gittel C[4], Böttcher P[5], Mülling CKW[1]

[1] Institute of Veterinary Anatomy, Histology and Embryology, Faculty of Veterinary Medicine, University of Leipzig, Leipzig, Germany
[2] Department of Small Animal Medicine, Faculty of Veterinary Medicine, University of Leipzig, Leipzig, Germany
[3] Chair of Anatomy, Histology and Embryology, Department of Veterinary Sciences, Ludwig-Maximilians-Universität, Munich, Germany
[4] University Equine Hospital, Faculty of Veterinary Medicine, University of Leipzig, Leipzig, Germany
[5] Small Animal Clinic, Faculty of Veterinary Medicine, Freie Universität Berlin, Berlin, Germany

INTRODUCTION

The superficial digital flexor tendon (SDFT) is one of the most injured structures of the musculoskeletal system in sport horses, especially the forelimb is affected1,2,3. The reconvalescence period after a tendinopathy lasts about 9 up to 18 months4. During a period of two years, 40% of those horses sustain a re-injury5. Due to its function, the SDFT works close to its physiological limit under maximal load6. The project's aim is to visualize and measure the strain of sound and injured tendons during loading using biplanar high-speed fluoroscopy (FluoKin). This part of the project consists of an ex vivo study (SDFTs loaded in a testing machine) and followed by an in vivo study. This presentation introduces the study design focusing on methods.

MATERIALS AND METHODS

Biplanar high-speed fluoroscopy (FluoKin)

FluoKin operates with two x-ray units which allow a biplanar, and therefore precise, motion analysis. The system has been retrofitted with high-speed video cameras recording 500 frames per second. In combination with CT-data, moving 3D-models of an object can be reconstructed. To visualize tendon kinematics, tantalum beads have been implanted into the tendon tissue. Tantalum is inert in the organism7, thus we are able to conduct a long term study. To confirm that small variations in tendon strain can be detected, we validated the FluoKin lab by measuring a known distance between pairs of tantalum beads embedded in an aluminium sheet.

Ex vivo tensile tests

18 SDFTs of forelimbs from Shetland ponies were examined with ultrasound to include only sound tendons in the study. The proximal tendon ends were mounted in a cryo-clamp and the os coronale was fixed in a special mounting device. Specimens were loaded cyclically in a testing machine (Zwick Z 010®) with 2.2% and 4.2% strain respectively to simulate walk and trot ex vivo. The moving specimens were also examined with FluoKin as preliminary tests for the in vivo study.

In vivo study

The animal experiment has been ethically approved by the local ethics committee (Landesdirektion Leipzig, Germany, no. TVV 20/16). A seven-year-old Shetland pony was used as a pilot animal to test the transferability of the ex vivo tests to living animals. A total number of five Shetland ponies will be examined with FluoKin during walk and trot. Additionally, an artificial tendinopathy was induced by collagenase injection in one of the legs. We want to analyse the biomechanics of the healing tendon over a period of months. Pain scoring was performed before surgery (baseline) and three times a day for an interval of ten days post operation.

RESULTS

Fluoroscopic examination of tendons in the ex vivo setup was technically possible.

Accuracy of the FluoKin lab ranged between 0.0287 mm to 0.0586 mm. These values describe

the difference between the known distance of the embedded beads in the sheet and the distance measured with FluoKin.
Cyclic tensile tests of up to 50 minutes in duration can be conducted with this new developed cryo-clamp and mounting device. There was no slippage out of the clamp even within rupture tests.
Tendon strain in motion can be recorded with FluoKin via changing inter-marker-distances of the implanted tantalum beads. No pain was detected after surgery. Currently, no more results can be reported, because the study is still in progress.

DISCUSSION

We expect a length variation of approximately 0.2 cm at walk and 0.4 cm at trot in the metacarpal region. Measuring such a small variation can be accomplished with FluoKin, as demonstrated by its validation.
In contrast to common clamps, it is possible to conduct cyclic tensile tests with cryo-clamps. Their wave profile is designed in order to prevent bruising of the tissue. The tendon is fixed only by freezing. Thus, all fibers of the tendon are equally loaded. The mounting device for os coronale imitates the distal shape of os compedale for optimal force transmission. A pulley simulates the proximal scutum. This set up enables a close to reality simulation.
First results indicate that implantation of tantalum beads is appropriate to investigate tendon strain ex and in vivo. With these prerequisites, transferring this method on other structures as well as future investigations of practical applications in regenerative medicine will be possible.

REFERENCES

(1) Williams R.B., Harkins L.S., Hammond C.J., Wood J.L.N. (2001). Racehorse injuries, clinical problems and fatalities recorded on British racecourses from flat racing and National Hunt racing during 1996, 1997 and 1998. Equine Vet J. 33 (5): 478-486.
(2) Butcher M.T., Hermanson J.W., Ducharme N.G., Mitchell L.M., Soderholm L.V., Bertram J.E.A. (2007). Superficial digital flexor tendon lesions in racehorses as a sequela to muscle fatigue: a preliminary study. Equine Vet J. 39 (6): 540-545.
(3) Patterson-Kane J.C., Firth E.C. (2009). The pathobiology of exercise-induced superficial digital flexor tendon injury in Thoroughbred racehorses. Vet J. 181 (2): 79-89.
(4) Davis C.S., Smith R.K. (2006). Diagnosis and management of tendon and ligament disorders. Equine Surgery, 3rd edition, Auer J.A., Stick J.A. Elsevier Saunders, St. Louis. 1086-1111.
(5) Dyson S.J. (2004). Medical management of superficial digital flexor tendonitis: a comparative study in 219 horses (1992-2000). Equine Vet J. 36 (5): 415-419.
(6) Dowling B.A., Dart A.J., Hodgson D.R., Smith R.K. (2000). Superficial digital flexor tendonitis in the horse. Equine Vet J. 32(5): 369-378.
(7) Aronson A.S., Jonsson N., Alberius P. (1985). Tantalum markers in radiography. An assessment of tissue reactions. Skeletal Radiol. 14 (3): 207-211.

MRI ASPECTS OF THE CEREBELLUM IN ADULT CHINCHILLAS (CHINCHILLA LANIGERA)

Irimescu I*[1, 2,] Turcu F[3], Chiriac L[3], Fărcăşanu A[3], Ştefan R[2], Damian A[2]

[1]Department of Biomedical Sciences, Ross University School of Veterinary Medicine, St. Kitts, West Indies
[2] Preclinical Department, University of Agricultural Sciences and Veterinary Medicine of Cluj-Napoca, Romania
[3] National Magnetic Resonance Centre, Physics Department, Babes-Bolyai University, Cluj-Napoca, Romania

INTRODUCTION

The chinchilla is one of the rodent species currently used as animal model in middle ear, cochlear and vestibular damage, due to particular features such as large tri-cameral tympanic bullae. As new connections with cerebellar functions emerge, such as involvement of the latter in tinnitus, the topography and in vivo anatomy of this brain segment of must be explored. Use of a non-invasive imaging tool, the MRI, offers a base for both imaging diagnosis and future development of experimental neurosurgical approaches.

MATERIALS AND METHODS

The study was performed on 5 adult clinically healthy chinchillas, with an average weight of 500 grams. Neuroleptanalgesia was induced using a mixture of Ketamine (20-40 mg/kg) and Xylazine (4-8 mg/kg) via i.m. administration. Image capture was performed using a Bruker PharmaScan Avance III digital console MRI scanner, equipped with a circular magnet generating a 7 tesla magnetic field. T1, T2 and gradient T2 (T2*) weighted protocols were applied. Coronal, parasagittal and axial cuts were scanned at a 300 µm width and at various distances in-between them. Images were viewed and processed with RadiAnt DICOM Viewer. Identification of anatomic structures was facilitated by qualitative comparison with the specimens extracted post mortem and preserved over 48 hours in a 10% buffered formalin solution.

RESULTS

Out of the three applied protocols, the T2 weighted protocol produced images with satisfactory clarity, contrast and absence of artefacts.

Coronal cuts through the caudal segment of the cerebellum, presented a hyperintense signal imaged as a thin white line of the cerebrospinal fluid contained within the IVth ventricle, clearly separating the cerebellum from the medulla. The vermis was viewed as an iso intensity signal, and higher details of its lobulation and folia were visible. On both lateral aspects of the vermis, the cerebellar hemispheres appeared similarly as an iso intensity signal, with thin hypointense signal lines indicating their lobulation. All three chambers of the tympanic bullae were visible, surrounding the both cerebellum and the medulla oblongata, with the exception of the dorsal aspect of the vermis and cerebellar hemispheres.

Further oral coronal cuts through the cerebellum continued to highlight the cerebrospinal fluid. The paraflocculus lobules became visible, including their internal structure. Part of the internal fluids of the cochlea became visible as hyper intense signals, immediately ventral to the two cerebellar expansions. The large chambers of the tympanic bullae continued to surround most of the cerebellum, the subjacent cochleae and the lateral aspect of the medulla.

Coronal cuts through the most oral segment of the cerebellum revealed part of the peduncular connection to the medulla in iso intense signal. The vestibulo-cochlear nerves has also been identified entering both cochleae. Part of the semicircular canals were also imaged as hyper intense signals. The ventral chambers of the tympanic bullae expanded to the ventrolateral aspects of the medulla.

A sagittal cut presented a good view of the normal topography of the hindbrain. Alternations

between iso and hypo intense signals highlighted the classic arbor vitae view within the cerebellum. Hyper intense signals placed caudally, centrally and rostrally indicated once again the presence of cerebrospinal fluid. A horizontal cut through the neurocranium highlighted the rostral extent of the lateral chambers of the tympanic bullae, completely surrounding the cerebellar hemispheres.

DISCUSSION

The results indicated that the T2 weighted protocol was the most useful for the imaging of the cerebellum on all three major types of cuts, without the help of a contrast medium, applicable as a in vivo diagnostic tool on small sized rodents.

Sagittal cuts offer a clear distinction between the hypo intensity signal aspect of the white matter arborization and the izo intensity signal of the grey matter lamellae, allowing evaluations of the internal cerebellar structure. Both the tectal recess, and the content of ventricular recesses (rostral and caudal) are identifiable on sagittal cuts, while the IV ventricle is visible on coronal sections

Coronal sequential cuts also allow imaging the surface and the inner structure of the cerebellum, including the paraflocculus lobes. The cochlea and the semicircular canals can be partially viewed, close to the latter. All of these structures are largely surrounded by the chambers of the tympanic bullae. Horizontal images offer a better view of the rostral extent of the middle chamber.

This topographic relationship between the structures of the inner ear, the cerebellum, the brainstem and the three chambers of the tympanic bullae suggests the potential for surgical access to the cerebellum, in addition to the existing experimental chinchilla models.

All husbandry and experimental procedures have been approved by the Bioethics Committee of the University of Agricultural Sciences and Veterinary Medicine of Cluj-Napoca (No. 14/ 24/10.2014). All MRI Images were obtained and processed at the National Centre of Magnetic Resonance of the Physics Faculty of Babes-Bolyai University, Cluj-Napoca, Romania.

REFERENCES

Hayden, R., Sawyer, S., Frey, E., Mori, S., Migliaccio, A. A., & Santina, C. D. (2011). Virtual labyrinth model of vestibular afferent excitation via implanted electrodes: validation and application to design of a multichannel vestibular prosthesis. Experimental Brain Research, (3-4), 623. doi:10.1007/s00221-011-2599-x

Irimescu I (2015), Morphological and nuclear magnetic resonance imaging research of the encephalon in chinchilla lanigera, PhD thesys, University of Agricultural sciences and Veterinary Medicine of Cluj-Napoca, Romania

Smit, J.V., Janssen, M.L.F., Schulze, H., Jahanshahi, A., Van Overbeeke, J.J., Temel, Y., Stokroos, R.J. (2015). Deep brain stimulation in tinnitus: Current and future perspectives, Brain Research, 1608:51-65.

COMPARISON OF THREE BLOOD DERIVED PRODUCTS ON PROLIFERATION AND MIGRATION CAPACITY OF EQUINE CORNEAL CELLS

Kammergruber E[1]*, Rushton JO[2], Tichy A[3], Egerbacher M[1], Nell B[2], Gabner S[1]

[1] *Institute of Anatomy, Histology and Embryology, University of Veterinary Medicine, Veterinaerplatz 1, 1210 Vienna, Austria*
[2] *Department of Companion Animals and Horses, University of Veterinary Medicine, Veterinaerplatz 1, 1210 Vienna, Austria*
[3] *Department for Biomedical Sciences, University of Veterinary Medicine Vienna, Veterinaerplatz 1, 1210 Vienna, Austria*

INTRODUCTION

Corneal ulcerative diseases are of major concern to both veterinarians and the equine industry. Despite advances in therapy of corneal diseases in horses, a vast number of cases require surgical intervention, due to insufficient treatment. Local application of serum has been used for many years, based on its properties to promote corneal wound healing [1,2]. Recently other blood derived products i.e. plasma rich in growth factors (PRGF) and platelet rich plasma (PRP), have been widely used in equine orthopaedics [3,4] and with promising results also in human ophthalmology [5,6]. The beneficial effects of PRGF and PRP on corneal wound healing have been attributed to the high amount of growth factors. However, no reports of the impact of these blood derived products exist in equine ophthalmology. The aim of this study was to determine the effects of equine PRP and PRGF on wound healing capabilities of equine corneal cells, compared to commonly used equine serum, and ultimately, to serve as a basis for subsequent in vivo studies in horses.

MATERIALS AND METHODS

Blood from 35 healthy horses was used to produce serum, PRGF (Endoret®), and PRP (E-PETTM). The study was part of an installed routine monitoring programme and procedures were approved by officials of the Spanish Riding School and the federal stud Piber. Equine corneal limbal (ECLCs) and stromal cells (ECSCs) were collected from globes of horses euthanized for reasons unrelated to this study and treated with 20% serum, 20% PRGF or 20% PRP. The impacts of the three blood derived products on proliferation and migration of ECLCs were evaluated using MT Cell Viability Assay (RealTime-Glo™) for proliferation, migration behaviour of ECLCs was analysed with a scratch assay. Proliferation rates and migration capacity were monitored in single cell cultures as well as co-culture systems, to better mimic the natural morphology of cornea tissue. Transwell permeable systems with an insert pore size of 0,4 µm were used to seed ECSCs in the upper compartment and ECLCs were seeded in the lower compartment. Proliferation rates of ECLCs were measured after 12, 24, 36, and 48 hours exposure to the respective blood derived products. After disrupting the monolayer with a pipette tip, the closure of cell free area was monitored over 42 hours.

RESULTS

ECLCs increased their proliferation after PRP treatment, remained constant with PRGF treatment, and declined upon serum treatment. A time dependent increased cell proliferation was only observed in PRP treatment group. During scratch assays, a significant effect on closure of the cell free area was observed in all three treatment groups. Serum and PRP treatment significantly enhanced cell migration, compared to PRGF treatment. At the end of experiment runtime (42 hours), closure was most complete in PRP control group. Within co- culture systems experiments revealed corresponding results to those in single cell culture, but PRP treated cells show significant faster closure compared to PRGF and serum

DISCUSSION

After PRP treatment migration rates of ECLCs were most progressed in comparison to serum and PRGF.

Consequently one may speculate that PRP is beneficial in corneal disorders requiring prolonged therapies. After corneal epithelial damage, the presence of underlying stroma has beneficial effects in rebuilding overlying epithelium. Essays in co-culture systems revealed approximate congruent results to those in single cell culture. An enhancing effect of substituted corneal stromal cells could not be identified.

In summary, PRP produced with the E-PETTM system showed promising results by enhancing proliferative, as well as migratory capacity of equine corneal cells in vitro.

PRP should further be tested in vivo to analyse its full potential for clinical ophthalmological use.

REFERENCES

Berman, M.B., Gordon, J., Garcia, L.A., Gage, J. (1975): Corneal ulceration and the serum antiproteases. II. Complex of corneal collagenases of α-macroglobulins. Exp Eye Res 20, 231-244.

Tsubota, K., Goto, E., Shimmura, S., Shimazaki, J. (1999) Treatment of persistent corneal epithelial defect by autologous serum application. Ophthalmology 106, 1984–1989.

Carter, C.A., Jolly, D.G., Worden, C.E., Hendren, D.G., Kane, C.J.M. (2003) Platelet-rich plasma gel promotes differentiation and regeneration during equine wound healing. Exp Mol Pathol 74, 244–255.

Torricelli, P., Fini, M., Filardo, G., Tschon, M., Pischedda, M., Pacorini, A., Kon, E., Giardino, R. (2011) Regenerative medicine for the treatment of musculoskeletal overuse injuries in competition horses. Int Orthop 35, 1569–1576.

Alio, J.L., Arnalich-Montiel, F., Rodriguez, A.E. (2012): The role of „eye platelet rich plasma" (E-PRP) for wound healing in ophthalmology. Curr Pharm Biotechno 13, 1257–1265.

Anitua, E., de la Fuente, M., Muruzabal, F., Riestra, A., Merayo-Lloves, J., Orive, G. (2015) Plasma rich in growth factors (PRGF) eye drops stimulates scarless regeneration compared to autologous serum in the ocular surface stromal fibroblasts. Exp Eye Res 135, 118-126.

THE ORBITAL REGION OF THE SKULL OF THE GREY HERON (Ardea cinerea)

Bavdek SV, Golob Z[2], Janžekovič F[3], Rutland C[4], Kubale V[1]*

[1] Veterinary Faculty, University of Ljubljana, Gerbičeva 60, 1000 Ljubljana, Slovenia
[2] Golob d.o.o. Clinic for small, wild and exotic animals, Glavni trg 7, 2366 Muta, Slovenia
[3] Faculty of Natural Sciences and Mathematics, University of Maribor, Koroška cesta 160, 2000 Maribor, Slovenia
[4] School of Veterinary Medicine and Science, University of Nottingham, Sutton Bonington Campus, Leicestershire, LE12 5RD, United Kingdom

INTRODUCTION

Herons belong to the family Ardeidae (order Pelecaniformes), which includes the grey heron (Ardea cinerea) and the great white heron (Ardea alba). These are large carnivorous birds, eating mainly fish, after standing stationary beside or in the water or stalking its prey through the shallows. They are measuring around 100 cm in height, have a wingspan around 155–195 cm and weight up to 2 kg. They have a white head and neck with a broad black stripe that extends from the eye to the black crest. The body and wings are grey above and the underparts are greyish-white, with some black on the flanks. The long, sharply pointed beak is pinkish-yellow and the legs are brown. They are native through Europe, Asia and parts of Africa, usually around rivers, ponds and the sea cost.
They have some special anatomical features in the skull bones. Dimensions of several bones (scapula, coracoid, humerus, ulna, femur and tibiotarsus) of the adult grey herons were measured and published. However there are not many publications available regarding the skeletal components of grey heron's skull. Therefore we aimed in the present study to evaluate the relationships between the bones of orbital area and in comparing the skeletons of a young grey heron with adult specimens.

MATERIAL AND METHODS

The skull of the grey heron (Ardea cinerea) was examined with an emphasis on describing the orbital region. We have used skulls of four adult and one circa three-month-old grey herons (Ardea cinerea) and one adult white heron (Ardea alba). Their sexes were unknown. Adult grey and white heron's skeletons and young grey heron were property of museums and University of Ljubljana, Slovenia. The anatomical descriptions were made by direct observation. The anatomical nomenclature followed the Nomina Anatomica Avium (Baumel and Witmer, 1993).

RESULTS

In the young (circa three-month-old) heron, the frontal bone (os frontale) and nasal bone (os nasale) comprised separate paired bones, connected by sutures (sutura interfrontalis, sutura internasalis, sutura frontonasalis plana). In adult animals, the relationship between these bones was very different: the left and right frontal bone and the left and right nasal bone had grown together, and the frontal bone and nasal bone had fused into a common frontonasal bone (os frontonasale). The lacrimal process of the frontal bone (processus lacrimalis frontalis) and the ectethmoid bone (os ectethmoidale) were also examined. In the latter, the main components comprised of the orbital and antorbital part of the ectethmoid plate (lamina ectethmoidalis orbitalis et antorbitalis), the lateral process (processus lateralis ectethmoidalis) and the tubercle (tuberculum ectethmoidalis); the left and right ectethmoid plates were fused together to form the ectethmoid sinus (sinus ectethmoidalis) between them. In the three-month-old grey heron, the anatomical and functional link between the frontal and lacrimal bones did not exist yet, nor did the osseous frame of the ectethmoid-lacrimal complex. Further research into the young heron skulls is needed but this article provides novel contributions, insights and knowledge into the young and adult grey heron's orbital region.

REFERENCES

1. Adams C.T. (1955). Comparative Osteology of the Night Herons. Condor 57, 55–60.

2. Atalgin S.H., Bozkurt Büyükçopur E.Ü., Kürtül I. (2014). A detailed evaluation of the skeletal elements of the skull in the grey heron (Ardea cinerea). Turkish Journal of Veterinary Animal Science 38, 370–376.
3. Baumel J., Witmer L.M. (1993) Osteologia. In: Baumel J., King A., Breazile J., Evans H., Vanden Berge J., eds. Handbook of Avian Anatomy: Nomina Anatomica Avium, Massachusetts: Publications of the Nuttall Ornithological Club. pp. 45–132.
4. Golob Z., Bavdek S.V., Zajc T., Janžekovič F., Klenovšek T. (2016). Some anatomical characteristics of the skeleton of grey heron, Ardea cinerea. Acta Biologica Slovenica 59, 55–75.
5. Livezey B.C., Zusi R.L. (2006). Phylogeny of Neornithes. Bulletin of Carnegie Museum of Natural History 37, 1–544.
6. Shufeldt R.W. (1889). Osteological studies on the sub-family Ardeinae. Part I. Journal of Comparative Medicine and Surgery 10, 218–243.
7. Zusi R.L., Livezey B.C. (2006) Variation in the os palatinum and its structural relation to the palatum osseum of birds (Aves). Annual Carnegie Museum 75, 137–180.

MECHANISM OF COMPLEX TOOTH SHAPE DEVELOPMENT IN REPTILES

Landová M[1,2], Zahradníček O[3], Dosedělová H[1], Kavková M[4], Zikmund T[4], Buchtová M[1,2]

[1] *Institute of Animal Physiology and Genetics, v.v.i., Academy of Science of the Czech Republic, Brno, Czech Republic*
[2] *Department of Experimental Biology, Faculty of Science, Masaryk University, Brno, Czech Republic*
[3] *Institute of Experimental Medicine, v.v.i., Academy of Science of the Czech Republic, Prague, Czech Republic*
[4] *CEITEC – Central European Institute of Technology, Brno, University of Technology, Brno, Czech Republic*

INTRODUCTION

Tooth shape formation in mammals is well known process thanks to the broad studies on the mouse molars. The main role in regulation of this process plays the enamel knot. Enamel knots are formed by cluster of cells, which serves as a source of numerous signalling molecules such as SHH or members of WNT, BMP and FGF families (Jernvall et al., 1994). All of these proteins help to determine process of tooth crown shaping and to establish final number of cusps. Several enamel knots can be distinguished such as primary, secondary and tertiary knots playing distinct role in odontogenesis. Primary enamel knot (PEK) is formed at the cap stage and it is characterized by the low proliferation rate and later by the high level of apoptosis (Vaahtokari et al., 1996). Its formation helps to drive the tooth development towards to next developmental stage. Secondary enamel knots take over the role at late cap/early bell stage and their numbers specify cusp number in each tooth and therefore the final shape of the teeth (Jernvall et al., 1998).
Almost all our knowledge about teeth came from study on the mouse model. For better understanding of odontogenesis, it is however necessary to compare developmental processes to another species. One of the most heterogenic group of dentition type and shape are reptiles. How the shape of their teeth completed is still unknown. Aim of our study is therefore to uncover developmental processes involved in cusp formation in non-mammalian species with focus on reptiles. As model species for this study, we selected chameleons where multicuspid teeth develop in the caudal area of the jaw.

MATERIAL AND METHODS

Animals (Chameleon calyptratus) were obtained from private breeders. Embryos and foetuses at different stages of development were collected to analyse progress of development. Eggs were incubated at the temperature of 27-29°C. At selected time points, eggs were opened and embryos were euthanized by decapitalization and fixed in 4% PFA at least overnight.
Specimens for immunohistochemical analysis were decalcified in 12.5% EDTA in 4% PFA at room temperature and then embedded into paraffin. Paraffin embedded tissues were cut in transverse and sagittal plane. All samples were deparaffinised and rehydrated through a series of ethanol. Water bath (97°C) in citrate buffer (pH=6) for 20 min was used for antigen retrieval. To prevent unspecific binding of antibodies, blocking serum was applied on the samples for 20 min. Next, slides were incubated with primary antibodies (SHH, FGF4, β-catenin, Lef1, ST14, PCNA) for 1 hour or overnight, alternatively. The secondary antibody was applied for 30 min and DAPI was used for the counterstaining. The photos were taken under a fluorescence microscope Leica DM LB2 (Leica Microsystems, Germany) and merged together in Adobe Photoshop 7.0 (USA).
Localisation of apoptotic cells was analysed by the detection of DNA fragments in situ by the TUNEL method (ApopTag Peroxidase in Situ Apoptosis Detection Kit). Counterstaining with Haematoxylin was performed.
Moreover, we prepared organ cultures from the lower and upper jaws by dissecting them out of embryos and placing them on Millipore filters and a metal mesh. They were cultured for 14-21 days at 29-30°C in advanced media supplemented by growth factors (SHH, FGF4, BMP2/7) or their inhibi

tors (cyclopamine, AZD4547, Noggin). Both jaws were photographed at the beginning and the end of each experiment to see possible differences in teeth shape during cultivation. For clear determination of changes in cusps formation under the influence of growth factors, jaws were analysed by microCT (GE Phoenix v|tome|x L 240 laboratory system) and then compared with the control ones.
All procedures were carried out according to the experimental protocol approved by the Laboratory Animal Science Committee of the IAPG, v.v.i. (Liběchov, Czech Republic).

RESULTS

Shape of chameleon teeth varied along the jaw: in the rostral part of the jaw there were teeth with simple monocuspid shape. In the caudal part of the jaws, teeth were larger and with more complex shape with one central and two lateral cusps. Moreover, there is ridge-shaped socket at the tip of the central cusps. To reveal mechanism, which drives the development of such structures in the chameleon dentition, we analysed sagittal sections to visualize cusps and transversal sections for observation of ridge formation.
Immunohistochemical analysis of transversal sections revealed the expression of several markers specific for the enamel knot at cap stage in chameleon teeth. We focused on proteins, which are important for the shaping of mammalian teeth. We were able to detect positive signal for FGF4 and SHH in the enamel knot zone. Beta-catenin also revealed high level of expression in the area of EK, which suggests possible link of WNT pathway in the process of tooth shape formation in reptilian dentition. Another member of WNT signalling family, transcription factor Lef1, was detected more on the labial side of the developing dental gland. Moreover, we detected matriptase ST14 in the cells of EK-like structure, which was previously found to be expressed in a cluster of EK cells in mouse. The bulge of the enamel knot cells in chameleon did not proliferate as we could not detect any PCNA-positive cells here. TUNEL analysis uncovered high level of the apoptosis in chameleon EK area similar to mouse. All these data point to the fact, that even in the reptiles, the shape of the teeth is driven by cells located in the area resembling enamel knot.
On the other hand, we were not able to detect any of above mentioned proteins in the forming cusps on sagittal sections. Later in the development, when central cusp is already formed and the deposition of hard tissue already started, the newly formed lateral cusps are negative for any of the above mention EK proteins such as FGF4 or SHH. Therefore, it seems that different developmental processes are involved in central ridge and lateral cusps formation.
To assess if previously mentioned signalling pathways play a role in the formation of lateral cusps, organ cultures from the lower jaws were established and incubated with growth factors (SHH, BMP2/7, FGF4) or their inhibitors (cyclopamine, Noggin, AZD4547). Contralateral side of the jaws were used as a control for every treatment. Up to now, our preliminary results using microCT analysis did not revealed any significant changes in the shape and average number of the cusps when compared treated and control jaws.

DISCUSSION

Reptilian tooth shape is heterogeneous from simple monocuspid to complex multicuspid teeth. However, developmental mechanisms involved in reptilian multicuspid teeth formation have not been studied previously in detail.
In recent study, we compared developmental processes of tooth shape establishment in reptiles and compared them to the mammalian model. At the cap stage, we detected the expression of growth factors known to be involved in mouse EK also in chameleon teeth. These results point to the fact that even in the reptiles is tooth development driven by cells located in the area resembling mouse enamel knot.
Whether lateral cusps are formed by SEK-like structure, or by different processes such as folding of the inner dental epithelium, is still debated question. Our recent data obtained by immunohistochemical analysis of sagittal sections and experiments using organ culture indicate that SEK probably is not present in reptiles and do not play role in lateral cusp formation. However, further experimental evidences are necessary to find processes involved in tooth shaping and lateral cusps formation in chameleon.

Moreover, we detected strong expression of the transcription factor Lef1 on the labial side in the oral epithelium close to the dentary gland. This can possibly play a role in the cell fate decision between the dental lamina and neighbour dental gland.

ACKNOWLEDGEMENT

This project was supported by the Czech Science Foundation (grant 14-37368G) and by the Ministry of Education, Youth and Sports of the Czech Republic from the Operational Programme Research, Development and Education (CZ.02.1.01/0.0/0.0/15_003/0000460).

REFERENCE

Jernvall, J., T. Aberg, P. Kettunen, S. Keranen, and I. Thesleff, 1998, The life history of an embryonic signaling center: BMP-4 induces p21 and is associated with apoptosis in the mouse tooth enamel knot: Development, v. 125, p. 161-169.

Jernvall, J., P. Kettunen, I. Karavanova, L. B. Martin, and I. Thesleff, 1994, Evidence for the role of the enamel knot as a control center in mammalian tooth cusp formation - nondividing cells express growth-stimulating FGF4 gene: International Journal of Developmental Biology, v. 38, p. 463-469.

Vaahtokari, A., T. Aberg, J. Jernvall, S. Keranen, and I. Thesleff, 1996, The enamel knot as a signaling center in the developing mouse tooth: Mechanisms of Development, v. 54, p. 39-43.

MODIFYING TRADITIONAL CLAW TRIMMING - ARE THERE ANY BENEFITS?

Munzel J[1]*, Oehme B[1], Geiger SM[1], Grund S[1], Röhrmann N[1], Weiß M[1], Mülling CKW[1]

[1]*Institute of Veterinary Anatomy, Histology and Embryology, Faculty of Veterinary Medicine, Leipzig University, Leipzig, Germany*

INTRODUCTION

Lameness in cows due to claw lesions continues to be a major problem in modern dairy farming. Flooring systems are among the predominant risk factors, thus numerous studies focusing on stable flooring and claw trimming have been carried out (2, 3). The “Dutch method” for claw trimming has been used many years but has been questioned recently by some authors due to development in dairy cow housing (10, 8). The claws of cattle kept on pasture develop a prominent weight bearing margin around the tip and the abaxial wall of the claw (1, 7). The hardest part of the claw is the wall horn which should therefore be the main weight bearing part (5). The aim of this study was to measure the pressure distribution under claws treated with a modified trimming method mimicking “pasture claws” on different floorings using a foil-based pressure sensor.

MATERIALS AND METHODS

The metatarsi of 10 severed distal hind limbs of Holstein Friesian dairy cows were fastened to a load applicator. Following functional trimming of all claws (“Dutch method”) (10, 4, 6), a 2 mm ridge around the tip and the abaxial wall of the claw was carved out. Metatarsi were arranged at a 90° angle towards the ground surface and approx. 150 kg of load applied. In order to ensure in vivo comparability tendon strain on the deep digital flexor tendon and the digital extensor tendons were realized with 50 kg and 5 kg weight respectively (9). Concrete and 3 different rubber mats (KARERA, KURA, profiKURA; KRAIBURG Holding GmbH & Co. KG, Waldkraiburg, Germany) were used as flooring. 4 measurements per ground surface and claw were carried out with a sensor foil (M3200E, HoofTM System, Tekscan Inc., Boston, MA, USA) positioned between flooring surface and claw. Maximum pressure, average pressure and contact area were analyzed.

RESULTS

Results show that contact area was 28.9±4.9 cm2 on concrete flooring and 48.8±5.6 cm2 max. on rubber mats. Average pressure was 49.8±9.0 N/cm2 on concrete and 32.6±3.6 N/cm2 max. on rubber mats (Table 1). Maximum pressure was located in the bulb area of the claw. Average ratio of weight distribution between lateral and medial claw was 1.7 on concrete as well as on rubber.

		overall		lateral		medial	
	Flooring	Contact area	Average pressure	Contact area	Average pressure	Contact area	Average pressure
Mean	Concrete	**28.9**	**49.8**	**16.6**	**53.8**	**12.2**	**42.2**
SD		4.9	9.0	3.1	11.1	4.2	12.5
Mean	KARERA	**42.8**	**32.6**	**24.9**	**34.5**	**17.9**	**28.9**
SD		4.7	3.6	4.8	5.4	5.0	6.1
Mean	KURA	**45.7**	**31.6**	**26.9**	**33.9**	**18.8**	**27.3**
SD		7.3	4.4	5.7	6.8	5.2	5.6
Mean	profiKURA	**48.8**	**28.9**	**28.1**	**30.8**	**20.5**	**26.0**
SD		5.6	3.3	5.6	4.9	4.9	4.8

Table 1: Contact area and average pressure on 4 different floorings DISCUSSION

Modifying traditional claw trimming benefits claws in terms of pressure distribution patterns. The sensitive sole carries less weight while the weight bearing margin is more heavily loaded. Maximum and average pressure are higher while the contact area is smaller on concrete which may lead to deteriorating claw health. A future study will compare the modified trimming method with traditionally trimmed claws according to the “Dutch method”.

ACKNOWLEDGEMENTS

The project is supported by funds of the Landwirtschaftliche Rentenbank.

REFERENCES

1. Benz, B. (2002): Elastische Beläge für Betonspaltenböden in Liegeboxenlaufställen. Dissertation. Universität Hohenheim, Hohenheim. Institut für Agrartechnik.
2. Bergsten, C.; Herlin, A. H. (1996): Sole haemorrhages and heel horn erosion in dairy cows: the influence of housing system on their prevalence and severity. In: Acta Vet Scand 37 (4), S. 395–408.
3. Carvalho, V. (2006): Effects of trimming on dairy cattle hoof weight bearing surfaces and pressure distributions. In: Braz J Vet Res Anim Sci 43 (4), S. 518–525.
4. Fiedler, A.; Maierl, J.; Nuss, K. (2004): Funktionelle Klauenpflege. In: A. Fiedler, J. Maierl und K. Nuss (Hg.): Erkrankungen der Klauen und Zehen des Rindes: Schattauer, S. 44–62.
5. Franck, A.; Cocquyt, G.; Simoens, P.; Belie, N. de (2006): Biomechanical Properties of Bovine Claw Horn. In: Biosyst Eng 93 (4), S. 459–467.
6. Greenough, P.R. (2007): Claw Trimming, Foot Baths, Restraint, Bandaging, Lifts, and Shoes. In: P. R. Greenough (Hg.): Bovine laminitis and lameness. A hands-on approach. Edinburgh, New York: Saunders Elsevier, S. 170–198.
7. Nuss, K.; Kolp, E.; Braun, U.; Weidmann, E.; Hässig, M. (2014): Klauengrösse von Schottischen Hochland-Kühen nach Weide- und Laufstallhaltung. In: Schweiz Arch Tierheilkd 156 (9), S. 433–440.
8. Ouweltjes, W.; Holzhauer, M.; van der Tol, P.P.J.; van der Werf, J. (2009): Effects of two trimming methods of dairy cattle on concrete or rubber-covered slatted floors. In: J Dairy Sci 92 (3), S. 960–971.
9. Riemersma, D. J.; van den Bogert, A J; Schamhardt, H. C.; Hartman, W. (1988): Kinetics and kinematics of the equine hind limb: in vivo tendon strain and joint kinematics. In: Am J Vet Res 49 (8), S. 1344–1352.
10. Toussaint-Raven, E. (1985): Cattle footcare and claw trimming. Ipswich, Suffolk.

USING OF 3D PRINTING DOG SKULL MODEL IN VETERINARY ANATOMY

Oto C[1]

[1]*Department of Anatomy, Faculty of Veterinary Medicine, University of Ankara, Turkey*

INTRODUCTION

In last decade, using of the 3D printing have gradually increased in medicine with the development of computerized medical imaging techniques. Virtual reconstructed and physical printing 3D models have been used teaching anatomy as well as for planning animal tests, training surgical procedures, and preparing operations. There is a growing trend for educators, operators and researchers to produce their own models for using their own purposes (Thomas, 2016)

The skull is the most complicated bony structure that forms of the head. It is made up of a number of fused bones and contains many foramina and processes, cavities and sinuses. Types of the skull can show a great variety and cephalic index is used the categorize animals especially in dogs. Therefore, learning the individual skull properties are important for veterinary anatomy and surgery. The aim of the preliminary study is to point out of 3D printing models usage as well as for determination of advantages and learning effects in veterinary medicine.

MATERIALS and METHODS

Different type of skulls and heads of the dogs that have been using in anatomy lab were used for the present study. The skulls and the heads were scanned by multi detector computed tomography (CT) and 3T magnetic resonance imaging scanner with 3D sequences.

Segmentation, surface generation and post-processing of the DICOM images were virtually performed by means of Mimics innovation suite and Simplify 3D (v3.1.1) software allowing the conversion of a stack of DICOM files into a STL files. The images were also processed to improve model quality by denoising, smoothing, and decimation procedures. The STL images of the dog skulls were used in 3D printing. The models were built layer-by-layer in 3D printer using PLA filaments.

RESULTS

The skull was printed as a solid structure both external and internal surface was scanned. The rapid prototyping skull replicas were smooth, durable and unscented. All the materials were drillable and fusible for making anatomical preparations.

All of the key anatomical features were shown in 3D digital and physical rapid prototyping models. All the bone processes were well distinguished as well as almost all of the foramina and the notches on the skull surface were present (e.g. foramina on the orbitosphenoidal crest). However data loss in the 3D print occurred especially at most of bone sutures. The anatomical differences among skulls of dogs according to type of cranial index were observed clearly.

DISCUSSION

The 3D printing skull replicas are anatomically accurate and identical to real organic skull specimens. These rapid prototypes can be manufactured and obtained by reasonable price. The purpose of this research was to clearly demonstrate 3D printing replicas could be used in understanding skull morphology in dog species. We have shown that it is possible to create an educational and training models for this goal. The 3D printed samples can be a convenient alternative for masserated skulls of animals.

REFERENCES

Badash I., Burtt K., Solorzano C.A., Carey J.N. (2016) Innovations in surgery simulation: a rewiev of past, current and future techniques. Annals of Translational Medicine, 4(23): 453-463

Kim Y.S., Shin Y.S, Park D.Y., Choi J.W., et al. (2015) The application of 3D printing in animal model of augmentation rhinoplasty.

Annals of Biomedical Engineering, 43 (9): 2153-2162
Raffan H., Guevar J., Poyade M., Rea P.M. (2017) Canine neuroanatomy: Development of a 3D reconstruction and interactive application for undergraduate veterinary education. Plos One, DOI: 10.1371/journal.pone.0168911
Ripley B., Levin D., Kelil T., Hermsen J.L., Kim S., Maki J.H., Wilson G.J. (2016) 3D printing from MRI data. Magnetic Resonance in Medicine, DOI: 10.1002/jmri.25526
Skrzat J., Spulber A., Walocha J. (2016) 3D model of the skull and the cranial bones reconstructed from CT scans designed for rapid prototyping process. Folia Medica Cracoviensia, 2: 45-52
Thomas D.B., Hiscox J.D., Dixon B.J., Potgieter J. (2016) 3D scanning and printing skeletal tissues for anatomy education. Journal of Anatomy, 229: 473-481.

Safe corridors for external skeletal fixation placement in cats - preliminary study

Prackova I[1], Kyllar M+

[1]Department of Anatomy, Histology and Embryology, Faculty of Veterinary Medicine, University of Veterinary and Pharmaceutical Sciences Brno, Czech Republic

The successful use of external fixators depends largely on the surgeon's knowledge of the possibilities and limitations of the technique and on careful adherence to the principles of fixator application: avoidance of damage to vital anatomical structures, the need to meet the biomechanical demands of the specific fracture and patient, and the provision of access to the injury in case of open fractures. Surgeons in both the human and veterinary orthopaedic field have, in recent years, become increasingly aware of the possible complications associated with the careless insertion of transfixation pins. Bilateral frames, despite their popularity, are not considered safe by many surgeons. Compartment syndromes, damage to neurovascular structures and impalement of musculotendinous units have been reported. Avoidance of these complications is possible if pin insertion is limited to regions where minimal soft tissue is present. Anatomical safe corridors for external skeletal fixator pin insertion have been well studied in human orthopaedic surgery and in dogs in veterinary surgery. However, to the author's knowledge, no anatomical studies have been published concerning the delimitation of such safe corridors for pin insertion in feline limbs. The purpose of this study is to identify and locate their extent in the feline front and hind limb.

Three feline front and hind limbs of frozen cadavers for a minimum of 24 hours were used for a cross sectional study and saline fixed front and hind limbs were used for a dissection study. The limbs were cross sectioned at three points of each long bone. Each region was divided in to three equal segments and transected. Relationship of the soft tissues, vital structures such as vessels and nerves and bones were assessed. Three types of corridors were recognized. Safe corridor, where bone was overlie directly by the fascia and skin. Unsafe corridors were those where vital structures such as nerves and vessels were present and finally intermediate corridor which was characterized as a bone covered by muscles, fascia and skin.

Safe corridors were identified only in the crural region medially and in antebrachial region caudo-latero-proximally. Unsafe corridors were localized on the medial aspect of the brachial region, medio-caudal aspect of the proximal antebrachium, medial femoral region and caudo-proximal region of the crus.

This study reports that the safe corridors for the placement of the pins of the external skeletal fixation do exist in feline, but to much lesser extent than in canines. Larger scale study is planned including advanced diagnostic imaging to confirm these findings.

MORPHOGENESIS AND ANGIOARCHITECTURE OF THE UTERINE TUBE IN DOMESTIC CAT

Prozorowska E, Jackowiak H

Department of Animal Histology and Embryology, Poznan University of Life Science, Poland

INTRODUCTION

Uterine tube in mammals develops from the tubal part of the paramesonephric duct, arranged laterally to the mesonephros. The wall of the tubal part of the paramesonephric duct is composed of pseudostratified epithelium and mesenchyme and during the fetal period differentiate into three layered duct i.e. tunica mucosa, tunica muscularis and tunica serosa. The processes of growth and histogenesis of the tubal part of paramesonephric duct require an early development of blood vessels, which develop by angiogenesis.

The aim of the study was to describe the morphogenesis of the domestic cat uterine tube and also to characterize the angioarchitecture of this developing organ, with indication of the process of angiogenesis.

MATERIAL AND METHODS

The domestic cat embryos and fetuses, aged 36 - 63 day p.c. were selected as the material used for the research. Two types of methods were used in the study, i.e. the light microscope (LM) technique and the vascular corrosion casts (VCC) technique.

For the LM observations the 4 μm slides of the paramesonephric ducts and uterine tubes were staining with Masson-Goldner topographic method and also with the orcein for elastic fibres. For the VCC technique the female cat fetuses were injected with the Mercox® resin, macerated in 15% NaOH solution, frozen in destilled water, dried in lyophilizer CHRIST ALPHA 1-2 LD and routinely prepared to observe in the scanning electron microscope Zeiss LEO 435VP.

RESULTS

36th – 39th day p.c: The tubal part of paramesonephric duct consists of pseudostratified epithelium covered by mesenchyme. The vascular system of the tubal part of paramesonephric duct is simple and consists of a single longitudinal feeding blood vessel and circumferential capillaries, which undergo intussusceptive angiogenesis. The blood vessels in the wall of paramesonephric ducts differ in diameter but have the structure of capillaries. The blood from the wall of paramesonephric duct is drained by a single wide collecting capillary.

42nd – 46th day p.c: The epithelium of paramesonephric duct is pseudostratified. The mesenchyme of the tubal part of the paramesonephric duct differentiate into inner and outer layer of loose connective tissue. The longitudinal blood vessel divide into two main supplying arterioles, which run together with the main collecting venule in the mesosalpinx area of the paramesonephric duct wall. The feeding arterioles give off circumferential capillaries for mesenchyme. The capillaries undergo intussusceptive and sprouting angiogenesis.

48th – 52nd day p.c: The wall of uterine tube consists of the pseudostratified epithelium and the loose connective tissue, which is still arranged in two layers and covered with serosal epithelium. The two main arterioles give off the circumferential arterial branches to the wall of uterine tube. These branches divide into subserosal capillaries and give off the capillaries, which form subepithelial vascular network. The circumferential venules collect blood from the subepithelial and subserosal capillary networks and merge with the main venule.

55th – 63rd day p.c. The wall of the uterine tube consists of the folded mucosa with simple cylindrical epithelium, thin and single muscular layer and serosa. The main blood vessels in the uterine tube wall became histologically arteries and veins. The two main longitudinal tubal arteries have an undulated course. The subserosal capillaries are arranged in dense network and the subepithelial mucosal capillary network adjust the shape of the folded mucosa. The blood vessels of both networks

undergo the intussusceptive angiogenesis.

CONCLUSIONS

In the prenatal development of the uterine tube in domestic cat two stages can be determined. First stage, between 27 – 43 day p.c. involves formation of the paramesonephric ducts, which are composed of the mesenchymal tissue lined by the pseudostratified epithelium.

The second stage, between 44 – 63 day p.c. involves the histogenesis of the oviduct wall. During this stage, between 53 – 55 day p.c., form the mucosa and muscular layer and the pseudostratified epithelium became cylindrical.

During the histogenesis of the uterine tube develops the nutritional vascular system, which consists of the pair of main supplying artery and draining vein and intramural system, composed by outer subserosal and inner mucosal network. The outer network is form by a circumferential interconnected blood vessels, which give off branches to the mucosa, where they form subepithalial capillary network.

Observations of the vascular corrosion casts showed that in the prenatal period most of the blood vessels, first in the tubal part of paramesonephric duct and then in the uterine tube develop as a result of intussusceptive angiogenesis. The sprouting angiogenesis is observed between 42th – 46th day p.c. in capillaries.

LET´S WORK TOGETHER! VET-SUSTAIN

Rieger J*, ... and YOU?

Institute of Veterinary Anatomy, Department of Veterinary Medicine, Freie Universität Berlin, Berlin, Germany

Sustainability is one of the biggest topics in our time and considerably affects veterinary medicine as well. In a broad sense, the definition is as follows: “Sustainability is the collective willingness and ability of a society to reach or maintain its viability, vitality, and integrity over long periods of time, while allowing other societies to reach or maintain their own viability, vitality, and integrity”(Wiek et al, 2015). In terms of food production and security, sustainability demands that economic, ecological and societal aspects are considered at the same time. The production of save food in an eco-friendly manner often stands in conflict with the use of common farming and animal treatment practices. For example, on the one hand the use of anti-microbials has improved food safety but on the other hand furthered anti-microbial resistance. Veterinarians work in this wide stretched field, covering the whole food chain from primary production to consumers. In the European Union, an extensive amount of research funding is currently invested in the field of sustainable food production. Especially veterinarians could take part in this endeavour, since they are experts in the management of farm animal health as well as food and feed production. International cooperation is often recommended in these research projects.

As example for a topic, and our current field of research, the pig as an important farm animal and moreover a model used in medical and nutrition research could be a point of interest. Thinking about the problems that are globally to be solved in pig farming, like manure overproduction, animal welfare and use of antibiotics, especially the gastro-intestinal system of the pig and its inhabiting microbiota are a suitable research field.

To bring together as much veterinary competence and influence as possible, we aim to start an open research network. We are looking for colleagues who are interested to work together with us on this challenging subject and explore the role of veterinary medicine in sustainable food production or already have some expertise in this line of work. We aim to connect with other networks and raise funding (e.g. Horizon 2020) for joint research projects.

REFERENCES

Wiek A, Bernstein MJ, Foley RW, Cohen M, Forrest N, Kuzdas C, Braden Kay, Withycombe Keeler L (2015) Operationalising Competencies in Higher Education for Sustainable Development. In Routledge Handbook of Higher Education for Sustainable Development, (London, New York: Routledge), pp. 241–260.

DISTRIBUTION OF THE α- AND β-KERATIN IN EPITHELIUM OF THE TONGUE IN THE DOMESTIC GOOSE

Skieresz-Szewczyk K[1], Jackowiak H[1], Buchwald T[2], Szybowicz M[2]

[1]Department of Histology and Embryology, Poznań University of Life Sciences, Poznań, Poland
2Division of Optical Spectroscopy, Institute of Materials Research and Quantum Engineering, Poznan University of Technology, Poland

INTRODUCTION

The tongue in the domestic goose is covered with the two types of the keratinized epithelium i.e. para- and orthokeratinized epithelium. The parakeratinized epithelium is present on the whole dorsal surface of the tongue, except the root of the tongue. The orthokeratinized epithelium cover the mechanical papillae of the tongue and is observed on the ventral surface of the lingual apex, where its keratinized layer forms the plate of the lingual nail. In birds the process of keratinization is best described in the epidermis and its cornified appendages (Alibardi, 2002, 2007; Sawyer and Knapp, 2003). Keratinization of the multilayered epithelium of the oral cavity have been investigated rarely in birds (Homberger and Brush, 1986; Carver and Sawyer, 1989). Generally during keratinization process in birds are synthesis two types of the cytokeratins: α- and β-keratin.
The aim of the presence study is to specify the range of the presence of α-keratin and β-keratin in the orthokeratinized epithelium on the ventral surface of the lingual apex and its keratinized layer, namely lingual nail in the domestic goose.

MATERIALS AND METHODS

Three tongues of the domestic goose collected from a local slaughterhouse after dissection were immersed in the 4% neutralized formalin. Tissue samples from the ventral surface of the apex of the tongue were dehydrated in a series of increasing concentration of ethanol (70%-96%) and routinely embedded in paraplast blocks and cut into sections of 4.5-5 mm. Tissue sections were stained using the Masson-Goldner trichrome histological staining technique. For immunohistochemistry tissue samples were incubated with the primary antibodies - monoclonal mouse antibodies directed against human antibodies: cytokeratin clone AE1/AE3 (DAKO) and then with secondary antibodies - goat anti-mouse IgG (Polymer-Labeled HRP-Anti-Mouse; Dako). The DAB solution (DAKO) was used to visualize binding of the secondary antibodies. To negative controls, the first antibody was omitted and instead the tissue samples was incubated with PBS (pH=7,4). The histological sections were examined using an Axioscope2plus light microscope (ZEISS, Germany).
The material to spectroscopic analysis were immersed in the 4% neutralized formalin and then rinsed in distilled water. The spectroscopic measurements were performed on confocal Raman microspectroscope (inVia made by Renishaw) equipped with diode pumped laser emitting 785 nm infrared wavelength.
According to the Polish law and the EU directive (no 2010/63/EU) the experiments conducted within the study do not require approval of the Local Ethical Committee for Experiments on the Animals in Poznan.

RESULTS

The histological observations in the light microscope show that orthokeratinized epithelium is composed of basal, intermediate and keratinized layer. In the intermediate layer due to the shape of cell nuclei and coloration of cytoplasm two zones are distinguished: the lower and upper zone. The keratinized layer, forming lingual nail, is consisted of flat cell without nuclei and the cell cytoplasm is stained red.

The immunohistochemistry staining reveals the strong reaction of α-keratin in basal layer. The upper zone of the intermediate layer is characterized with stronger staining reaction than the lower zone. In the keratinized layer the staining reaction is weak.
The Raman spectroscopy specifies that percentage distribution of α- and β-keratin in the particular layers of the epithelium. The amount of α-keratins in the lingual nail is 25% and the amount of β-keratin reaches 70%. Raman maps shows also that amount of β-keratin increases from lower layers of the epithelium to the lingual nail from 45% to 70%, whereas the amount of α-keratin decreases from lower layers of the epithelium in the direction of the lingual nail, from 43% to 25%. Raman spectra of the orthokeratinized epithelium demonstrate that secondary structure of keratins is different in lingual nail and intermediate and basal layer. Amide I and amide III bands associated with α- and β-keratins change the intensity in Raman spectra recorded in lingual nail and lower layer of the epithelium. Deconvolution of amide I band allowed to estimating precisely the content of various types of conformation. Curve-fitting process indicates that lingual nail as well as lower layers of the orthokeratinized epithelium consists of the proteins in β-sheet, β-turn, α-helix conformation and unordered structure.

DISCUSSION

The IHC study in the present work reveals the presence of α-keratin in the orthokeratinized epithelium on the ventral surface of the lingual apex and its keratinized layer – lingual nail in the domestic goose. Comparing own results to studies of the tongue in the chicken, we identify species-specific variation in the distribution of α-keratin.
The results obtained by Raman spectroscopy confirm IHC staining detecting alpha-keratin and also demonstrate the presence of beta-keratin in the lingual nail and lower layers of the orthokeratinized epithelium. The application of the Raman spectroscopy is very good alternative method to IHC studies, in the absence of specific antibodies, and gives detailed information about the structure of proteins and their conformation.
The cytokeratins are characterized by different mechanical and non-mechanical functions. The α-keratin in the basal and intermediate layer of the orthokeratinized epithelium is responsible for the formation of a stable cytoskeleton providing an adequate connection between neighboring cells and with the basal membrane. This is particularly important, because this epithelium is exposed to major mechanical pressure during pecking of grains. Additionally, the epithelium on the ventral surface of the apex of the tongue in the domestic goose is at risk of damage during uptake of food varying in consistency and hardness. The presence of α-keratin may indicate intensive reconstruction processes of these epithelia and the potential for rapid healing of possible damage. β-keratin detected in reptile scales exhibits limited extensibility, microbiological resistance, hydrophobicity and serves a protective function. Thus the β-keratin accumulates in the keratinized layer of the orthokeratinized epithelium called lingual nail sustains mechanical stress.

REFFERENCES

1. Alibardi L. 2002. Keratinization and lipogenesis in epidermal derivatives of the zebra finch, Taeniopygia guttata castanotis (Aves, Passeriformes, Ploecida) during embryonic development. J Morphol 251: 284-293.
2. Alibardi L. 2007. Keratinization of sheath and calamus cells in developing and regenerating feathers. Ann Anat 189: 583-595.
3. Carver W., Sawyer R.H. 1989. Immunocytochemical localization and biochemical analysis of alpha and beta keratins in the avian lingual epithelium. Am J Anat 84: 66-75.
4. Homberger D.G, Brush A.H. 1986. Functional-morphological and biochemical correlations of the keratinized structures in the African Grey Parrot, Psittacus erithacus (Aves). Zoomorphol 106: 103-114.
5. Sawyer R.H, Knapp L. 2003. Avian skin development and the evolutionary origin of feathers. J Exp Zool 298 B: 57-72.

IDENTIFICATION OF TELOCYTES IN THE PORCINE HEART

Hanna Tay[1]*, Tim Vandecasteele[1], Wim Van den Broeck[1]

[1] *Department of Morphology, Faculty of Veterinary Medicine, Ghent University, Merelbeke, Belgium*

INTRODUCTION

Telocytes are considered as a new type of interstitial cell, characterized by their long and thin prolongations called telopodes. They are believed to be ubiquitously present and so far, have been found in humans and various vertebrate animals such as mice, dogs, chickens and salamanders, where their presence was shown in different organs including heart, lungs, gut, and uterus. As telocytes are currently described and evaluated by their ultrastructural features, electron microscopic techniques, such as transmission electron microscopy (TEM), are essential for their correct identification. More precisely, it is the telopodes that are indispensable for telocyte recognition. Telopodes typically emerge thin from the cell body, are able to branch dichotomously, measure tens of µm in length, and have a moniliform (beads-on-a-string) aspect. The thin segments are called podomers while the dilated regions are called podoms. The thickness of the telopodes is usually below 0,2 µm, the resolving power of light microscopy. Few organelles are present; they are located mostly in the cell body and podoms and consist mainly of mitochondria, endoplasmic reticulum and caveolae. Telocytes are found in the interstitium where they are located in the vicinity of other cells such as endothelial cells or organ-specific cells, making it possible to form heterocellular junctions with them just as they are able to make homocellular connections with other telocytes. Furthermore, telocytes have been observed to release extracellular vesicles. These observations have led to many hypotheses about telocyte functions, in which intercellular communication is regarded a key function. Participation in mechanical support and tissue regeneration are other popular theories. For this reason, telocytes are hypothesized to have various interesting implications in medical research. Therefore it seemed interesting to look for telocytes in pigs as they have many similarities with man. This study focusses on the presence of telocytes in porcine heart.

MATERIAL AND METHODS

Hearts were collected from 6 pigs with ages ranging from 8 to 16 weeks. These animals were intended for other studies, which all got approval from the local ethical committee. Immediately after euthanasia, the heart was removed and within an hour samples from both atria and ventricles were obtained, cut in pieces of +/- 1 mm³ and put in Karnovsky fixative (2% paraformaldehyde and 2,5% glutaraldehyde in 0,1M cacodylate buffer, pH 7,2). After fixation for 24 hours at 4°C, samples were further processed for TEM according to routine procedures, which include post-fixation with 1% osmium tetroxide and embedding in EPON. Semi-thin sections were cut with a thickness of 1 µm and stained with toluidine blue in order to evaluate tissue morphology and select areas for ultrathin sectioning. Ultrathin sections (90 nm) were cut on a Leica EM UC6 ultramicrotome using a diamond knife (DiATOME, ultra 45°) and collected on Formvar-coated copper grids. Sections were stained with uranyl acetate, briefly rinsed with double-distilled water, stained with lead citrate, and rinsed again. Examination of the sections was done using a JEM-1400 Plus transmission electron microscope (JEOL, Benelux).

RESULTS

Transmission electron microscopy showed the presence of telocytes in porcine heart, in the myocardium of both atria and ventricles. Based on the ultrastructural features described in the literature, it was possible to distinguish telocytes from other interstitial cells. The cell body is small, and a thin brim of cytoplasm surrounds the large nucleus. Long, cytoplasmic processes emerge from the cell body and possess distinct characteristics:

1. Length: tens of micrometers, as measured on EM images. The length of 14 telopodes was measured, and the mean length was 23,63 µm ± 14,19 µm (min = 8,32 µm; max = 66,97 µm).
2. Thickness: usually below 0,2 µm. Telopodes emerge abruptly from the cell body as they have a thin aspect from the beginning.
3. Moniliform aspect: telopodes show an alternation of thin segments and thicker segments, which leads to the resemblance of beads on a string (fig. 1).
4. Organelles: there are few organelles. Mitochondria, endoplasmic reticulum and caveolae can be observed in the podoms, while mitochondria are seen in the cell body as well.
5. Dichotomous branching pattern.
6. Basal lamina: when looking at telocytes in a higher magnification, it becomes clear that they lack a basal lamina.

Telocytes are usually present in the vicinity of cardiomyocytes and/or blood vessels (fig. 1). Furthermore, telocytes are also observed in the tunica adventitia of a larger blood vessel in the heart, where they are surrounded by collagen fibrils. Close presence to mononuclear cells is observed as well. This vicinity to other cells enables telocytes to interact with them in different ways. First of all, telocytes can be seen releasing extracellular vesicles to neighboring structures. Secondly, intercellular contacts are established between telocytes and other cells. Electron-dense structures can be observed between telopodes and endothelial cells or pericytes, forming a connection. These dense structures seem to range from very small, being only nanometers in width and length, to

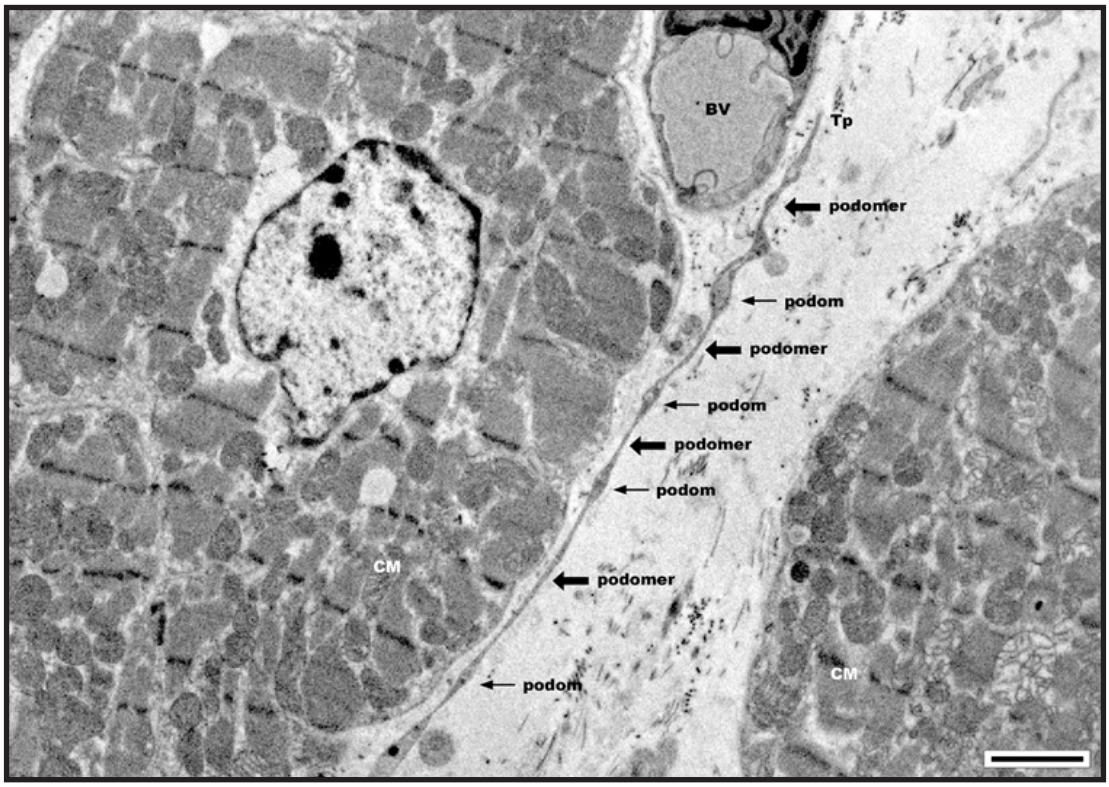

Fig. 1. Transmission electron microscopic image of a telopode (Tp). The typical moniliform aspect is unmistakable here: an alternation between thick (podoms) and thin (podomers) sections. The length of the sections varies, although the podomers are usually longer than the podoms. CM = cardiomyocyte; BV = blood vessel. Scale bar = 2 µm.

bigger and more elaborative structures. Next to these heterocellular junctions, homocellular junctions between telocytes can be found as well.

DISCUSSION

The results of this study show the presence of telocytes in the porcine heart, based on their distinct morphology as seen on transmission electron microscopic images. The most important characteristic, the cytoplasmic processes, measure tens of µm in length. This length makes it possible for one

telopode to span multiple structures such as adjacent blood vessels or cells. As telopodes are able to branch dichotomously as well, it is not unlikely to think that they form a 3D-network that delivers mechanical support to the surrounding tissues. The podoms, present along the telopodes and giving them their moniliform aspect, are another typical morphological feature. As in other studies, mitochondria, endoplasmic reticulum and caveolae are found in these dilatations. However, it is not clear what their exact purpose is. The vicinity between telocytes and nearby structures makes it possible for telocytes to make contacts with them if the distance is close enough. In this study, these neighboring structures are usually endothelial cells, pericytes and/or cardiomyocytes. Furthermore, homocellular contacts between telocytes can be observed as well. These intercellular junctions are thought to include both anchoring and communicating junctions, which contributes to the belief that telocytes have roles in both mechanical support and intercellular communication. Another means of communication is the exchange of vesicles. Our pictures show extracellular vesicles that seem to be released from telopodes. Furthermore, they are also present between telocytes and other cells, which suggest vesicle exchange between the cells. Additionally, telocytes seem to lack a basal lamina which could facilitate this form of cellular interaction. To conclude, this study has revealed the presence of telocytes in porcine heart. It might prove useful to perform future perform research regarding telocytes on porcine tissue as pigs have many similarities with man.

ABSTRACTS
of
POSTER PRESENTATIONS
IN ALPHABETICAL ORDER
OF
PRESENTING SPEAKERS

MICROSCOPIC ANATOMY OF THE VISCERAL ORGANS – AN INTERACTIVE ON-LINE ATLAS

Cizek P[1]*, Hamouzova P[1]

[1] *Department of Anatomy, Histology and Embryology, Faculty of Veterinary Medicine, University of Veterinary and Pharmaceutical Sciences, Brno, Czech Republic*

INTRODUCTION

Veterinary histology as a subject belongs to the core medical disciplines. It represents an integral part of the curriculum of the veterinary studies taught at the Faculty of Veterinary Medicine, University of Veterinary and Pharmaceutical Sciences Brno, Czech Republic. During two semesters, undergraduate students attend lectures and courses emphasising work with microscopes. The most common bibliography is available in the form of textbooks. Nevertheless, widely used modern electronic devices such as laptops and tablets increase the demand for new and innovative didactic methods. Thus, the interactive atlas of veterinary histology was created.

MATERIAL AND METHODS

Appropriate slides of the visceral organs were chosen. Seventy pictures of the slides under various microscope lenses were photographed and processed. Important structures were labeled so that a student can easily recognize and consequently remember the typical signs of the respective organs. An on-line version of the atlas was created. The slides were divided into six groups based on the organ systems to which the featured slide belonged. Students are free to self-evaluate since the label stays hidden until the cursor is moved to the designated area. The atlas is available at www.veterinarnihistologie.cz. The site uses the latest WordPress content management system. Data are built with powerful jQuery image map editor using modern web technology for creating live shapes as dynamic layers above the source image. The atlas is responsive and optimized for touch screens.

RESULTS

This is another form of study material available to students. Its interactivity helps them to recognize the slides more easily and describe the microscopic structure of visceral organs more profoundly.

CONCLUSION

This study demonstrates the potential of modern electronic devices for educational enrichment and their contribution to both the attractiveness of veterinary histology as a discipline and today's students effort which should result in their attaining greater success in studying the clinical subjects.

REFINING EXPERIMENTAL DENTAL IMPLANT TESTING USING 3D COMPUTED TOMOGRAPHY – A MORPHOMETRIC STUDY OF THE MANDIBULAR CANAL IN GÖTTINGEN MINIPIGS™

Corte GM[1*],Hünigen H[1],Niehues SM[2], Plendl J[1]

[1]Institute of Veterinary Anatomy, Department of Veterinary Medicine, Freie Universität Berlin, Germany
[2]Department of Radiology, Charité Universitätsmedizin Berlin, Berlin, Germany

INTRODUCTION

Because the omnivorous Göttingen Minipig is small in size, has a low body weight, and resembles human anatomy in being diphyodont, heterodont, having brachydont incisives and bunodont molars, it is frequently used as large animal model in dental research, which often involves the in vivo testing of endosseus dental implants. Frequently, these interventions have failed entirely or have had less than satisfactory results. One reason was that the assumption of a similar anatomy as in humans often resulted in the penetration of the mandibular canal which caused injury to the neurovascular bundle (A., V. and N. alveolaris inferior), leading to bleeding, swelling, neurosensory alterations like hyperaesthesia and postoperative pain. In addition, it might negatively affect implant stability and can jeopardize the whole experiment. Because there is limited information about the size and shape of the mandibular canal in Göttingen Minipigs, the objective of this study was to provide detailed morphometric data using computed tomography and 3D visualization and compare it with human mandibles. By doing so, we contribute to the 3R principles. The results will help to avoid complications during surgery and to find animal-friendly surgical procedures and also facilitate the selection of suitable age groups.

MATERIALS AND METHODS

CT scans were collected from a group of 18 female minipigs consisting of six animals examined at the age of 12 months (357±39 d) (group 1) and 12 animals examined at 17 and 21 months (511±24 d and 620±37 d) (group 2 and group 3, respectively). Their body mass was measured using a decimal scale. The data was gathered on a 64-slice scanner (Lightspeed 64®; GE Medical Systems, Milwaukee, USA). Full-body CT scans with a slice thickness of 0.5 mm were taken in prone and supine positions. The image analysis was performed using Vitrea Advanced® from Vital Images Incorporated (Minnetonka, MN, USA). The following parameters of the mandibular canal and the alveolar ridge were defined and measured: Volume of the mandibular canal; Length of the mandibular canal; Maximal vertical depth; Maximal oblique depth; Maximal width of mandibular canal; Alveolar bone height; Inferior bone thickness and Alveolar ridge width.

RESULTS

The volume of the mandibular canal increases with age. Highly significant differences within animals of the same age groups could be observed. The biggest range was in group 3 (21 months), where the largest volume was 13.41 ml and the lowest one 4.71 ml, which is a percentage difference of 285%. In addition, the length and depth increase with age. The width, the inferior bone thickness and the alveolar ridge width do not significantly change over time. The alveolar bone height, a parameter that is very important when to correctly evaluate the available space for dental implant placement to avoid the penetration of the canal, diminishes over time, with the 12 months old minipigs having the highest distance. The body mass does not have an influence on any of the measured parameters.

DISCUSSION

Compared to humans, Göttingen Minipigs have a longer, deeper and wider mandibular canal. Humans have a circular shaped and very thin canal, whilst the canal in minipigs is oval-shaped and much larger. Older minipigs have a shorter alveolar bone height compared to humans. This should be taken into account when positioning a dental implant without risking the penetration of the mandibular canal. The increase in canal volume appears to be due to loss of deep spongy bone in the posterior premolar and molar regions. This reduces the available space for dental implantation, negatively affecting implant stability and potentially the integrity of the neurovascular

bundle. Dynamic anatomical changes occur until 21 months. This suggests, on ethical grounds, not using minipigs younger than 21 months in experimental implant dentistry. Paradoxically the measurements of the 12 months old pigs indicate a closer alignment of their mandibular anatomy to that of humans suggesting that they may be better models for implant studies. Given the variability in mandibular canal dimensions in similar age cohorts, the use of imaging techniques is essential for the selection of individual minipigs for dental prosthetic interventions as well as presumably for higher success rates and thus the use of fewer animals in the long run.

THORACIC LIMB SKELETON IN CAMEL AND MARE

Crișan M.I.[1,2*], Dezdrobitu C.[2], Stan F.[2], Chirilean I.[2], Gudea A.[2], Martonoș C.[2], Damian A.[2], Aire T.[1] and Rennie E.[1]

[1]Anatomy, Physiology and Pharmacology Academic Programme, School of Veterinary Medicine, St George's University, Grenada, West Indies
[2]Department of Anatomy, Faculty of Veterinary Medicine, University of Agricultural Sciences and Veterinary Medicine of Cluj-Napoca, Romania.

INTRODUCTION

The camel (*Camelus Dromedarius*) is one of the oldest domesticated mammals and one of the first ever domesticated, playing a very important socio-economic role in some countries from southern Atlantic to Pacific

This comparative study of the thoracic limb skeleton in camel and mare can serve for teaching, research, private practice, food inspection service, research and/or paleontological studies.

MATERIALS AND METHODS

The current study was performed on 4 bodies coming from 2 mares and 2 camels. The bones were obtained through classical anatomical techniques (tissue removal, boiling and bleaching). Pictures were taken and interpretation was done by a group of specialists.

RESULTS

The acromion of the scapula was present in camel and the coracoids process in camel was located at mid distance between glenoid cavity and supraglenoid tubercle. The bicipital groove was double in mare and simple in camel. Three interosseous spaces of the forearm (one proximal and to distal) were noticed in camel. The carpal skeleton consisted of 7 bones in both camel and mare. The distal epiphysis of the metacarpus had two condyles, each articular condyle being divided by a sagittal ridge on its palmar aspect. Horse has one digit (the third) and camel has two digits (third and fourth). The small sesamoid bone was absent in camel.

DISCUSSIONS

These two species have developed in parallel starting 54 million years ago. The appendicular skeleton showed some clear differences between both species and most likely they are related to the biomechanics of their locomotion.

REFERENCES

Ghetie, V., A. Hillebrand (1971) Anatomia animalelor domestice, vol.I - Aparatul locomotor, Ed. Academiei Republicii Socialiste România, București.

Janis, M. Christine, Jessica M. Theodor, B. Boisvert (2002). Locomotor Evolution in Camels Revisited: A Quantitative Analysis Of Pedal - Anatomy And The Acquisition Of The Pacing Gait, Journal of Vertebrate Paleontology 22(1): 110–121, USA.

AGGLOMERATED SALIVARY GLANDS IN GUINEA PIGS (CAVIA PORCELLUS)

Matosz Bianca[1], V. E. Luca[1], C. C. Dezdrobitu[1*], C. Martonos[1], A. Damian[1]

[1)]University of Agricultural Sciences and Veterinary Medicine Cluj-Napoca, Calea Manastur, 3-5, 400372 Cluj-Napoca, Romania

INTRODUCTION

In rodents, there are dissimilarities between the major salivary glands, even if the diet is similar. Differences can be found between the salivary glands in mammals, depending on the species and the type of food (herbivorous, carnivorous or omnivorous) (Baciu, 1970). They develop in different locations, having a very various architecture, secreting different types of saliva (Jaskoll et al., 2002).

MATERIALS AND METHODS

For this study, the biologic material was represented by 5 adult guinea pigs of both sexes. The animals were euthanized by exposure to prolonged inhalatory anesthesia (Isoflurane). The stratigraphic dissection of the major salivary glands region was performed after euthanizing the subjects.

RESULTS

The macroscopic examination revealed that the parotid gland is found at the ear base, extending ventral reaching the ventral cervical region. The mandibular gland in guinea pig is found precervical anterior from the larynx and ventral from the recurved mandibular branch, subtracheal and is partially covered by the parotid gland. The sublingual gland is found on the both sides of the tongues ventral root ridge, with elongated appearance.

DISCUSSION

The results regarding major salivary glands were compared to literature data on other similar species such as rat, mice, rabbit and dog. In special literature are reported studies about the major salivary gland morphology on the species studied by us, but most were retrospective, focusing on several aspects. The vast majority of the studies were focused on the pathological, imunohistochemical or structural parts of these glands.

REFERENCES

Baciu I., (1970). Fiziologie, Editura didactică și pedagogică, București.

Jaskoll T., Y.M. Zhou, C.Y. Makarenkovahp, J.M. Collinson, J.D. West, A.D. Carvalho, (2002). Embrionic submandibular gland morphogenesis: stage specific protein localization of FGFs, BMPs, Pax6 and Pax9 in normal mice and abnormal SMG phenotypes in FgfR2-IIIc (+/Delta), BMP7 (-/-) and Pax6 (-/-) mice,Cells tissues organs, 170:83-90.

MORPHOMETRICAL DATA OF THE SPLANCHNOCRANIUM AND BONY ORBIT OF THE MOKRA GOAT IN ALBANIA

Duro S[1*], Kambo A[2], Çaushi A[3], Bakiasi I[4], Boçari A[5], and Kurti F[6]

[1]*Department of Morphofunctional Matters, Faculty of Veterinary Medicine, Agriculture University of Tirana, Albania*
[2]*Department of Economy and Rural Development Policies, Faculty of Economy and Agribusiness, Agriculture University of Tirana, Albania*
[3]*Department of Foreign Languages, Faculty of Economy and Agribusiness, Agriculture University of Tirana, Albania*
[4]*Department of Clinical subjects, Faculty of Veterinary Medicine, Agriculture University of Tirana, Albania*
[5]*Department of Mathematics, Faculty of Economy and Agribusiness, Agriculture University of Tirana, Albania*
[6]*National Food Authority, Elbasan, Albania*

INTRODUCTION

Mokra goat is a native breed that is found in the eastern part of Albania, near Lake Ohrid Currently, its population counts less than 10 thousand heads, with a tendency to be reduced constantly. In a near future, the risk of its disappearance is very high. So far in the literature there are no investigations focusing on morphometric parameters of this goat's skull. The purpose of this study was to identify all morphometric parameters of the Mokra goat, in particular those of clinical relevance.

MATERIALS AND METHODS

Sixteen heads of Mokra goats (8 females and 8 males aged over two years), coming from slaughtered animals, were measured and evaluated between January - December 2016. The skulls were prepared in our Anatomy Laboratory by using the boiling maceration techniques. Measurements were made by electronic calibre, goniometer and thread fibre. The results were evaluated and presented booth's average and standard deviations and as confidence interval estimator of the

mean with formula: $\text{confidence interval} = \text{observed mean} \pm t_{n-1,\alpha/2} * (\frac{s}{\sqrt{n}})$, where observed mean is the mean of the sample, $t_{n-1, \alpha/2}$ is the probability of t – distribution for α/2 and n-1 degree freedom, s is standard deviations and n is the total number of items for samples.

RESULTS

We have evaluated almost all morphometric parameters of splanchnocranium of Mokra goat.
The Skull length, height and width were 232.56 mm (±10.70) [223.615-241.51], 116.38 mm (±5.88) [111.461-121.289], 106.64 mm (±4.49) [102.887-110.391], respectively. Facial length, facial width (just caudal orbits) and facial index were 134.90 mm (±6.78) [129.233-140.576], 118.6 mm (±4.79) [114.605-122.02], 88.07 (±3.71) [84.9686-91.1648], respectively.

Length of lacrimal, zygomatic and nasal bone were 45.09 mm (±4.85) [41.0356-49.1494], 73.64 mm (±3.63) [70.6067-76.6683], 76.91 (±7.88) [70.32-83.5025], respectively.
Orbital length, width, depth and orbital index were 39.99 mm (±1.21) [39.0066-40.9741], 34.50 (±1.65) [33.1382-35.8625], 51.48 mm (±3.29) [48.7636-54.2033], and 86.27(±3.08) [83.8593-88.6732], respectively.
Perimeter of bony orbit were 126.32 mm (±6.21) [123.562-129.077]; composed by frontal 63.28 mm (±2.59) [61.6188-64.9437], zygomatic 47.32 mm (±2.07) [46.0724-48.5588], and lacrimal bone 15.72 mm (±1.56) [14.8722-16.5728]; or, 50.1%, 37.46% and 12.45% respectively.
There are not significant differences in all morphometric parameters of the skulls of Mokra goats between male and female except the differences in the skull high (diff. of means = -14 ±8.87912).
Conclusions: This study provided us with valuable data on morphometric and clinical parameters of the skull of Mokra goat, which will serve us as a basis for comparative studies with other ruminates species and important data on the clinical anatomy in the nearest future.
Key words: Mokra goat, skull, splanchnocranium, morphometric parameter, orbit

REFERENCES

1. Ali Louei Monfared. 2013. Clinical Anatomy of the Skull of Iranian Native Sheep. Global Veterinaria 10 (3): 271-275, 2013. ISSN 1992-6197. © IDOSI Publications, 2013.
2. Isaac Karimi, Vedat Onar, Gülsün Pazvant, Mohammadmehdi Hadipour and Yazdan Mazaheri. 2011. The Cranial Morphometric and Morphologic Characteristics of Mehraban Sheep in Western Iran. Global Veterinaria 6 (2): 111-117, 2011. ISSN 1992-6197.
3. K. Sarma, "Morphological and craniometrical studies on the skull of Kagani goat (Capra hircus) of Jammu region," International Journal of Morphology, vol. 24, no. 3, pp. 449–455, 2006.

Nader Goodarzi and Toraj Shah Hoseini. 2014. Morphologic and Osteometric Analysis of the Skull of Markhoz Goat (Iranian Angora). Veterinary Medicine International. Volume 2014, Article ID 972682, http://dx.doi.org/10.1155/2014/972682.

Olopade J.O. and Onwuke, S.K. (2005): Morphometric study of the skull of the West African Dwarf goat from South West Nigeria. Nigerian Veterinary Journal, Vol.26(2): 18-21.

Petrit Dobi, Anila Hoda, Enkelejda Sallaku, Valbona Kolaneci. The autochtonous breed of small ruminants. Tirane, 2006. Pp. 48-50

USE OF BOOTSTRAP STATISTICS METHOD FOR MEASURE AND REPORT OF ANATOMIES DATA. A CASE STUDY OF RUDA SHEEP IN ALBANIA

Duro S[1*], Kambo A[2], Çaushi A[3], Bakiasi I[4], Boçari A[5], and Kurti F[6]

[1]*Department of Morphofunctional Matters, Faculty of Veterinary Medicine, Agriculture University of Tirana, Albania*
[2]*Department of Economy and Rural Development Policies, Faculty of Economy and Agribusiness, Agriculture University of Tirana, Albania*
[3]*Department of Foreign Languages, Faculty of Economy and Agribusiness, Agriculture University of Tirana, Albania*
[4]*Department of Clinical subjects, Faculty of Veterinary Medicine, Agriculture University of Tirana, Albania*
[5]*Department of Mathematics, Faculty of Economy and Agribusiness, Agriculture University of Tirana, Albania*
[6]*National Food Authority, Elbasan, Albania*

INTRODUCTION

"Ruda" sheep is a native breed that is found mostly in the north-eastern Albania. The head of this sheep is without wool, distinguished orbits with very protruding eyes and a quite convex profile.

Referred of some publications on the past about morphometric parameters of the skull's Ruda sheep (Duro. S., et al. 2015) the results contain inaccuracies due to the small number of animals evaluated as well as the data distribution asymmetry. Using the bootstrapping method exceeds these limits and yields more accurate results compared to the classical methods of parameter estimation.The evaluation and statistical accuracy of morphometric parameters is related to the construction of confidence interval of indicators with a probability of security.

The methods traditionally used for this are available only for a small set of statistics and often make unrealistic assumptions about the variables' distributions. These assumptions are often particularly unrealistic in data derived from skull of Ruda sheep samples.

Bootstrapping estimation is a computer intensive procedure that offers a flexible and automatic alternative. The computer takes thousands of bootstrap samples from the observed data and from these bootstrap samples estimates the precision of the statistic.

High-speed personal computers make available the bootstrapping technique. Data from morphometric parameters of sheep's skull are often particularly prone to having non-normal distributions. Substantial skew has been shown in outcome measures relevant to morphometric parameters. Perhaps most problematic for experimental in veterinary anatomy research is the fact that measures of samples constructs are often heavily skewed in normal populations. Bootstrapping offers a flexible and general alternative that can be used to find statistic of anatomy. Bootstrapping makes fewer assumptions than the traditional approaches.

The aim of this study is to record, report and compare the morphometric indicators of Ruda sheep

skulls, based on the Bootstrapping method with traditional methods of distribution interval based on the t-distribution.

MATERIALS AND METHODS

This article offers applying bootstrap estimation to data from anatomic samples from Ruda sheep. Seventeen skull of Ruda sheep (8 females and 9 males aged over two years, coming from slaughtered animals, were measured and evaluated). The skulls were prepared in our Anatomy Laboratory by using the boiling maceration techniques. Measurements were made by electronic calibre, goniometer and thread fibre in millimetres. The results were evaluated and presented as average and standard deviations. We use traditional way of interval evaluation with stat graphics program p value = 0,05. After that we used SPSS version 23 program estimating the same data of Ruda sheep's scull using bootstrapping. We construct the percentile bootstrap interval with confidential level 95% (Davidson and Hincly, 1997; Efron & Tibshirani, 1993). The percentile method is most straight forward approach to bootstrapping.

Number of samples estimated with Bootstrap method were 50000, sampling method: simple.

RESULTS

In this study, we evaluated 12 morphometrical parameters from the skull of Ruda sheep.
The interval value of t-student of Skull length, skull high skull width and skull index were [253,41900 - 263,52200] mm, [107,13100 - 110,98700] mm, [106,58800 - 112,25300] mm, [41,67230 - 42,98620] respectively. Cranial length, Maximum width of neurocranium, cranial index, facial length, facial width and facial index value with t-student were [133,30200 - 138,46500] mm, [66,75790 - 68,92210] mm, [49,07180 - 50,85380], [150,011 - 159,93] mm, [77,5316 - 83,8531] mm and [78,0209 - 81,4782] respectively. The value of the same parameters as above with Bootstrapping method were: [254,0000000 - 263,0000000] mm, [107,4117650 - 110,8235290] mm, [106,8830740 - 111,8787200] mm, [41,8050180 - 42,9583380] respectively for the Cranial length, Maximum width of neurocranium, cranial index, facial length, facial width and facial index. Also, [133,5600440 - 138,1822940] mm, [66,8882500 - 68,7686910] mm, [49,1858880 - 50,7410380], [150,6429560 - 159,4298520] mm, [77,7359410 - 83,4804850] mm and [78,1988140 - 81,2833240] respectively for the Cranial length, Maximum width of neurocranium, cranial index, facial length, facial width and facial index. The differences in intervals value between two methods are very significates which vary from 0,146905 to 1,044176 as low interval and from -0,025214 to – 0,67255 as upper intervals. The same value in average percentage were about 10.84%.

CONCLUSIONS

The bootstrapping is a flexible method that enables the evaluation of different statistical parameters. In our study, it was found that use of this method for the evaluation of the morphometric parameters of the skull of Ruda sheep improved the accuracy of the results with an average of 10.84%, compared to the traditional method of interval evaluation with the student distribution (t). We recommend Bootstrapping method as a method more accurate and efficiency in evaluations and publications the values in all anatomical parameters especially in imagery and zooarchaeology study.

REFERENCES

1. A. C. Davison and D. V. Hinkley. Bootstrap methods and their application. 1997. Cambridge University Press. ISBN 0 521 57391 2 (hb). ISBN 0 521 57471 4 (pb).
2. Ali Louei Monfared. 2013. Clinical Anatomy of the Skull of Iranian Native Sheep. Global Veterinaria 10 (3): 271-275, 2013. ISSN 1992-6197
3. Dyce, K.M., W.O. Sack and C.J.G. Wensing, 2002. Textbook of Veterinary Anatomy, ed 3. Philadelphia,WB Saunders.
4. Efron B. and Tibshirani, R.J (1993), An Introduction of the Bootstrap. Chapman and Hall/CRC: New York.
5. Efron, B. (2002). The bootstrap and modern statistics. In Statistics in the 21st Century (A. E. Raftery, M. A. Tanner, and M. Wells, editors), pp. 326 – 332 . Chapman & Hall , London .
6. Isaac Karimi, Vedat Onar, Gülsün Pazvant, Mohammadmehdi Hadipour and Yazdan Mazaheri. 2011. The Cranial Morphometric and Morphologic Characteristics of Mehraban Sheep in Western Iran. Global Veterinaria 6 (2): 111-117, 2011. ISSN 1992-6197.
7. Nader Goodarzi and Toraj Shah Hoseini. 2014. Morphologic and Osteometric Analysis of the Skull of Markhoz Goat (Iranian Angora). Hindawi Publishing Corporation Veterinary Medicine International Volume 2014, Article ID 972682.
8. SOKOL DURO and ILIRJAN BAKIASI. The skull of the “Ruda” sheep in Albania: Morfological and Morphometrical data. Poster Nr. 7 presented on the 6th Internacional Scientific Meeting Days of Veterinary Medicine 2015. Struga, Republic of Macedonia 24-26 September 2015. Proceedings. ISSN 1409-7621.
9. Th. W. Fossum. 2013). Small Animal Surgery. Fourth edition. Elsevier 2013.

HISTOLOGICAL AND ULTRASTRUCTURAL STUDY OF THE TONGUE AND CHEEK OF THE PHILIPPINE MOUSE-DEER (TRAGULIDAE: TRAGULUS NIGRICANS)

Goździewska-Harłajczuk K[1*], Janeczek M[1], Nawara T[2], Paszta W[3], Marycz K[2]

[1]Department of Animal Physiology and Biostructure, Faculty of Veterinary Medicine, Wroclaw University of Environmental and Life Sciences, Wroclaw, Poland,

[2]Faculty of Biology, Electron Microscopy Laboratory, Wroclaw University of Environmental and Life Sciences, Wroclaw, Poland

[3]Wroclaw Zoological Garden

INTRODUCTION

The Philippine mouse-deer (Tragulus nigricans), also known as the Balabac chevrotain, is a species at a high risk of extinction and is endemic to a small island region in the Philippines. It is classified as a ruminant due to the anatomy of its gastrointestinal tract. To date, the tongue anatomy of the lesser mouse deer (Tragulus javanicus), belonging to the Tragulidae family (Agungpriyono, 1995), has been described. There are no reports of the microstructure of the tongue and cheeks of the Philippine mouse-deer Tragulus nigricans. Thus, the aim of this study was the examination of the tongue and cheek morphology in the Philippine mouse-deer using light microscopy and scanning electron microscopy (SEM).

MATERIAL AND METHODS

The study was performed on three tongues and cheek samples collected from the Philippine mouse-deer (one female and two males). The research material was obtained from the Wroclaw Zoological Garden. According to the Polish law, tissues obtained post-mortem do not require the permission of the ethics committee (Act of Animal Protection passed on August 21, 1997 by the Parliament of the Republic of Poland; No. 111/724). A histological, histochemical and ultrastructural analysis of the collected tissue was performed. Two tongues and two cheek samples fixed in 4 % buffered formalin were used for the histological and histochemical analysis. One tongue and two cheek samples fixed in 2% glutaraldehyde dissolved in 0.1 M phosphate buffer at pH 7.4 were used for the SEM. The sections were stained with hematoxylin and eosin (H&E), Masson-Goldner trichrome and Azan trichrome in order to identify the structure of the tissues. Glycans, glycoconjugates and neutral glycoproteins were identified using the periodic acid-Schiff method (PAS), while acid sialylated glycosaminoglycans were identified using the alcian blue pH 2.5 (AB pH 2.5) method. Prior to SEM, the samples were dehydrated and coated with gold using ScanCoat (Edwards). They were then assessed using SE1 at 10 kV filament tension (SEM, Zeiss Evo LS 15).

RESULTS

The tongue of the Philippine mouse-deer was elongated with a rounded apex. It was approximately 9 cm long and consisted of an apex, body and root. There was no lingual prominence. The only present mechanical papillae were the filiform papillae, which had a conical shape. They formed the largest group of papillae on the dorsal surface of the tongue, excluding the caudal part of root. At the apex of the tongue, the filiform papillae usually had two additional pseudopapillae (located anterior to the filiform papillae base). The body of the tongue contained taller filiform papillae also with two or three additional pseudopapillae, located at their base. The pseudopapillae were thin and elongated. The superficial layer of the filiform papillae contained keratin spines. Keratohyaline granules located

in the anterior part of the filiform papillae were present in deeper epithelial layers. The surface of the Philippine mouse-deer tongue was covered by a thin layer of keratin. The fungiform papillae were round and were dispersed on the surface of the apex and the body of the tongue. The SEM study revealed the presence of over a dozen taste bud openings in these papillae. Microfolds and microridges were also clearly visible. The surface of the fungiform papillae was covered by a thin layer of keratin. The foliate papillae were well developed and were located in the caudo-lateral part of the tongue. Macroscopically, they formed folds. Pseudopapillae resembling fungiform papillae were present in those folds. The histological assessment revealed the presence of numerous taste buds in the lateral walls of the foliate papillae. Taste buds were also present in area of the pseudopapillae, in the dorsal part of these structures. There were few (4-6) round or elongated vallate papillae. They were surrounded by a round papillary groove with a clearly visible annulary pad. Microfolds and microridges were visible on the surface of the vallate papillae. Numerous taste buds were present in the internal wall of the vallate papillae and in the wall of the annulary pad. There were numerous openings of the posterior lingual glands on the root of the tongue. The histochemical study showed that the glands accompanying the foliate and vallate papillae were serous.

The buccal papillae of the Philippine mouse-deer were conical. Some of them were pointed sharply while others were rounded at the apex. Sharply pointed buccal conical papillae were approximately 0.2-0.4 cm high. SEM study revealed that the surface of these papillae was smooth. On cross-section, a keratin layer was visible on the surface of these papillae. Numerous sebaceous glands were present in the cheeks.

DISCUSSION

The presence of well-developed foliate papillae was one of the main features of the Philippine mouse-deer that distinguishes it from other ruminants (Adyane et al., 2011; Emura et al., 2013; Erdoğan and Pérez, 2013). This was also a feature of the lesser mouse-deer (Agungpriyono et al., 1995). Another feature of the Philippine mouse-deer was the presence of small pseudopapillae with characteristics of fungiform papillae within foliate papillae area. Similarly to the lesser mouse-deer, there was soft keratinization of the surface of the tongue. The structure of the filiform papillae in the Philippine mouse-deer, including the presence of additional projections, was similar to that in the lesser mouse-deer (Agungpriyono et al., 1995). The lack of standard conical or lenticular lingual papillae is associated with the Philippine mouse deer diet, which consists of fruits, especially figs, young leaves and grasses that do not require long pretreatment. The fungiform papillae had also similar features to those in the lesser mouse-deer (Agungpriyono et al., 1995). Interestingly, they had many more taste bud openings on their surface. Unlike other ruminants, the Philippine mouse-deer had few lingual vallate papillae. They were round or elongated, as in the lesser mouse-deer (Agungpriyono et al., 1995). The buccal papillae were similar to those found in other ruminants.

REFERENCES

Adyane I.K.M., Zuki A.B., Noordin M.M., Agungpriyono S. (2011). Morphological study of the lingual papillae in the barking deer (Muntiacus muntjac). Anatomia Histologia Embryologia 40, 73-77.

Agungpriyono S., Yamada J., Kitamura N., Nisa C., Sigit K., Yamamoto Y. (1995). Morphology of the dorsal lingual papillae in the lesser mouse deer, Tragulus javanicus. Journal of Anatomy 187, 635-640.

Emura S., Okumura T., Chen H. (2013). Morphology of the lingual papillae in giraffe. Okajimas Folia Anat. Jpn. 89, 99-103.

Erdoğan S., Pérez W. (2013). Anatomical and scanning electron microscopy characteristics of the tongue in the Pampas deer (Cervidae: Ozotoceros bezoarticus, Linaeus 1758). Microscopy Research and Technique 76, 1025-1034.

COMPARISON OF THE MORPHOLOGY OF THE SELECTED GENITAL ORGANS AND THE SEX HORMONE LEVELS IN QUEENS

Hamouzova P[1]*, Cizek P[1], Bartoskova A[2], Novotny R[3]

[1] *Department of Anatomy, Histology and Embryology, Faculty of Veterinary Medicine, University of Veterinary and Pharmaceutical Sciences Brno, Czech Republic*

[2] *Institute of Life-Long Education and Informatics, University of Veterinary and Pharmaceutical Sciences Brno, Czech Republic*

[3] *Ruminant and Swine Clinic, Faculty of Veterinary Medicine, University of Veterinary and Pharmaceutical* Sciences Brno, Czech Republic

INTRODUCTION

The aim of this study was to determine whether a morphological description and measuring of oestradiol and progesterone levels give the same result when assessing the oestrous cycle phases and thus, whether the blood serum examination can be replaced with a morphological evaluation of the particular organs. Feline ovaries and the uterine horns were evaluated macroscopically and microscopically. The sex hormone levels were measured in the blood serum. The results might be useful in studies that focus on research which is dependent on detecting the stage of the oestrous cycle.

MATERIALS AND METHODS

Samples were collected from 40 healthy cats (sexually mature cats up to the age of 2 years with oestrous cycles), which were kept as pets. The cats were brought to the Small Animal Clinic, University of Veterinary and Pharmaceutical Sciences Brno, Czech Republic, because the owners required an ovariectomy. Blood samples were taken as a part of a preoperative examination.

Ovaries and proximal parts of the uterine horns were collected. The material was immediately fixed in 4% formaldehyde after the ovariectomy. After fixing had been completed, the samples were dehydrated in a graded alcohol series, acetone and xylene. At the end of the dehydration process, the samples were infiltrated with hot paraffin and embedded in paraffin wax. Sections of 3–4 μm were cut in a routine manner. The sections were dried, stained with haematoxylin and eosin, mounted and examined under an Olympus BX 51 light microscope.

The samples were divided into 4 groups according to the oestradiol and progesterone levels in the blood serum. The organs from the first group were taken from cats with an oestradiol level < 15 pg/ml (they were classified as in anoestrus). The organs from the second group were taken from cats with oestradiol levels > 15 pg/ml (they were classified as in prooestrus). The organs from the third group were taken from cats with oestradiol levels > 20 pg/ml (they were classified as in oestrus). The organs from the fourth group were taken from cats with progesterone levels > 1.5 ng/ml (they were classified as in dioestrus).

The macroscopic description of the genital organs (size of the ovarian follicles and luteal corpuscles, uterine edema) was determined immediately after the ovariectomy.

	Oestradiol	Progesterone	Macroscopic evaluation
Anoestrus	< 15 pg/ml	< 1.5 ng/ml	Follicles < 1 mm
Prooestrus	15 – 20 pg/ml	< 1.5 ng/ml	Follicles 1 – 2 mm
Oestrus	> 20 pg/ml	< 1.5 ng/ml	Follicles > 2 mm, edematized uterus
Dioestrus		>1.5 ng/ml	Luteal corpuscles

The macroscopic assessment was followed by a microscopic examination where the type of the ovarian

follicles and luteal corpuscles, follicular atresia, uterine gland development and the height of the uterine epithelium were described.

The results were compared with the stages of the oestrous cycle determined by measuring the oestradiol and progesterone levels.

RESULTS

Anoestrus was more often recognized by macroscopic evaluation (in 4 cases) compared to the microscopic assessment (only in 2 cases). However, anoestrus was incorrectly determined by macroscopic evaluation in 6 cases in queens with oestradiol levels higher than 15 or even 20 pg/ml. Microscopic evaluation revealed that no cat was in deep seasonal anoestrus. All ovaries of cats in anoestrus contained tertiary follicles, even if atretic.

Prooestrus was often confused with oestrus and vice versa. This is the reason why prooestrus and oestrus are often included in the follicular phase. The follicular phase (prooestrus + oestrus) was correctly described in 22 cases by microscopical evaluation and only in 16 cases by macroscopical evaluation (6 cases were confused with anoestrus).

Dioestrus was easily determined. All 12 cats with the high progesterone levels revealed structures typical for dioestrus. Nevertheless, 2 of these cats were incorrectly evaluated as they were in the follicular phase by macroscopic evaluation. Therefore, the microscopic evaluation was more accurate in evaluating dioestrus.

DISCUSSION

Frequent misinterpretation of prooestrus and oestrus based on macroscopic and microscopic evaluation compared to the sex hormone concentration indicates that the prooestrus is difficult to detect. Therefore, including those cats in only one (follicular) phase is an option (especially in cases when the sex hormone levels are not measured). Only 3 phases of the oestrous cycle are used in some studies which focused on the oestrous cycle in queens (Chatdarong et al., 2005; Hamouzova et al., 2017).

The fact that no cat was found in the deep seasonal anoestrus, as confirmed by microscopic assessment of the ovaries, could lead to a more difficult detection of anoestrus by morphological methods. Anoestrus was detected macroscopically in more cases than microscopically (4:2). However, oestrus was confused with anoestrus by the macroscopic assessment in 6 cases.

Dioestrus can be determined both macroscopically and microscopically. Nevertheless, microscopic assessment showed a higher reliability (12: 10).

To conclude, measuring the sex hormone levels is not necessary for the detection of dioestrus. Morphological methods are reliable in these cases. Macroscopic or microscopic evaluation could be used as the only method also for the detection of the follicular phase of the cycle. Nevertheless, whenever it is necessary to distinguish between prooestrus and oestrus, morphological evaluation is not reliable. Short anoestrus which is between two follicular phases is difficult to determine by both morphological methods.

REFERENCES

Chatdarong K., Rungsipipat A.,Axner E., Forsberg C. L. (2005). Hysterographic appearance and uterine histology at different stages of the reproductive cycle and after progestagen treatment in the domestic cat. Theriogenology 64,12-29.

Hamouzova P., Cizek P., Novotny R., Bartoskova A., Tichy F. (2017). Distribution of mast cells in the feline ovary in various phases of the oestrous cycle. Reproduction in Domestic Animals 52, 483-486.

SCRATCH ASSAY OF HUMAN AND EQUINE ENDOTHELIAL CELLS – COMPARISON OF THE MIGRATION PATTERN IN VITRO

Hopperdietzel C*, Rieger J, Käßmeyer S, Plendl J

Institute of Veterinary Anatomy, Department of Veterinary Medicine, Freie Universität Berlin, Berlin, Germany

INTRODUCTION

Endothelial lesions induce migration and proliferation of neighboring cells in vivo and in vitro, aimed at closing the damage as quickly as possible. Thereby, different endothelial cell populations (tip- and stalk cells) play a specific role.
In horses it has been known for a long time that thrombosis evolves frequently in both, arterial and venous localizations. In contrast, this phenomenon is not often seen in other domestic animals. To examine the role of migration of venous and arterial endothelial cells in equine thrombosis, a scratch assay was established. As a control group, different human endothelial cell lines were used.

MATERIALS AND METHODS

Human endothelial cells of the skin (HDMEC), the umbilical vein (HUVEC) and the abdominal aorta were bought from different manufactures and cultivated in endothelial cell growth medium (EGM-2 MV, Lonza). Equine endothelial cells were isolated from the Arteria carotis communis and the Vena jugularis externa via enzymatic digestion. Identification and sorting of these cells was performed by flow cytometry with the endothelial marker CD31. Additionally, equine endothelial cells were identified by labelling immunohistochemically with anti-von Willebrand factor and Weibel-Palade-bodies, i.e., endothelial marker organelles were visualized using transmission electron microscopy. After the emergence of a complete monolayer, a lesion was set using a sterile Eppendorf pipette tip (10µl). The cellular migration was investigated over a period up to 60 hours using an air-conditioned Life Science Microscope (Olympus IX81). For documentation, the shooting interval was set to one picture per 30 minutes.

RESULTS

Human endothelial cells
All of the three cell lines examined displayed continuous migration and proliferation towards the middle of the scratch. Tip-cells could be observed at the monolayer edges consistently. The joining stalk-cells were following permanently. The scratch area was closed by the migrating cells after about 16 hours and a complete monolayer was reconstructed. Endothelial cells presented the typical cobblestone pattern and a slight reduction of the cell density, as well as a hypertrophy of single cells could be observed at the periphery of the field of view.
Equine endothelial cells
Immunohistochemical and electron microscopic examinations confirmed endothelial identity of the isolated equine cells.
The induced lesion in the arterial endothelial cell monolayer was closed after 33 hours. Migration of these cells towards the middle of the scratch was not continuous but showed focal sprouting of tip- and stalk-cells. In addition, single cells (especially tip-cells) displayed a specific migration pattern. They detached from the cell complex a few times and migrated up to 20 hours in the denuded scratch area. Neither reduction of the cell density nor hypertrophy of single cells could be monitored. The cells displayed an elongated shape but also in a cobblestone pattern.
The equine endothelial cells from the Vena jugularis externa displayed an increased migration compared to the arterial equine endothelial cells. A complete monolayer was rebuild after around 23

hours. The migration pattern was equate to that of the arterial equine endothelial cells.

DISCUSSION

A fast and uniform migration of human endothelial cells to close the wound in scratch assays is described in many studies (e.g. Liang et al., 2007). In our study, we were able to confirm this. For the equine endothelial cells this was not true. Wound closure in equine cells was not uniform and also slower than in the human cultures. The solitary migrating cells might be a special subpopulation of tip-cells.

REFERENCES

Liang, C. C., Park, A. Y., & Guan, J. L. (2007). In vitro scratch assay: a convenient and inexpensive method for analysis of cell migration in vitro. Nature protocols, 2(2), 329-333.

THE VARIATIONS OF THE VARUS AND PROCURVATUM ANGLES OF THE DISTAL FEMORAL SHAFT ON DOGS

Kara ME[1]*, Sevil-Kilimci F,[1] Dilek ÖG[2], Onar V[3]

1. Adnan Menderes University, Faculty of Veterinary Medicine, Department of Anatomy, 2. Mehmet Akif Ersoy University, Faculty of Veterinary Medicine, Department of Anatomy, 3. Istanbul University, Faculty of Veterinary Medicine, Department of Anatomy

INTRODUCTION

Many researchers are interested in the femoral conformation because the most of the orthopaedic problems have been occurred in the femur and it's joints. The neck-shaft and the anteversion angles are two parameters that are frequently measured when the femur is assessed. The orientation femoral head directly affects the transmission of loads from hip to knee. The geometry of the proximal femur may be related to some knee disorders. The excessive femoral varus is a contributing factor to patellar luxation. Both of the femoral varus and the procurvatum are also considered essentially on the corrective osteotomies and for the success on the optimal alignment of the femoral implant of the total knee arthroplasty. To the best of our knowledge only few reports highlighted to evaluate variations in the bends of the distal femoral shaft in dog. Besides of this, no report had been demonstrated the sexual dimorphism for the femoral angles and the relationship between the proximal and distal angles of femur in dog yet.

MATERIALS AND METHODS

A total of seventy-five cleaned femur from the eight different breed of dogs were used. The three-dimensional images were reconstructed from the computed tomographic images. The anteversion, neck-shaft angels were measured at the proximal femur as well as the anatomic lateral distal femoral angle (femoral varus) and the anatomical caudal distal femoral angle (procurvatum) at the distal. The mean values, standard deviations and 95% confidence intervals were calculated for each parameter. The statistical comparison was performed between sexes. The correlation coefficients were also calculated among the measured angels for all the dogs.

RESULTS and DISCUSSION

The neck shaft angle has no correlations among the procurvatum and varus angles. There was a weak inverse correlation between the version and procurvatum angles while there was a weak positive correlation between the version and varus angles. The 95% of confidence intervals of the varus and procurvatum angles were 92.62^0-94.08^0 and 89.09^0-91.94^0, respectively. The differences in the distal femoral angles between male and female dog were not significant. The data of this study may be used in the orthopaedic studies and the clinical applications on the distal femur of dog.

REFERENCES

Dudley R.M., Kowaleski M.P., Drost W.M.T., Dyce J. (2006). Radiographic and computed tomographic determination of femoral varus and torsion in the dog. Veterinary Radiology & Ultrasound 47, 546-552

Oxley B., Gemmill T.J., Pink J., Clarke S., Parry A., Baines S., Malcolm M.W. (2013). Precision of a novel computed tomographic method for quantification of femoral varus in dogs and an assessment of the effect of femoral malpositioning". Vet Surg. 42, 751-758

Paley D. (2002) Principles of deformity correction. Springer-Verlag,

Tomlinson J., Fox D., Cook J.L., Keller G.G. (2007). Measurement of femoral angles in four dog breeds. Veterinary Surgery 36, 593-598.

Wright S.J, Boymans T.A, Grimm B, Miles A.W, Kessler O. (2014) Strong correlation between the morphology of the proximal femur and the geometry of the distal femoral trochlea. Knee Surg Sports Traumatol Arthrosc. 22, 2900-10.

* This study was supported by TÜBİTAK (114O094).

HISTOLOGICAL COMPARISON OF FOUR ANATOMICAL REGIONS OF PORCINE SKIN TO HUMAN ABDOMINAL SKIN.

M. Khiao In[1]*, S. Kaessmeyer[1], KC. Richardson[2], J. Plendl[1]

[1] *Institute for Veterinary Anatomy, Department of Veterinary Medicine, Freie Universität Berlin, Germany*

[2] *College of Veterinary Medicine, Murdoch University, Murdoch, WA, Australia*

INTRODUCTION

Human skin is the gold standard for in-vitro skin experiments. Unfortunately, the availability of human skin for research is limited, so alternatives are required. Because of its similar structure, porcine skin has been used frequently as a model of human skin for *in vitro* studies. Human skin used in dermatological research, is usually abdominal or chest skin obtained from plastic surgery. However, pig skin can be sampled from many locations, even though there are structural variations between different regions (Turner et al,2015). The aim of this study is to identify a region of the body to obtain porcine skin that can be used as the best possible model for human abdominal skin.

MATERIALS AND METHODS

Samples of German Landrace pig skin (10–11 weeks old, n = 8; female = 4, male = 4) were collected from immediately caudal to the ear, lumbar flank, mid-back and the caudal abdomen. Human abdominal skin samples were excised during plastic surgery (n = 3). The skin samples were processed using routine techniques for analysis by light microscopy (LM). Qualitative assessment of the morphology was carried out. Quantitative assessments included counting the number of cell layers in each stratum. Statistical analysis was performed to compare quantitative parameters of each pig skin region to human abdominal skin using a linear mixed model method. A P value of less than 0.05 was considered statistically significant and tests were performed using SPSS version 24 (IBM Deutschland GmbH, Ehningen).

RESULTS

Histologically, morphologic features of all regions of porcine skin studied were similar to human abdominal skin. The overall appearance of the pig epidermis, notably behind the ear and from the flank, was gently folded, similar to that seen in the human skin samples. Elsewhere, the pig samples of the back had a flattened appearance, and those of the caudal abdomen were greatly folded.

The number of layers within the **stratum spinosum** of porcine skin ranged from 6.94 ± 0.39 to 7.63 ± 0.38 layers, he human abdominal skin had 4.00 ± 0.58 layers. All sampled regions of porcine skin showed significantly more layers of s. spinosum when compared to the human skin. However, there was no significant difference of numbers of cell layers in **s. granulosum and s. corneum** from pig and human skin. The stratum **granulosum** of pig skin from all regions showed only 1–2 layers and human skin showed only 1 layer. In the pig, the number of cell layers in the s. **corneum** ranged from 9.44 ± 0.54 to 15.63 ± 1.44 layers. In the human skin samples, there were 13.33 ± 0.88 layers.

DISCUSSION

While the morphological studies found a remarkable similarity between the pig skin samples and the human abdominal skin, the statistical analysis revealed specific differences: significantly more layers in the stratum spinosum in all pig samples. Interestingly, the comparison between the pig samples showed no differences. From the results of this study, we can conclude that the German Landrace skin from all regions could potentially be used as a substitute for human skin.

REFERENCES

Turner NJ., Pezzone D., Badylak SF. (2015). Regional variations in the histology of porcine skin. Tissue engineering Part C 21,373–384

THE EFFECT OF WNT5A AND WNT7A ON CARTILAGE FORMATION AND ANTERIOR-POSTERIOR PATTERNING OF THE LIMB

Killinger M[1,2,*], Buchtova M[1,2]

[1]*Laboratory of Molecular Morphogenesis, Institute of Animal Physiology and Genetics, Brno, Czech Republic*
[2] *Institute of Experimental Biology, Masaryk University, Czech Republic*

INTRODUCTION

Growth and patterning of the vertebrate limb is controlled by signals produced in the apical ectodermal ridge (AER) and by the zone of polarizing activity (ZPA). Limb development requires tight interactions between these signaling centers to keep asymmetrical arrangement of all skeletal elements and their growth. Here, we examined the role of non-canonical WNT signaling in limb development. Activation of the non-canonical WNT pathway is initiated by binding of WNT proteins to their specific receptors and co-receptors and later activating downstream targets. WNT pathway is essential for the establishment of size and general morphology of zeugopodial and autopodial skeletal elements. Mutations in this pathway have been shown to cause severe limb malformations. Our aim is to uncover a possible role of WNT5a and WNT7a in anterior-posterior patterning of limb development using gain-of-function approaches.

MATERIAL AND METHODS

The chicken embryos (ISA Brown) were obtained from private breeder (farm Integra a.s., Žabčice, CR). First, we analyzed the effect of WNT5a and WNT7a ectopic application *in ovo* using microinjection into chicken limb buds. Fertilized chicken eggs were incubated horizontally on the plate at 37.8°C for 3.5 days until the embryo develops into a stage suitable for further manipulation. Limb buds at stage HH20-22 were microinjected with WNT5a or WNT7a (500 µg/ml) in the apical, anterior and posterior areas. Proteins were applied also separately into just anterior or posterior areas to analyze area-specific phenotype. Left non-treated wings were used as controls. Wings were collected into 100% ethanol after 11 days of incubation and stained with 3% Alcian Blue for cartilage visualization and 0.1% Alizarin Red to analyze bone morphology. Samples were cleared in 4% KOH and photographed in 50% glycerol. The embryos not surviving whole incubation period were collected to 4% PFA and analyzed for external phenotype.

To study cellular and molecular mechanisms underlying specific development of anterior and posterior areas of developing limb, we isolated radius and ulna from different stages of chicken development. We started at the stage HH36 when the first lacunae were observed and continued up to stage HH41 when the bone is almost fully ossified. Organ explants were cultivated up to 8 days. We optimized suitable time of incubation for following histological analysis. The length of bones were measured at the first day at time of embryo harvesting as well as at the last day of incubation to analyze growth differences. Cultures were treated with WNT5a, WNT7a (40 ng/ml), FGF2 (50 ng/ml) or their combination to find differences in chondrocyte differentiation during endochondral ossification.

RESULTS

The application of WNT5a and WNT7a into three areas of chicken limb bud caused shortening of the zeugopodial and the autopodial areas. Moreover, alteration of the limb shaping was observed following both treatments. The ectopic application WNT5a initiated bending of radius together with shortening of ulna and digits were missing in some embryos. The microinjection into the anterior area of the limb bud leads to malformation in radial area while the application into posterior area caused abnormal phenotype in ulnar area together with rudimental wing formation. Following the application of WNT7a, the treated wings were shorter and thinner than control wings. We also observed morphological differences in zeugopodial and autopodial part of the wings such as curved bones and abnormal fingers. Moreover, some bones were missing or rudimental wings developed. Separate anterior or posterior applications of WNT7a caused distinct phenotypes similarly to the

WNT5a application.

Cultivation of zeugopodial long bones dissected from different stages of chicken embryos exhibited dependence of length gain on the age of cartilage at the onset of experiment. The length of bones isolated from the stage HH36 was almost 5 times higher than using stage HH41. In contrast, the bones isolated earlier were more curved and bended than elements isolated later, which resulted in difficulties to analyze the length and unfeasibility to prepare histological sections. For this reason, we selected for further analysis stage HH39 when the bone is well developed and the deformities during cultivation are not so remarkable. Radius and ulna isolated from HH39 were cultivated for 2 to 5 days to uncover suitable period of incubation. The cartilages grew normally until the day 4 when they started to bend due to massive cartilage proliferation especially in radius. Therefore, 3 days of incubation seem to be optimal for chicken in vitro cultures in contrast to 8 days in mouse.

DISCUSSION

Abnormalities of the human limb development caused by non-canonical WNT signaling are recently in center of attentions. *Wnt5a*, which is expressed the apical ectodermal ridge and in the mesoderm, was shown to affect chondrogenesis due to modulation of cell polarity in the developing limb (Conte et al., 2016; Gros et al., 2010). WNT5a has also the ability to reduce the size of the zeugopodial long bones, suggesting its involvement in proximal–distal bone patterning through regulation of chondrogenic differentiation (Kawakami et al., 1999). Robinow syndrome and brachydactyly type B, which are caused by missense mutations in *Wnt5a* or its receptor *Ror2*, exhibit a prominent limb shortening (Wang et al., 2011; Takeuchi et al., 2000). In contrast, *Wnt7a* expression is located in the dorsal ectoderm and it is essential for dorso-ventral patterning. Alteration in WNT7a signaling produce several clinically relevant conditions such as the palmar duplication syndrome, nail patella syndrome, ulnar ray deficiency, limb hypoplasia, polysyndactyly and the palmar nail syndrome. Homozygous missense mutations in *Wnt7a* cause Awandi/Raas-Rothschild/Schinzel syndrome and Fuhrman syndrome that are characterized by ulnar ray deficiency and the reduction of limb length with hypoplasia of distal skeletal elements (Woods et al., 2006). Similar to our embryos with ectopic application of WNT ligands, human malformation included mostly hypoplasia or aplasia of bones with effect observed mainly in the areas of zeugopod and distal autopod. Further study of interplay between FGF and non-canonical WNT signaling during limb formation can help to determine the mechanisms of species-specific zeugopod patterning during evolution and disruption leading to syndromes in human. Moreover, we hope that establishment of chicken explant cultures and the comparison of growth potential between radius and ulna will help us to uncover the molecular bases of interaction between these two pathways with focus on different sensibility of anterior and posterior skeletal elements during endochondral ossification.

ACKNOWLEDGEMENTS The project was supported by the Czech Science Foundation (14-31540S) and by the Ministry of Education, Youth and Sports of the Czech Republic from the Operational Programme Research, Development and Education (CZ.02.1.01/0.0/0.0/15_003/0000460).

REFERENCES

Conte, D., G. Garaffo, N. Lo Iacono, S. Mantero, S. Piccolo, M. Cordenonsi, D. Perez-Morga, V. Orecchia, V. Poli, and G. R. Merlo, 2016, The apical ectodermal ridge of the mouse model of ectrodactyly Dlx5;Dlx6-/- shows altered stratification and cell polarity, which are restored by exogenous Wnt5a ligand: Hum Mol Genet, v. 25, p. 740-54.

Gros, J., J. K. Hu, C. Vinegoni, P. F. Feruglio, R. Weissleder, and C. J. Tabin, 2010, WNT5A/JNK and FGF/MAPK pathways regulate the cellular events shaping the vertebrate limb bud: Curr Biol, v. 20, p. 1993-2002.

Kawakami, Y., N. Wada, S. I. Nishimatsu, T. Ishikawa, S. Noji, and T. Nohno, 1999, Involvement of Wnt-5a in chondrogenic pattern formation in the chick limb bud: Dev Growth Differ, v. 41, p. 29-40.

Takeuchi, S., K. Takeda, I. Oishi, M. Nomi, M. Ikeya, K. Itoh, S. Tamura, T. Ueda, T. Hatta, H. Otani, T. Terashima, S. Takada, H. Yamamura, S. Akira, and Y. Minami, 2000, Mouse Ror2 receptor tyrosine kinase is required for the heart development and limb formation: Genes Cells, v. 5, p. 71-8.

Wang, B., T. Sinha, K. Jiao, R. Serra, and J. Wang, 2011, Disruption of PCP signaling causes limb morphogenesis and skeletal defects and may underlie Robinow syndrome and brachydactyly type B: Hum Mol Genet, v. 20, p. 271-85.

Woods, C. G., S. Stricker, P. Seemann, R. Stern, J. Cox, E. Sherridan, E. Roberts, K. Springell, S. Scott, G. Karbani, S. M. Sharif, C. Toomes, J. Bond, D. Kumar, L. Al-Gazali, and S. Mundlos, 2006, Mutations in WNT7A cause a range of limb malformations, including Fuhrmann syndrome and Al-Awadi/Raas-Rothschild/Schinzel phocomelia syndrome: Am J Hum Genet, v. 79, p. 402-8.

CONJUNCTIVA-ASSOCIATED LYMPHOID TISSUE (CALT) IN THE PRIMITIVE BREED – BILGORAJSKA GOOSE (*ANSER ANSER*)

Klećkowska-Nawrot J[1], Kowalczyk A[2], Łukaszewicz E[2]

[1]Department of Animal Physiology and Biostructure, Faculty of Veterinary Medicine, Wroclaw University of Environmental and Life Sciences, Kozuchowska 1/3, 51-631 Wroclaw, Poland; [2]Division of Poultry Breeding, Institute of Animal Breeding, Wroclaw University of Environmental and Life Sciences, Chelmonskiego 38a, 51-631 Wroclaw, Poland.

INTRODUCTION

The Bilgorajska goose is an indigenous breed descended from primitive geese from north-eastern Poland (Bilgoraj region), kept as a closed population since 1971. The population of the national Bilgorajska goose breed is actively preserved, and is included in the World Watch List for Domestic Animal Diversity (FAO) (Książkiewicz, 2006; Scherf, 2000). Since 2011, the Bilgorajska goose is included in a preservation program for genetic resources of goose populations; it is bred in two research centers in Poland (Wroclaw and Puchaczow). The ocular surface of the Bilgorajska goose is protected from infectious disease or allergic factors by lymphoid tissue as part of the CALT (Bayraktaroglu and Asti, 2009). The CALT in birds is assumed to play a key role in the eye protection by initiating and regulating immune responses and is presumed to partake in the mucosal immunity of the nasopharynx (Steven et al. 2008, 2009; Seo et al., 2010; Siebelmann et al., 2013).

MATERIAL AND METHODS

In the present study, we describe the histology and histochemical analysis of the upper and lower eyelids of 13 adult female Bilgorajska geese (Anser anser) (8-12 months old). The material was obtained from the Division of Poultry Breeding of the Institute of Animal Breeding at the Wroclaw University of Environmental and Life Sciences and was collected during a 1-year period. The geese were not killed for the purpose of this study and died under natural circumstances. According to the Polish law, studies on tissues obtained post-mortem do not require the Ethics Committee approval (Parliament of the Republic of Poland 2012) (Act of Animal Protection passed on August 21, 1997 by the Parliament of the Republic of Poland; No. 111/ 724). The goose eyelids were examined under light microscopy (histological analysis – H&E, azan trichrome staining and histochemical analysis – periodic acid-Schiff and alcian blue pH 2.5 staining).

RESULTS

The skin surface was lined by a keratinized stratified squamous epithelium with 2-3 rows of nucleated cells in upper and lower eyelids. The marginal zone of the conjunctival surface was covered by a stratified columnar epithelium with 9-10 rows of cells. The orbital zone was covered by to 3-4

non-keratinized rows with numerous goblet cells. The connective stroma of the eyelids contained densely packed collagen fibers, blood vessels and numerous Zeis glands located at the base of the eyelash bulbs. The tarsal plate, formed from dense connective tissue containing elastic fibres, was located beneath the conjunctival surface. Well-developed, diffuse lymphatic tissue was present in the upper eyelids, while numerous lymphatic follicles mostly under the conjunctival epithelium were present in the lower eyelids. Numerous lymphocytes were also found within the loose connective tissue. PAS staining of the eyelids demonstrated the presence of mucous goblet cells (mucoprotein and neutral mucopolysaccharydes), and AB pH 2.5 staining indicated the presence of sulfated acid mucopolysaccharrides.

DISCUSSION

In domestic birds, the structure of the eyelids and the CALT is crucial in the prevention of viral respiratory tract infections (Fix and Arp, 1991, Klećkowska-Nawrot et al., 2016; van Ginkel et al., 2012). The CALT in birds plays an important role in building local resistance, which also promotes the health of upper respiratory tract (Bayraktaroglu et al. 2011; Klećkowska-Nawrot et al. 2016). In the Bilgorajska goose, the CALT was present mostly under the conjunctival epithelium of the lower eyelid. According to Klećkowska-Nawrot et al (2016b), the lymphoid follicles were more abundant in the lower eyelid than in the upper eyelid in adult African black ostrich. Fix and Arp (1991) reported that the CALT in chickens and turkeys is characterized by the presence of lymphoid follicles within the conjunctival folds and fissures at the medial canthus of the lower eyelid only. As reported by van Ginkel (2012), the lymphoid follicles in upper eyelid are much smaller and are located near the lacrimal ducts. The human conjunctiva contains lymphoid follicles in the lower and upper eyelid. Interestingly, studies of the CALT in rodents (such as rats and mice) revealed the presence of very little lymphoid tissue, which does not physiologically contain lymphoid follicles and has very few diffusely interspersed lymphoid cells (Klećkowska-Nawrot et al. 2016, Knop and Knop, 2005). Studies carried out on the rabbit eye found diffuse lymphocytes (Franklin and Remus, 1984). There were few diffuse lymphocytes and no components of the secretory system in the rat conjunctiva (Knop and Knop, 2005). The study by Siebelmann et al. (2013) on a novel Bagg Albino (BALB/c strain) mouse model after a splenectomy and a lymphadenectomy, kept under different housing conditions, subjected to topical surface-stimulation, showed that there were similarities between the mouse and human CALT (Klećkowska-Nawrot et al. 2016).

REFERENCES.

Bayraktaroglu AG, Kormaz D, Aşti RN, Kurtdede N, Altunay H. 2011. Conjunctiva Associated Lymphoid Tissue in the Ostrich (Struthio camelus). Kafkas Univ Vet Fak Derg 17:89–94.

Fix AS, Arp LH. 1991. Particle uptake by conjunctiva-associated lymphoid tissue (CALT) in turkeys. Avian Dis 35:100–106.

Khan MZI, Jahan MR, Islam MN, Haque Z, Islam MR, Kon Y. 2007. Immunoglobulin (Ig)- containing plasma cells in the Harderian gland in broiler and native chickens of Bangladesh. Tissue & Cell 39:141–149.

Klećkowska-Nawrot J, Goździewska-Harłajczuk K, Nowaczyk R. 2016a. Morphological study of the upper, lower and third eyelids in the African black ostrich (Struthio camelus camelus L., 1758) (Aves:Struthioniformes) during the embryonic and postnatal period.

Italian J of Zoology. 83: 312-328.

Knop E, Knop N. 2005. The role of eye-associated lymphoid tissue in corneal immune protection. Journal of Anatomy 206:271–285.

Książkiewicz J. 2006. The role and importane of geese species included by genetic stock protection program. Wiadomości Zootechniczne. 4:34-38.

Scerf BD (ed). 2000. World watch list for domestic animals diversity, 3rd edn,. Food and Agriculture Organization of the United Nations, Rome.

Seo KY, Han SJ, Cha H-R, Seo S-U, Song J-H, Chung S-H, Kweon M-N. 2010. Eye mucosa: An efficient vaccine delivery route for inducing protective immunity. The Journal of Immunology 185:3610–3619.

Siebelmann S, Gehlsen U, Hüttmann G, Koop N, Bölke T, Gebert A, Stern ME, Niederkorn JY, Steven P, Stover CM. 2013. Development, alteration and real time dynamics of conjunctiva-associated lymphoid tissue. PloS One 8:e82355.

Steven P, Rupp J, Hüttmann G, Koop N, Lensing C, Laqua H, Gebert A. 2008. Experimental induction and three-dimensional two-photon imaging of conjunctiva-associated lymphoid tissue. Investigative Opthalmology & Visual Science 49:1512–1517.

Steven P, Gebert A. 2009. Conjunctiva-associated lymphoid tissue – current knowledge, animal models and experimental prospects. Ophthalmic Research 42:2–8.

Van Ginkel FW, Gulley SL, Lammers A, Hoerr FJ, R Gurjar R, Toro H. 2012. Conjunctiva-associated lymphoid tissue in avian mucosal immunity. Dev Comp Immunol 36:289–297.

COMPARATIVE HISTOLOGICAL AND ULTRASTRUCTURAL STUDY OF THE EYELIDS AND CONJUNCTIVA-ASSOCIATED LYMPHOID TISSUE (CALT) IN SELECTED WILD BIRDS

Klećkowska-Nawrot J[1], Olszewska K[2], Podzielny O[2], Marycz K[3], Nawara T[3], Paszta W[4], Zagórski K[4], Łupicki D[5].

[1]Department of Animal Physiology and Biostructure, Faculty of Veterinary Medicine, Wroclaw University of Environmental and Life Sciences, Kozuchowska 1/3, 51-631 Wroclaw, Poland; [2]Students of 1rd year of the Faculty of Veterinary Medicine, Wroclaw University of Environmental and Life Sciences, Poland; [3]Electron Microscopy Laboratory, Faculty of Biology, University of Environmental and Life Sciences Wroclaw, Kozuchowska 5b, 50-631 Wroclaw, Poland; [4]Zoological Garden in Wroclaw, Wróblewskiego 1-5, 51-618 Wroclaw, Poland; [5]Museum of Natural History of the Faculty of Biology and Animal Science, Wroclaw University of Environmental and Life Sciences, Kozuchowska 1/3, 51-631 Wroclaw, Poland.

INTRODUCTION

The upper and lower eyelids are dermomuscular folds that surround the palpebral fissure. In birds, both eyelids protect the eye from injury and control the amount of light entering the eye through opening and closing of the palpebral fissure (Klećkowska-Nawrot et al., 2016a; Nickel et al., 2004). The eyelids in birds consist of the three layers: the skin covered with delicate feathers or unfeathered, a middle musculofibrous layer containing the m. levator palpebrae dorsalis and m. depressor palpebrae ventralis,vsebaceous glands (Zeis glands), ciliary sweat glands (Moll's gland) as well as a mucous membrane, known as the palpebral conjunctiva with goblet cells (NAA, 1993; Nickel et al., 2004; Jochems and Philips, 2015). In mammals and birds, the ocular surface is protected from different bacterial, viral and toxic agents (which cause conjunctivitis), allergic factors and the dry-eye syndrome by lymphoid tissue which forms the conjunctiva-associated lymphoid tissue (CALT) (Siebelmann et al., 2013). The CALT contains antigen-specific immunoglobulin A (IgA)-secreting plasma cells and cytokine-producing T and B-cells, which are very important in maintaining ocular immunity (van Ginkel et al., 2012; Klećkowska-Nawrot et al., 2016b).

MATERIAL AND METHODS

The study was conducted on four species of ornamental and wild birds (greater flamingo Phoenicopterus roseus, African penguin Spheniscus demersus, tawny owl Strix aluco and golden-breasted Starling Lamprotornis regius) belonging to four supraorders (Procellariimorphae, Phoenicopterimorphae, Strigimorphae, Passerimorphae). All of the material was obtained from the Wroclaw Zoological Garden (Poland) and Museum of Natural History of the Faculty of Biology and Animal Science, Wroclaw University of Environmental and Life Sciences (Poland). The permission of the District Veterinary Office for carrying out the study on the post-mortem samples was obtained (Wrocław, Poland; No. PIW Wroc. UT-45/5/16, PIW Wroc UT- 45/6/16, PIW Wroc. UT-45/8/16). The birds were not killed for the purpose of this study and died under natural circumstances. A histologic examination with hematoxylin and eosin, Masson-Goldner trichrome and picro-Mallory trichrome staining was carrying out scanning electron microscopy was performed.

RESULTS

Phoenicopterus roseus. A keratinised startified squamous epithelium with five to six layers of nucleated cells was present on the skin surface of the upper and lower eyelids. The marginal zone of the conjunctival surface was covered by a stratified columnar epithelium containing seven to nine layers of cells. Up to three to five non-keratinized layers of the orbital zone were covered with numerous goblet cells. The connective stroma of the eyelids contained fibrocytes, a dense network of collagen fibers, single lymphocytes, bundles of muscles, blood vessels and HEV. The connective stroma contained numerous clusters of melanocytes located in the marginal zone. Short eyelashes with numerous sweat and sebaceous glands were located on the anterior palpebral margin of the eyelids. No tarsal plate was found. In the upper and lower eyelids, lymphocytes were present in the form of numerous small lymphoid follicles located in the connective tissue in the in orbital zone. Spheniscus demersus. The skin surface of the upper and lower eyelids was covered by a keratinised squamous epithelium containing six to seven layers of nucleated cells in both eyelids. The marginal zone of the conjunctival surface was lined by a stratified columnar epithelium with seven to nine layers of cells. Up to 3-5 non-keratinized layers of the orbital zone were covered with numerous goblet cells. Within the connective tissue, numerous sebaceous glands and single sweat glands were located at the root of the eyelashes. There were numerous melanocytes between the glandular epithelium in the sebaceous glands. In the lower eyelid, the stromal connective tissue comprised of densely packed collagen fibers, fibrocytes, blood vessels, single HEV and numerous lymphoid follicles. Numerous diffuse lymphocytes were found in the stromal connective tissue of the upper eyelid. There was an adipose pad in the connective stroma of both eyelids. There was no tarsal plate in the lower eyelid.Strix aluco. A keratinised stratified squamous epithelium with two to four layers of nucleated cells was present on the skin surface of the upper and lower eyelids. In both eyelids, the marginal zone of the conjunctival surface was covered by a stratified columnar epithelium with 8-9 layers of cells. The orbital zone was covered with 3-4 non-keratinized rows of cells and had numerous goblet cells. A dense network of collagen and elastic fibers with fibrocytes, bundles of the m. levator palpebrae dorsalis and m. depressor palpebrae ventralis fibers, and numerous clusters of melanocytes were present within the connective tissue of both eyelids. There were few sweat glands near the eyelash bulbs. Many blood vessels and single HEV were observed in the conjunctival stroma of the lower eyelid. In the upper eyelid, a very large adipose pad was present. The tarsal plate was very long and ridged and measured approximately 4-6 mm. It was composed of dense elastic fibers with numerous blood vessels. Few lymphoid follicles were also located in the orbital zone of the conjunctival surface of the lower eyelid.Lamprotornis regius. The skin surface of the eyelids was lined by a keratinised stratified squamous epithelium with 3-4 layers of cells. The marginal zone of the conjunctival surface –of the eyelids was covered by a stratified columnar epithelium with 7-10 layers of nucleated cells. The orbital zone was covered to 2-4 non-keratinized rows with numerous goblet cells. The connective stroma of the eyelids contained a dense network of collagen fibers with fibrocytes and numerous adipocytes, blood vessels and high endothelial venules. Zaobserwowano There were several clusters of melanocytes in the connective tissue of the upper and lower eyelids. Numerous sebaceous glands were located at the base of the eyelash bulbs in both eyelids. The tarsal plate was oval in shape and composed of dense connective tissue containing elastic fibers

and numerous blood vessels. It was 3-4 mm long. Lymphoid follicles located under the conjunctival epithelium and diffuse lymphatic cells located in the connective tissue were present in both eyelids.

DISCUSSION

Our study indicated diverse upper and lower eyelid conformation in the studied bird supraorders. There were various numbers of layers of nucleated cells forming the keratinized stratified squamous epithelium of the skin of both eyelids. According to Jochems and Phillips (2015) the keratinized stratified squamous epithelium contained 2-3 layers of typically nucleated cells in the Barred owl (Strix varia, Strimimorphae). We also observed differences in the anatomy of the eyelid stroma. In the tawny owl (Strigimorphae), the great cormorant (Pelecanimorphae) and the African penguin (Procellarimorphae), a large adipose pad was present. Melanocyte clusters of various size were present in all the birds either exclusively in the marginal zone or in all the zones in both eyelids, as in the Barred owl (Jochems and Phillips, 2015). According to Klećkowska-Nawrot et al. (2016a) there were no melanocytes in in the stroma of upper and lower eyelids of the Bilgorajska goose. In all the studied birds, the tarsal plate, which was oval, was composed of dense connective tissue containing elastic fibers and numerous small blood vessels or single large blood vessels. This is similar to the findings reported by Klećkowska- Nawrot et al. (2016b) in the adult African ostrich, where the tarsal plate was thicker and was also composed of dense connective tissue containing elastic fibers and single large blood vessels. Jochems and Phillips (2015) found a slightly elevated, fibrous, oval tarsal plate in the Barred owl.

REFERENCES

Nickel R, Schummer A, Seiferle E. 2004. Lehrbuch der Anatomie der Haustiere. Band V. Berlin und Hamburg: Verlag Paul Parey.

Nomina Anatomica Avium. 1993. Second edition. Published by the Club. Cambridge Massachusetts.

Jochems B, Phillips TE. 2015. Histological and ultrastructural studies on the conjunctiva of the barred owl (*Strix varia*). PloS One 10:e0142783.

Klećkowska-Nawrot J, Goździewska-Harłajczuk K, Nowaczyk R. 2016a. Morphological study of the upper, lower and third eyelids in the African black ostrich (*Struthio camelus camelus* L., 1758) (Aves:Struthioniformes) during the embryonic and postnatal period. Italian J. Zool. 83: 312-328.

Klećkowska-Nawrot J, Nowaczyk R, Goździewska-Harłajczuk K, Barszcz K, Kowalczyk A, Łukaszewicz E. 2016b. Light and electron microscopic study of the eyelids, conjunctiva-associated lymphoid tissue and lacrimal gland in Bilgorajska Goose (*Anser anser*). Anat. Sci. Int. 91:74-88.

Siebelmann S, Gehlsen U, Hüttmann G, Koop N, Bölke T, Gebert A, Stern ME, Niederkorn JY, Steven P, Stover CM. 2013. Development, alteration and real time dynamics of conjunctiva-associated lymphoid tissue. PloS One. 8:e82355.

Van Ginkel FW, Gulley SL, Lammers A, Hoerr FJ, R Gurjar R, Toro H. 2012. Conjunctiva-associated lymphoid tissue in avian mucosal immunity. Dev. Comp. Immunol. 36:289–297.

RESEARCH POSSIBILITIES USING CONFOCAL MICROSCOPIC TECHNIQUES FOR THE MEASUREMENT OF CELLULAR RESPONSE IN INTRACELLULAR Ca^{2+} ACTIVITY, CELLULAR LOCALIZATION AND DIMERIZATION OF G PROTEIN COUPLED RECEPTORS (GPCR)

Kubale V *, Frangež R, Fazarinc G, Vrecl Fazarinc M

Institute of Preclinical Sciences, Veterinary Faculty, University in Ljubljana

INTRODUCTION

In the Institute of preclinical sciences at Veterinary faculty in Ljubljana inverted Leica multispectral laser scanning confocal microscope (Leica Microsystems, Heidelberg, Germany) is used principally for two various research areas - calcium activity measurements in different individual mammalian cells (e.g. neuroblastoma and rat glioma cell line, A10 cell line – model for vascular smooth muscle cells) and for cellular detection of different receptors of the superfamily of GPCRs (e.g. neurokinin receptor, dopamine receptor, ghrelin receptor), their internalization and dimerization properties and interaction with actin cytoskeleton.

MATERIAL AND METHODS

To follow the cellular response in intracellular Ca^{2+} activity ($[Ca2+]_i$) in individual mammalian cells, cells were exposed to different biologically active compounds. As Ca^{2+} indicator Fluo-4 were used and excited by the use of an argon laser excitation line at 488 nm. Time series (10-30 min, 1 frame/1.67 s) were typically collected using a scanning format of 512×512 pixels. For the time scan, fluorescence intensity analysis of digital images, Leica image software was used. The CellMask orange plasma membrane stain (Invitrogen) excited by laser line at 543 nm has been used to follow time-dependent changes in morphology and cell volume of individual mammalian cells. An oil immersion objective lens (Leica, Planapo × 40 NA = 1.25) was used to obtain cell optical confocal sections. A series of optical sections were collected using a scanning format of 1024 × 1024 pixels. A series of 1 μm optical sections was collected through the entire mammalian cells before (time 0) and at different time intervals after the addition of tested substance. The effects of biologically active compounds were quantified using the Leica digital image software for morphometric analysis. The adverse effects of xenobiotic microcystin-LR on morphology and cytoskeletal elements of blastomeres in different stages of early embryonal development have also been studied using different fluorescent cytoskeletal markers.

To observe biology of different GPCRs we have expressed receptors in transiently- or stably-transfected HEK-293 cells, which were grown on poly-D-lysine-coated glass coverslips. After 48 h, cells were fixed with 4% paraformaldehyde, washed with phosphate-buffered saline (PBS), permeabilized with 0.01% Triton X-100 in PBS, and then incubated in a blocking solution (1% bovine serum albumin (BSA) in PBS to reduce the nonspecific binding. Further on, cells were incubated overnight at 4 °C with case specific dilutions of primary antibodies. If colocalization with intracellular compartments or other type of receptor was to be observed also primary antibodies targeting different species were used against compartment/other protein. After extensive washing, cells were incubated for 60 min at room temperature in the dark with different dilutions of secondary antibodies. After washing, cells were mounted using an anti-fading ProLong®Gold reagent (Molecular Probes, Leiden, The Netherlands), sealed and examined under an oil immersion objective (Planapo 40×, numerical aperture (N.A.) = 1.25) using a Leica TCS NT microscope. Sequential images were collected in an eight-fold frame with an average resolution of 1024 × 1024 pixels. Representative sections corresponding to the middle of the cells are presented using Adobe Photoshop 7.0. The degree of co-localization was quantified using ImageJ (National Institute of Health) and the colocalization plugin image analysis software. Pearson's correlation coefficient for image above

thresholds (Rcoloc) was calculated, which represents pixels where both channels (red and green) were above their respective threshold; its values range between −1.0 and 1.0, where −1, 0, and +1 indicate complete negative correlation, no significant correlation and perfect correlation, respectively. Five to seven individual cells showing co-localization were analysed.

RESULTS

In the part of the research, where effect of the ostreolysin on the intracellular Ca^{2+} activity in neurons and membrane bleb formation and cellular swelling in neurons was observed we were the first to demonstrate the effect of the OlyA/PlyB-induced swelling and plasma membrane blebbing of neuroblastoma NG108-15 cells. Formation of cellular oedema involved the presence of Na^+ and/or Cl^- in the extracellular space and might be connected to an influx of Na^+ and/or a shift in Cl^-, which induced a marked influx of water that was finally responsible for cellular swelling. OlyA/PlyB induced Ca^{2+} influx into the NG108-15 cells. A switch in the NCX mode to mediate Ca^{2+} influx, related with the de novo formation of non-selective ion pores by OlyA/PlyB in plasma membranes of mammalian cells, appeared to play an important role in this effect. The described morphological effects and the underlying cellular mechanisms responsible for these observations are important steps toward understanding the toxic cardiorespiratory effects of the OlyA/PlyB protein complex in vivo.

In the part of the research, where we have studied the conserved arginine cluster in the 29-amino acid insert of the third cytoplasmic loop of the long form of the D2 dopamine receptor (D2L-R), we have described insret as an intracellular retention signal. This insert could act as an ER motif and be a part of the intricate underlying mechanisms responsible for differentially-regulated anterograde trafficking of the D_2-R isoforms and their plasma membrane availability.

In the part, where we have characterized the morphological alterations in HEK-293 cells, transfected with mutants of ghrelin receptor (GHS-R1a), impaired in binding or intracellular signalling, we have demonstrated that α subunits of G proteins $G\alpha_{12}$ and $G\alpha_{13}$ had a role in the rearrangement of the actin cytoskeleton, especially in the formation of stress fibres in GHS-R1a. In highly constitutive mutant of GHS-R1a even more pronounced changes were observed in the cytoskeleton rearrangement, stress fibre formation and the role of $G\alpha_{12}$ and $G\alpha_{13}$ subunits of G-proteins. In the receptor mutated in conserved DRY motif differences in the polymerization of microtubules were observed. Similar phenotype of cell morphology, rearrangement of microtubules and actin cytoskeleton was observed in the cells co-expressing mutants of GHS-R1a with disabled ligand binding function and signal transduction capacity in comparison to WT receptor.

REFERENCES

Vrecl M., Babnik M., Diacci U., Benoit E., Frangež R. (2015). Effect of the ostreolysin A/pleurotolysin B pore-forming complex on neuroblastoma cell morphology and intracellular Ca^2 activity. Toxicological Sciences 144:276-83.

Vrecl M., Babnik M., Sepčić K., Žužek MC., Maček P., Diacci U., Frangež R. (2015). Effect of the ostreolysin A/pleurotolysin B pore-forming complex on intracellular Ca^{2+} activity in the vascular smooth muscle cell line A10.Toxicolgy In Vitro 29:2015-21.

Kubale V., Blagotinšek K., Nøhr J., Eidne KA., Vrecl M. (2016). The Conserved Arginine Cluster in the Insert of the Third Cytoplasmic Loop of the Long Form of the D_2 Dopamine Receptor (D2L-R) Acts as an Intracellular Retention Signal. International Journal of Molecular Sciences 17. pii: E1152.

Frangez R., Žužek MC., Mrkun J., Šuput D., Sedmak B., Kosec M. 2003. Microcystin-LR affects cytoskeleton and morphology of rabbit primary whole embryo cultured cells in vitro. Toxicon 41:999-1005.

Immunohistochemical analysis of TNF α and TGF β1 expression in healing wounds covered by chemically modified cellulose.

Jiří Lenz[1-3], Gabriela Kuzmínová[4], František Tichý[1], Alžběta Kružicová[4]

1 Department of Anatomy, Histology, and Embryology, Fakulty of Veterinary Medicine, University of Veterinary and Pharmaceutical Sciences, Brno, Czech Republic
2 Department of Pathology, Znojmo Hospital, Czech Republic
3 Cytohisto s.r.o., Breclav, Czech Republic 4 Department of Human Pharmacology and Toxikology, Faculty of Pharmacy, University of Veterinary and Pharmaceutical Sciences,

INTRODUCTION

Wound healing is a complex and dynamic process that occurs in several consequential and intermingling steps. The priority in wound care nowadays is mainly diminishing traumatisation of the patient, influence of the external and internal risk factors on the wound healing and also the length of the treatment. Therefore it is important to choose an appropriate therapeutic medium which means applying modern bandaging and covering materials such as moist therapy. The aim of this study was to evaluate wound healing process and investigate the immunohistochemical expression of cytokines TNF α and TBF β1 using different types of cellulose material.

MATERIAL AND METHODS

We used seven different types of cellulose material: Hcel® nat - NAT, Hcel® caht - CAHT, Hcel® htb – HTB, Aquacel® - AQCl, Traumacel biodress comfort – TBC, Hcel® ht- HHT, Aquacel® with 1,2 % Ag – AAG. Gauze as a secondary wound covering was used for the control group. We worked with 120 rats of the Wistar tride which we divided into eigth groups with 15 animals in each of them. The covering material was applied on the suprascapular area of the experimental animal wound. We evaluated the wound condition and process of healing macroscopically, histopathologically and immuhistochemically in 2, 7 and 14-days interval.

RESULTS

Histopathological examination showed highest effect on re-epithelization and lowest rate of granulomatous inflammation while using HHT material. Conversely, materials HTB, NAT and AQCl showed low effect on re-epithelization and higher rate of granulomatous inflammation. Using immunohistochemistry, weak to moderate immunopozitivity for TNFα after 2 days, strong immunopozitivity after 7 days and weak to moderate immunopozitivity after 14 days for NAT, CAHT, HTB, TBC, HHT and AAG materials were showed. Higher level of TNF α expression after 14 days as a result of granulomatous inflammation while using AQCl material was found. Weak immunopozitivty

for TGF β1 expression for all materials after 2,7 and 14 days was showed. The only exception was AQCL material with higher levels of expression after 2 and 7 days.

CONCLUSION

Histopathological examination revealed the HHT material as the best covering while the worst results for HTB, NAT, AQCL materials were found. Immunohistochemmical expression of cytokines TNF α and TGF β1 in the wound is affected by several factors: amount of leukocytes, presence of granulatious tissue and granulomatous inflammation. The overall higher level of TNF α expression compared with TGF β1 indicates a more significant role of TNF α in the wound healing process.

THE ROLE OF HYPOXIA IN EPIDERMAL CLAW KERATINOCYTES

Luebbe K[1*], Wielsch B[2], Bosse I[2], Bahramsoltani M[1] and Muelling CKW[3]

[1]*Institute of Veterinary Anatomy, Department of Veterinary Medicine, Freie Universität Berlin, Berlin, Germany*

[2]*Department of Cell Therapy, Fraunhofer Institute for Cell Therapy and Immunology IZI, Leipzig, Germany*

[3]*Institute of Veterinary Anatomy, Histology and Embryology, Faculty of Veterinary Medicine, University of Leipzig, Leipzig, Germany*

INTRODUCTION

The question of epidermal oxygen concentration is of controversial nature. With increasing distance to dermal microvasculature, hypoxic conditions are predominating in the epidermis and are discussed to range from 0,5% and 10% oxygen. Therefore, in vitro cultivation of keratinocytes should be performed under slight hypoxic conditions, which may reduce oxidative damage and improve keratinocytes' growth. However, epidermal cells are often exposed to normoxic culture conditions with atmospheric oxygen concentrations of 21%. This may cause oxidative stress and DNA damage in keratinocytes. Until now, there is a lack of knowledge of specific oxygen concentrations in the epidermis. Therefore, it is difficult to provide recommendation for optimal oxygen concentration for in vitro cultured keratinocytes. Therefore, the objective of the present study was the analysis of cell viability of keratinocytes after exposure to different hypoxic concentrations compared to atmospheric culture conditions.

MATERIALS AND METHODS

Keratinocytes were isolated from bovine claws and exposed to atmospheric as well as hypoxic conditions with 1% and 5% oxygen. Subsequently, keratinocytes' viability was measured by using LDH (lactate dehydrogenase) and MTT (3-(4,5-dimethylthiazol-2-yl)-2,5-diphenyltetrazolium bromide) cell viability assays. In a second step, differentiation patterns of the keratinocytes after exposure to hypoxia with 1% oxygen were detected by western blot analysis using the differentiation markers involucrin and loricrin.

RESULTS

The results show no significant differences of cell viability between exposure to 5% oxygen and atmospheric culture conditions. A decrease of cell viability with high cytotoxicity was only measured after exposure to 1% oxygen for two weeks. This effect was accompanied by slight changes in keratinocytes' morphology. Furthermore, keratinocytes showed an increased expression pattern of involucrin and loricrin after exposure to hypoxia with 1% oxygen.

DISCUSSION

As the results show, the viability of keratinocytes was only slightly affected by the different oxygen concentrations. This might be based on keratinocytes' ability to adapt their glucose metabolism and cell function to different environmental conditions alike the hypoxic milieu in the epidermis. One example is the upregulation of LDH to force the anaerobic glycolysis in keratinocytes, which could also be observed within this study. However, results also show that only hypoxic conditions lead to an appropriate differentiation of keratinocytes.

A GUINEA PIG IN VITRO SKIN MODEL FOR INFECTION STUDIES WITH DERMATOPHYTES

Baumbach CM[1,2], Schrödl W[2], Michler JK*[1]

[1]*Institute of Veterinary Anatomy, Histology and Embryology, Leipzig University, Leipzig, Germany*
[2]*Institute of Bacteriology and Mycology, Leipzig University, Leipzig, Germany*

INTRODUCTION

The dermatophyte Trichophyton (T.) benhamiae represents an emerging pathogen with a high risk for long lasting dermatophytosis especially in children and young people. Guinea pigs as pets are a source of infection with this zoonotic disease. The named dermatophyte is known to express different virulence factors growing on agar plates in vitro versus in vivo on experimentally or naturally infected guinea pigs. Studying the course of infection in animal trials requires high numbers of guinea pigs. Therefore, the aim of the study was to develop an in vitro model using guinea pig skin explants that can be infected under standardized conditions allowing for multiple approaches with less animals sacrificed. We hypothesized that the guinea pig skin explants may shed light on the different growing and infection behaviors of the dermatophyte in vitro (agar plates) versus in vivo (animal experiments).

MATERIALS AND METHODS

Guinea pig skin was harvested from 12 cadavers of adult animals (>400g) of either sex with an age range between one month and one and a half years. Animals were sacrificed for two research projects not related to this study (ethical approval No. 04/16 and 48/16). The flank area was clipped, disinfected using 70% ethanol and a skin patch of 4x3cm^2 was excised. Small pieces of skin were prepared under a stereo microscope and transferred to ThinCerts® (Greiner BioOne, Frickenhausen, Germany) in a 12-well cell culture plate. The skin was incubated at a 5%CO_2 atmosphere and at 37°C versus 30°C for up to 14 days. A basic medium consisting of DMEM and Ham´s F12 supplemented with growth factors (EGF and bFGF) was either enriched with allogeneic guinea pig serum (GPS) or fetal calf serum (FCS) to determine the optimal nourishing procedure. Skin samples were harvested at day 0, 4, 7, 10 and 14 for evaluation of the explants. The structure and the integrity of the skin explants were investigated histologically and immunohistochemically. Therefore, standard hematoxylin-eosin staining and immunohistochemistry with an anti-Ki67 antibody (Dako, Hamburg, Germany) were performed.

RESULTS

11 of the 12 cultivations could be conducted without fungal or bacterial contamination. In one culture, a contamination with coccoid motile bacteria was observed in the culture medium and therefore discarded. The absence of naturally occurring epidermal scaling led to a thickened stratum corneum in the course of culture. These microscopically visible parakeratotic alterations were mainly observed up to day 4. In some areas, this was accompanied by hypogranulosis and pyknotic nuclei. In other regions, hyperplasia and signs of akantholysis above the stratum basale could be observed. Apart from these findings, the morphology did not change further until day 14. In addition to that, anti-Ki67 antibody staining revealed viable basal keratinocytes.No differences were found in cultivations at 30°C or 37°C as well as with different serum types.

DISCUSSION

First results of this ongoing study indicate that the guinea pig skin explant approach is a suitable way to enable the investigation of dermatophyte infections. The established culture conditions are crucial for the following infection studies. Firstly, immunohistochemistry provided evidence that the epithelium of the cultured skin explants maintained its abilities to divide and differentiate in vitro. Secondly, optimal growth conditions such as culture temperature for T. benhamiae (30°C) are met. The data presented here offer promising basics for our further experiments concerning the pathomechanisms of T. benhamiae during adherence to and invasion of guinea pig skin.

COMPARATIVE ANATOMY E-BOOK WITH EMBEDDED QUIZZES: AN ACTIVE LEARNING STRATEGY

Noble P[1] , Domett K[2]

[1] College of Public health, Biomedical and Veterinary Sciences, James Cook University, Townsville, Queensland, Australia.
[2] College of Medicine and Dentistry, James Cook University, Townsville, Queensland, Australia.

INTRODUCTION

The subject "Anatomy: structure and movement" is a first year anatomy course compulsory for Biomedical Science students and elective for Bachelor of Science students. This subject includes modules on both human and comparative vertebrate musculoskeletal systems (MSS). Whereas there is an excellent textbook for human MSS we have not found an adequate textbook that targets the key learning outcomes for the comparative vertebrate MSS module. We believe that this is one of the primary reasons that students struggle with this module, much more so than the human module, as borne out in the assessment data. Our aim was to create a targeted learning resource for the students and to encourage more independent and active learning through this resource.

MATERIALS AND METHODS

A blended learning tool (comparative vertebrate MSS ebook) was developed using ibook author (Apple). The text has been written according to specific learning outcomes for the comparative vertebrate MSS module and peer reviewed by experienced anatomists. The movies and pictures were edited using Camtasia (Techsmith) and fireworks (Adobe) and were inserted in the ebook. Finally some interactive MCQs have been added at the end of each chapter of the ebook. In order to investigate the effect of the ebook on the student learning, the assessment data from two cohorts with a similar overall position score (tertiary entrance rank used in Queensland for selection into universities) respectively without ebook (Y1, n=93) and with ebook (Y2, n=73) was compared using a Mann-Whitney test ($p<0.05$).

RESULTS

This new teaching resource clearly aligns with the learning outcomes and includes some self-assessment tools. The cohorts Y1 and Y2 that have been selected for the study with a respective OP score mean of 9.54 (+-6.53) and 7.55 (+-4.3) were found to be not significantly different (p-value = 0.15). According to the assessment data for the comparative MSS module, the Y1 and Y2 quiz mean was 63.95% ±24.23 and 63.44% ±15.21; practical mean was 65.83% ±27.84 and 75.84% ±18.18; final exam mean was 59.89% ±26.83 and 67.60% ±16.93, respectively. Whereas the introduction of the ebook did not significantly change the marks along the assessments between Y1 and Y2, it may have improved the assessment outcomes in reducing the subject failure rate from 22% to 10%. Finally, according to the subject feedback report, the introduction of the ebook may have improved the motivation and engagement of students in the vertebrate module of this subject (Overall Subject satisfaction scores were 4.6 in Y1 and 4.8 in Y2 out of a maximum of 5).

DISCUSSION

The production of the comparative vertebrate MSS ebook with embedded quizzes has provided students with another type of learning resource, addressing the issue of variability in learning styles and promoting a more active learning. As the assessment outcomes have improved after the introduction of this interactive teaching resource, its concept should be generalised in the future to cover all of the comparative anatomy course.

MACRO – AND MIKROSCOPIC STUDY OF THE TONGUE AND LINGUAL PAPILLAE IN BISON BONASUS HYBRID; PRELIMINARY STUDIES

Plewa B[1*], Skieresz – Szewczyk K[1,] Jackowiak H[1]

[1]Department of Histology and Embryology, Poznań University of Life Sciences, Poznań, Poland

INTRODUCTION

The characteristic anatomical features and arrangement of lingual papillae on the tongue in ruminants particularly is connected with the kind of food. In ruminants develops a number of structural adaptations which help in consumption of plant food. One of the most characteristic for ruminants, is lingual prominence responsible for trimming, chewing and transport of food to the esophagus (1,2,4). Bison bonasus hybrid is a interspecific animal between cow (Bos taurus) and the bull of bison (Bison bonasus). The first breeding was created by Leopold Walicki in Poland in order to create an animal resistant like a bison and meat efficient like a cow. Nowadays the biggest breeding is in Białowieża National Park (3).The aim of the study is to compare the morphology of the tongue in Bison bonasus hybrid with features in the parental speciesas well to indicate the species-specific features in examined breed as to define the degree of heredity of the anatomical features in the Bison bonasus hybrid.

MATERIALS AND METHODSThe observations were conducted on a tongue of 3 years old female of the Bison bonasus hybrid . The tongue was fixed in 10% neutral formalin. The tissue samples collected from the dorsal and ventral surface of the apex,, the body, the prominence and root were perform for observations the light microscopy (LM) and scanning electron microscopy (SEM). The tissue samples for the light microscope were dehydrated in a series of increasing concentrations of ethanol (70-96%). The 4,5-5 µm paraplast sections were stained Masson-Goldner trichrom staining technique (Romeis, 1989). Observations of the slides were performed using an Axioscope 2 plus (Zeiss)Tissue samples for the SEM were dehydrated in a series of ethanol (70-99,8%), the mixture of 96% ethanol and 100% acetone and 100% acetone. The tongues were then dried at critical point using CO_2 (CPDK850, EMITECH). All samples were mounted on aluminum stubs covered with carbon tabs, sputtered with gold (Sputter Coater S 150B) and examined under a SEM ZEISS435 VP. Multiscan computer morphometric system (CSS, Warsaw, Poland) was used for morphometry.

RESULTS

The elongated tongue of Bison bonasus hybrid 44,1 cm in length is divided into four parts:apex, body, lingual prominence and root of the tongue. ON the dorsal surface of the the apex and body of tongue the median sulcus observed. On the dorsal and ventral surface of the anterior part of tongue are observed two types of lingual papillae: the mechanical filiform papillae and gustatory fungiform papillaFiliform papillae have one large main processes and 2 or 3 smaller lateral processes. Filiform papillae are directed caudally. Lm observations of the processes reveal elongated connective tissue cores covered with strongly keratinized stratified squamous epithelium .

Rounded fungiform papillae surrounded by furrow are distributed on the tip of lingual apex, ventral surface of the tongue, on the lingual body, whereas on the dorsal surface of apex and lingual prominence fungiform papillae are flattened. Histological observations showed weak keratinisation of the stratified squamous epithelium covering the connective tissue core of the fungiform papillae. On the ventral surface of the tongue the filiform and fungiform papillae are arrange in the shape of V letter separating the surface covered with papillae from the smooth surface.

On the lingual prominence four types of lingual papillae are present. The conical papillae are observed on the anterior and medial part of the lingual prominence. The filiform papillae are present on the lateral and caudal part of the lingual prominence. The fungiform papillae are observed on the medial, caudal and lateral parts. The vallate papillae occur on the caudolateral part of the lingual

prominence. The conical papillae with width base and narrowed, blunt tip posses. On the top of prominence, these papillae are arranged towards lingua fossa, laterally or slantwise towards dorsal surface of the tongue and create a form of rosette, whereas on the median part of th prominence are directed laterally. The conical papillae revealed a stratified squamous epithelium with thick horny layer.

The filiform papillae posses only one main process covered with hard horny layer of epithelium. The structure of fungiform papillae on the caudal part of prominence is similar as on anterior part of the tongue. Vallate papillae are arranged in two rows, but only external row extend to the lingual root. A single vallate papillae is created often from a one or few connected bodies of the papillae surrounded by ridge. Histological observations confirm that Each papillary body has own connective tissue core. Macro- and microscopic observations of The surface of the root of the tongue is flat with slightly rows in mucosa.

DISSCUSION

Referring to earlier published articles, results of this study proved that Bison bonasus hybrid inherits some structural features after parental species and at the same time creates own features. Our studies confirm presence of the differences in morphology of the tongue and distribution and microstructure of lingual papillae.

The specific trait for Bison bonasus hybrid is the presence of median furrow on the body of tongue and arrangement of lingual papillae in letter V shape on ventral surface of tongue. The filiform papillae with lateral processes occur in Bison bonasus hybrid and and in the cattle, but are not present in bison. Additionally the smaller lateral processes in the Bison bonasus hybrid are presented on the filiform papillae on the lingual apex, lingual body and ventral surface of the tongue. In turn in the cattle the smaller lateral processes of the filiform papillae are only on the apex of the tongue. Moreover, conical papillae at the lingual prominence in the cattle are wide and reduced, while in the Bison bonasus hybrid are directed in different sides creating a form of rosette. On the surface of the median part of lingual prominence in Bison and cattle are many short reduced conical papillae and Bison bonasus hybrid the surface of mucosa is rather smooth.

The arrangement and appearance of vallate papillae of Bison bonasus hybrid. is species- specific characteristic. The distribution of such papillae in two rows is the same as in the cattle. Locally, was observed that one ridge of the papillae surrounding bodies of two neighboring vallate papillae, what is similar feature to the bison. In parental species vallate papillae are rather separated, while in Bison bonasus hybrid are close each other. The number of vallate papillae is different in every species and vary on right and left side of the prominence i.e. in Bison bonasus hybrid is about 17-18, in bison 15-20 and in the cattle 7-10.

The absence of lingual papillae on the root of tongue could be a features inherited after bison, because this part of the tongue of the cattle posses small, reduced conical papillae.

REFFERENCES

1. Emura S., Okumura T., Chen H. (2011). Morphology of the lingual papillae in the roan antelope. Okjimas Folia Anat. Jpn. 88, 127 – 131.
2. Jackowiak H., Skubis J., Łakomy P., Nasiadka P., Godynicki Sz. (2017). Anatomy of the tongue and microstructure of the lingual papillae in the fallow deer (Dama dama, Linnaeus, 1758). Mamm. Biology, 85: 14-23.
3. Krasińska M. (1988). Hybrydy żubra i bydła domowego. Wydawnictwo Polskiej Akademii Nauk, Wrocław
4. Nickel R., Schummer A., Seiferle E. (1973). The Viscera of the Domestic Mammals. Verlag Paul Parey, Berlin, Hamburg

ROLE OF PLANAR CELL POLARITY PATHWAY IN AMELOBLASTOMA WITH FOCUS ON FRIZZLED 6

Barbora Putnová[1,2], Iveta Putnová[1,3], Eva Hrubá[1], Hana Dosedělová[1], Jan Štembírek[1,4], Zdeněk Daněk[5], Marcela Buchtová[1,6]

[1] Laboratory of Molecular Morphogenesis, Institute of Animal Physiology and Genetics, Academy of Sciences, Brno, Czech Republic
[2] Department of Pathological Morphology and Parasitology, University of Veterinary and Pharmaceutical Sciences, Brno, Czech Republic
[3] Department of Anatomy, Histology and Embryology, University of Veterinary and Pharmaceutical Sciences, Brno, Czech Republic
[4] Department of Maxillofacial Surgery, University Hospital Ostrava, Ostrava, Czech Republic
[5] Clinic of Oral and Maxillofacial Surgery of Faculty Hospital, Masaryk University, Brno, Czech Republic
[6] Department of Animal Physiology and Immunology, Institute of Experimental Biology, Masaryk University, Brno, Czech Republic

INTRODUCTION

Ameloblastoma is the most common epithelial odontogenic tumour in the oral cavity. Its progression is usually slow and the surface is covered by an oral mucosa with physiologic appearance. These tumors do not cause any pain to the patient and therefore it is difficult to diagnose them on time and the first signs are often missed by clinician leading to late diagnosis.
The majority of ameloblastomas are benign in their biological behaviour, but they can be very locally invasive and recidivism after a surgery is very usual phenomena. Ameloblastoma grows into the surrounding tissues and they form very complex interlacing structures. However, what regulates this kind of aggressive behaviour reminds unknown. We focused on the expression pattern and possible role of Planar Cell Polarity Pathway (PCP) in pathogenesis of thise neoplasm. One of the very important molecules in this cell signalling pathway is receptor Frizzled 6 (FZD6), which we selected for further immunohistochemical analysis with the aim to evaluate its expression in tissues as well as on subcellular levels. Moreover, we used cytokeratin as a marker of epithelial cells, SOX2 as a marker of progenitor cells and PCNA to evaluate proliferating cell distribution.
We also compared an expression pattern of these molecules in ameloblastoma with their distribution in a radicular and follicular cysts, which represent common pseudo tumorous lesions of odontogenic origin.

MATERIAL AND METHODS

Tissue samples were obtained from the Clinic of Oral and Maxillofacial Surgery of Faculty Hospital in Ostrava and from the Clinic of Oral and Maxillofacial Surgery of Faculty Hospital in Brno. Tissues were processed by standard histological techniques and stained by Haematoxylin and Eosin. Alternative sections were used for an immunohistochemical analysis of FZD6, cytokeratin, PCNA and SOX2 expression. Following primary antibodies were used for the detection: FZD6 antibody (Frizzled Family Receptor 6 (FZD6); Antibodies-online.com; 1:200 dilution), cytokeratin antibody (ab961; Abcam; 1:1 dilution), SOX2 antibody (2748; Cell Signalling Technology; 1:50 dilution) and PCNA (PCNA Staining kit, Invitrogen, USA). Alexa-fluor secondary antibody (Thermo Fisher Scientific; 1:200 dilution) was used to visualize positive cells and ProLong® Gold Antifade Mountant with DAPI (Thermo Fisher Scientific, USA) to counterstain nuclei. The fluorescent microscope Leica DMLB2 (Leica Microsystems, Germany) was used for a photodocumentation and these pictures were merged together in Adobe Photoshop (CC 2017, Adobe, USA).

RESULTS

The morphological appearance of ameloblastoma is very complex, so to define the presence of particular molecules in distinguished areas was not always easy. The expression of cytokeratin was weaker on the edges of the tumorous islets of ameloblastoma. The palisade-like arranged cells

surrounding the basal lamina were only weakly positive. At the same time, we found a stronger FZD6 signal in the middle of tumorous islets of ameloblastoma, usually corresponding with a stronger signal of cytokeratin. Only occasionally, FZD6-positive cells were located in the basal layers of finger projections.
SOX2-positive cells were found around the basal layer of ameloblastoma epithelium. Interestingly, they were also spread randomly in the tumorous tissue forming nest-like structures. PCNA positive cells were present in the surrounding mesenchymal tissue, but also spread in the tumorous epithelial part.
We observed different expression patterns in odontogenic cyst. The epithelium lining of cysts was strongly positive on cytokeratin. Expression of FZD6 was also present in odontogenic cyst, however in comparison to the ameloblastoma, it was spread randomly and FZD6-positive cells were located around the basal lamina. However, cellular arrangement of the FZD6 expression in odontogenic cysts was comparable to the ameloblastoma cells. Presence of PCNA and SOX2 positive cells was observed evenly spread in the lining epithelium.

DISCUSSION

Ameloblastoma grows invasively to form the intertwining epithelial structures. This tumour does not grow infiltratively, but can be very invasive because of its ingrowing pattern. This can lead to complications like is often reoccurrence after the surgical removal. The mechanism of this type of aggressive behaviour remains unknown. Probably this very complex growing pattern arises from the dysregulation of cell signalling pathways. We selected FZD6 as a receptor of PCP pathway that plays an important role in the establishment of planar cell polarity. Moreover, it participates on multiple cellular processes during ontogenesis and postnatal growth. Even though the pathogenesis of odontogenic tumours is still not well understood, it was proposed that arise from the residual cells of the dental lamina. Our recent study revealed that FZD6 has a distinct expression pattern in the dental lamina (Putnova et al., 2017). High expression of FZD6 in tumorous tissue together with similar cellular location of protein in protruding cells such we observed during degradation of dental lamina indicate common molecular signalling driving this process.
Furthermore, we detected cytokeratins in tumorous tissues. Cytokeratins are proteins of intermediate filaments found in the intracytoplasmic cytoskeleton of epithelial cells. The level of expression of this epithelial marker could be modified according to differentiation status of cells with upregulation during keratinization or can be downregulated during an epithelial-mesenchymal transition (EMT) observed in malignant neoplasms. In agreement, we found weaker expression of this marker on the edges of the epithelial structures of ameloblastoma.
The analysis of possible co-localization of FZD6 and cytokeratin revealed that the expression of FZD6 is located in the already differentiated cells of ameloblastoma. However, this can be caused also by another facts such as for example cellular hypoxia (Cantilena et al., 2011). As a receptor participating on the cell polarity establishment, we expected FZD6 to be located asymmetrically in migrating cells what we did not confirmed. Furthermore, the expression site of progenitor markers and proliferating cells were different than FZD6-positive areas. Based on our results, we propose, that the ameloblastoma islet grows from the central area and spread aside pushing its own cells into the surrounding tissue and these results will be necessary to follow in future by functional experiments.
Comparison of pseudotumorous lesion like are odontogenic cysts with a tumour is certainly challenging task just because of the different growing pattern of these two lesions. For the further studies comparing pathogenesis of these lesions it will be necessary to apply also different approaches using molecular biology to identify more precisely the expression of our selected markers.
Based on our recent study, we cannot suggest FZD6 as a reliable prognostic marker in case of odontogenic tumours. Nevertheless, PCP pathway acts an important role in the ameloblastoma growth as FZD6 is strongly expressed in the deregulated growth of ameloblastoma. Simultaneously, deregulation of FZD6 function also play a role in epithelial cells of pseudotumorous lesions of odontogenic character.

GRANT
This research was supported by the Czech Science Foundation (14-37368G) and by the Ministry of Education, Youth and Sports of the Czech Republic from the Operational Programme Research, Development and Education (CZ.02.1.01/0.0/0.0/15_003/0000460).

REFFERENCES

Cantilena, S., Pastorino, F., Pezzolo, A., Chayka, O., Pistoia, V., Ponzoni, M., & Sala, A. (2011). Frizzled receptor 6 marks rare, highly tumourigenic stem-like cells in mouse and human neuroblastomas. *Oncotarget, 2*(12), 976-983. doi: 10.18632/oncotarget.410

Putnova, I., Dosedelova, H., Bryja, V., Landova, M., Buchtova, M., & Stembirek, J. (2017). Angled Growth of the Dental Lamina Is Accompanied by Asymmetrical Expression of the WNT Pathway Receptor Frizzled 6. *Front Physiol, 8*, 29. doi: 10.3389/fphys.2017.00029

"CAT HOUSE" FROM ORLI STREET – AN UNUSUAL OSTEOARCHEOLOGICAL FINDING

Pyszko M[1]*, Loskotova I[2], Paral V[1], Pyszkova L[1], Goetzova T[1], Frgelecova L[3], Stehlik L[4]

[1] Department of Anatomy, Histology and Embryology, Faculty of Veterinary Medicine, University of Veterinary and Pharmaceutical Sciences, Palackeho 1, 612 42, Brno, Czech Republic (address for correspondence)

[2] Department of Archaeology and Museology, Faculty of Arts, Masaryk University, Brno, Czech Republic

[3] Department of Pathological Morphology and Parasitology, Faculty of Veterinary Medicine, University of Veterinary and Pharmaceutical Sciences, Brno, Czech Republic

[4] Department of Diagnostic Imaging, Faculty of Veterinary Medicine, University of Veterinary and Pharmaceutical Sciences, Brno, Czech Republic

INTRODUCTION

The skeletal remains of animals found during archaeological surveys of medieval areas are an irreplaceable source of knowledge. They inform us not only about the meaty diet of human in the past but also about the cultural, social and health conditions at one historical era. As a common finding we can mention bones of large and small ruminants, the pig and the fowl. These species which have been a part of human diet since time immemorial. On the other hand, our study revealed many interesting issues and differences from the information described in specialized publications.

MATERIALS AND METHODS

The total number of bones or their fragments was 979 and 925 were identified thereof. The composition of species was highly varied. It included nine mammals and three bird species. Namely, it was the cattle, the horse, the pig, the sheep, the goat, the dog, the cat, the rabbit, the rat, the fowl, the goose and the pigeon. The material was cleaned, classified and identified by species and type. In order to determine the bones and their fragments we used comparative collections of skeletons of each animal species inhabiting Central Europe. The bones that showed signs of pathology were further subjected to a pathomorphological analysis, also X-ray images were made and samples were taken for future tests.

RESULTS

Compared to a "common" finding typical for the urban environment of medieval Europe, there was high proportion of fowl bones (36.6%) and low proportion of bovine bones (21.1%) confirmed in the studied sample.

The large number of domestic cat bones (12.7%), coming from at least five individuals, was a very unusual finding itself. Most of them died at the same age (estimated according to the bones sizes and conditions of epiphyseal plates) which indicates a serious infectious disease or euthanasia.

Among others, there were also bones from at least three different dogs (3.8%) at the archaeological site. One of them measured only 26-28 cm at the withers (less than an adult cat) according to the osteometric analysis. A dog of that size was not commonly bred in the Czech lands during the Middle

Ages and it must have been very rare. The individual was definitely adult and without evident signs of nanism or dyschondroplasia.

In the sample of bovine and pig bones the juvenile stages dominated. At least two piglets with a

height of 25 and 30 cm at the withers and a calf under 1 month of age were found. On the other hand, there were also fragments of the skull and the long bones of an old bull's limbs. Most probably, it did not serve human diet, rather it was used as a basis of a quality stock for dogs and cats.

Two bones (ulna and tibiotarsus) of the domestic pigeon with obvious signs of bone form of avian tuberculosis represent another remarkable finding. Most probably, this individual was not able to fly and even walking may have been difficult for it.

The results of the skeletal material analysis from the archaeological area in Orlí street 19–21 indicate that some wealthy animal lovers lived here. Although it was a "shanty town" at the city walls, where the poorer social class used to live, they were able to "keep up" several cats and dogs and consume a diet typical rather for the "higher class".

"WATER COW" AND "RIVER HORSE" – ANATOMICALLY INCORRECT NAMES OF PYGMY HIPPOPOTAMUS (HEXAPROTODON LIBERIENSIS)

Pyszko M[1]*, Kana V[2], Paral V[1], Pyszkova L[1], Habova M[1], Malac M[3], Nemecek P[4]

[1] Department of Anatomy, Histology and Embryology, Faculty of Veterinary Medicine, University of Veterinary and Pharmaceutical Sciences, Palackeho 1, 612 42, Brno, Czech Republic (address for correspondence)

[2] Department of Natural Sciences Collections, Muzeum Blanenska, p. o., Blansko, Czech Republic

[3] Zoo Jihlava, Jihlava, Czech Republic

[4] Gymnazium Jiriho Ortena, Kutna Hora, Czech Republic

INTRODUCTION

Pygmy hippopotamus (Hexaprotodon seu Choeropsis liberiensis Morton 1849) is a critically endangered species, which was scientifically recognized only in 1914. The last two or three thousand individuals live in the wild, while 300–350 animals are held captive. Unfortunately, these numbers are only indicative. Every year, their quantity changes because they are losing their natural habitat and are hunted for meat and (according to one legend) also for the "diamonds" in their eyes (tapetum lucidum), which they use to shine their way to grating. Unlike its relative, the hippopotamus amphibius, the pygmy hippopotamus does not spend most of the time in the water, since it prefers wet, swampy areas of rainforests and rivers. It belongs to the order of the Artiodactyla, the suborder of the Nonruminantia, and the family of the Hippopotamidae. It is genetically nearest to cetaceans, but there are significant morphological similarities between hippo and some artiodactyls and perissodactyls.

MATERIALS AND METHODS

Therefore, our aim was to compare the anatomy of pygmy hippopotamus with the findings described in other ungulates. We worked with a male born in 1979 at the Rostov-upon-Don zoo. In that time it was the oldest individual of this species in the Czech Republic and died at the age of 37 at the Jihlava zoo. In order to achieve the goals, we followed the anatomic autopsy. The animal was dissected in the lateral position according to the autopsy protocol used for large ungulates.

RESULTS

The autopsy proved that the anatomical structure of the pygmy hippopotamus is unique. Some organs were similar to those known from ruminants (e.g. lobular kidney, colon ascendens without taeniae and haustra, fibroelastic type of penis). However, the dentition resembled rather the non-ruminant animals (the incisors were directed forward, the canines were transformed into "tusks", premolars and molars with a bunodont occlusal surface).

Many findings indicated a proximity to perissodactyls. Particularly high number of thoracic vertebrae and ribs and identical lung lobes (right lung without lobus medius and bronchus trachealis). The unique findings of the pygmy hippopotamus anatomy consists in the formation of its stomach, larynx and the absence of the caecum.

The stomach was clearly divided into a larger, non-glandular section with a lot of protrusions (fundus et corpus ventriculi were lined with a mucous membrane with many low papillae) and a smaller smooth glandular part located around the pylorus. We found two particularities on the larynx. The first was the cutting of the epiglottis tip into the form of the “V” and the second were the vocal folds. They were not oriented perpendicularly downward, as it is usual in case of the ungulates, but in the caudal direction to the first tracheal ring.

The pygmy hippo’s skin was very similar to those described at the amphibian hippo. Its strength ranged from 0.5 cm on the belly to 2.0 cm on its back. The skin was hairless (except of protective hair on the head and tail end) and contained a large number of special glands. These glands produce a secretion (a red liquid) which protects the body surface from drying out and UV rays.

In conclusion, with some exaggeration, we may say that from the anatomical point of view, the pygmy hippopotamus is neither a “water cow” nor a “river horse”. The pygmy hippo is simply the pygmy hippo.

THE SUPERIOR OLIVARY COMPLEX IN TWO AFROTHERIAN SPECIES: THE ELEPHANT AND THE ROCK HYRAX - A NEUROANATOMICAL INVESTIGATION

Sophie Rasenberger*[1,2], Mandy Sonntag[2], Katja Reimann[2], Thomas Hildebrandt[3], Tina Risch[4], Johannes Seeger[1], Markus Morawski[2]

[1] *Institute of Veterinary Anatomy, Histology and Embryology, Faculty of Veterinary Medicine, University of Leipzig*
[2] *Paul Flechsig Institute of Brain Research, Faculty of Medicine, University of Leipzig*
[3] *Leibnitz Institute for Zoo and Wildlife Research*
[4] *Zoopark Erfurt*

INTRODUCTION

Acoustic communication is essential for the survival of most mammals. Some use frequencies far-out of human acoustic perception for long- distance- communication as the elephant with ranges from 0,017 kHz to 5 kHz (Comparison mouse: 2,3 kHz to 85,5 kHz).

Rock hyraxes engage in a rich and complex vocalizing behaviour that some authors describe as 'singing'. Their "songs" provide accurate information regarding body weight, size and condition, social status and hormonal state of the singer and are thought to advertise individual attributes similar to chemical scent marks.

Acoustic signals reach the brainstem by one first interconnection in the dorsal and ventral cochlear nucleus (DCN and VCN), being processed and evaluated in the binaurally connected superior olivary complex (SOC). This part of the brainstem contains a large number of cell groups of which the medial and lateral superior olivary nucleus (MSO and LSO) are the most prominent nuclei. The other smaller nuclei are addressed as periolivary nuclei and can be classified into a dorsal, ventral, lateral and medial group e.g. containing the medial nucleus of the trapezoid body (MNTB). Their task is the sequential processing of sound origin, calculated by the interaural time difference, especially used by animal with a low- frequency hearing range and the interaural level difference. Most of the anatomical and morphological information on the SOC and the processing of sound in these nuclei derive from small rodent species (mouse, rat and gerbil). Knowledge on the larger species especially the afrotherian Hyrax and Elephant are virtually absent or sparse.

All nuclei of the SOC and their neuronal connections consist of neurons and glial cells, as commonly known in the central nervous system (CNS). Nevertheless about 20% of the CNS consists of extracellular matrix (ECM). Perineuronal nets (PNs), in this regard are classified as a specialized composition of ECM molecules which surrounds the soma, dendrites and the axon initial segment of particular neurons in the CNS. The nuclei of the auditory brainstem are characterized by an exceptionally high density of PN-positive neurons. While it is clear that neurons in the SOC show prominent PNs, these nuclei were so far not explicitly targeted in studies on the ancient clade of afrotherians (Sonntag et al. 2015).

The ECM of neurons in the CNS is an important organizer of the extracellular space and plays a crucial role in maturation, stabilization, and modulation of synapses (Frischknecht et al. 2009) and may therefore contribute to the modulation of synaptic plasticity. PNs of the ECM can thus be seen as basic components of the cellular and systemic organization of the CNS (for reviews, see Zimmermann, 2008 and Sonntag et al., 2016). The potential contribution of PNs to maintenance of the structural and functional integrity of the nervous system is not well understood. With the postnatal differentiation completed, PNs determine the microenvironment of neurons including their afferent synaptic terminals by which they are contacted together with the neighboring perineuronal astrocytic processes. The structural and chemical organization of PNs is rather heterogeneous and varies with neuronal cell types (Matthews et al. 2002; Morawski et al. 2009).The significance of this heterogeneity and the basic functions of PNs are unknown. Currently discussed hypotheses on the function of PNs focus on tree major functional aspects:

1) Mechanical stabilization of synaptic contacts via aggregated proteoglycans (Faissner et al. 2010).
2) Securing high-rate synaptic transmission through buffering of physiologically relevant cations

such as calcium, potassium and sodium (Morawski et al. 2015).
3) Neuroprotective actions by reducing oxidative stress through scavenging redox active cations ,(Morawski et al. 2004, 2010, (Suttkus et al. 2016) Suttkus et al., 2016).
For an evaluation of the above mentioned potential functions of PNs in signal processing it is necessary to consider the specific molecular und structural organization of the ECM.
As the elephant is using acoustic signals in a very unique way (infrasound), conducted by seismic waves over long distances, it is important to investigate the fundamental morphology of the auditory brainstem nuclei and the distribution of ECM within the SOC. The study will help us to draw conclusions on the functions of PN's regarding low frequency hearing and comparing these findings to those of an elephant- relative, the Rock Hyrax.

MATERIAL AND METHODS

Animals

The data were collected from two juvenile Elephants and two juvenile Rock Hyraxes.

Species	Scientific name	Age	Year of death	Origin
Elephant	Elephas maximus	P7	(2015)	Zoo Leipzig, IZW
	Loxodonta africana	P0	(2015)	Bergzoo Halle, IZW
Hyrax	Procavia capensis	Adult	(2016)	Zoopark Erfurt, TÄ Tina Risch
	Procavia capensis	Juvenil	(2016)	Zoopark Erfurt, TÄ Tina Risch

As there is no neuroanatomical atlas of the Elephant or the Hyrax, identification of the SOC was done using Klüver-Barrera-stained sections as well as comparing our findings to the „Topographische Hirnatlas der Katze für experimental- physiologische Untersuchungen" (F. Reinoso- Suárez; E. Merck-AG Darmstadt, 1961) and to the publications of the Manger group for the elephant (Maseko et al. 2013).

Cytochemistry

For cytochemistry the brains were immersion fixed in 4% paraformaldehyde in 0.1 M phosphate buffer (PBS, pH 7.4) for 3- 12 weeks. The tissue was cryoprotected in 30% sucrose, cut in 30 µm thick slices with a cryo-microtome in frontal direction and collected in PBS + 0.1% azide.
The following antibodies were used for staining: anti- brevican (brevican Core Protein), anti- Calbindin (Calbindin D-28k), anti- GAD65/67 (cytoplasmatic Glutamat- Decarboxylase), anti- Parvalbumin (PV 27 calcium binding protein), anti- Gly-T2 (Glycin- 2 transporter), anti-aggrecan (aggrecan core protein), anti- HuC/D (neuronal Protein C/D), -anti - VGlut1 (vesicular glutatmate transporter 1)
Immunoreactivity was either visualized using standard chromogen or fluorescent methods.

RESULTS

A well-developed and mammalian-like SOC could be identified on ~250 slices in the Elephant, and on ~ 100 slices in the Hyrax. In both species we were able to identify the MSO, the LSO, the MNTB and further periolivary nuclei. The MSO is the most noticeable of these nuclei as it shows significant characteristics: we could detect its well-defined layering with parallel glutamatergic and glycinergic dendrites that enter and exit the nucleus all in the same angle. The nucleus was highly reactive for brevican immunostaining which can be detected around dendrites in both species. The LSO is clearly identifiable in histological stainings in the Hyrax but hard to distinguish in the elephant. The cytoarchitecture of the LSO is rather divers and there is no unique and characteristic immunoreactivity to this nucleus. The MNTB in contrast is reactive for GlyT2 and Calbindin and could therefore easily be identified. It shows clear differences in the Elephant and the Hyrax: The Elephant has a small MNTB only containing a few principal cells; at its largest extent we estimated ~ five principal cells ensheathed by a PN per slice. In contrast the MNTB of the Hyrax contains up to 100 principal cells.

DISCUSSION

The results of the present study show that the ECM is an integral part of the unique SOC architecture of the Elephant and the Hyrax. Different structural phenotypes of PNs are associated with neurons in region-specific patterns. This is clearly evident in the SOC. In addition, basic molecular properties of the ECM are evolutionary conserved. Aggrecan and Brevican are the major chondroitin sulfate proteoglycan specifically related to the chemoarchitectural organization of the neuronal microenvironment in the mammalian brain (Blosa et al. 2013)). They are known to have changed their molecular structure during evolution of vertebrates (Schwartz et al. 1999)The ECM antibodies used in the present study as sensitive marker of PNs indicates that immunoreactive molecular epitopes are identical in Elephant, Rock hyrax, mice, rats and human (Virgintino et al. 2009; Morawski et al. 2010; Blosa et al. 2013) We provide a detailed description of PN distribution in the SOC of the Hyrax and the Elephant. PNs are found in almost all nuclei along the ascending auditory pathway, though only specific neuron types are associated with this specific form of the ECM. Prominent PNs were found in the VCN around octopus cells and in the MNTB around principal cells. Also, the fine structure and chemical heterogeneity of PNs might differ between distinct neuron populations and also across mammals of the same afrotherian clade as the PNs might be an adaptation to the species dependend individual task of the ensheathed neurons. Though PNs are hypothesized to control synaptic activity, and especially have a role in synaptic plasticity, the detailed function of PNs and the mechanisms through which the different PN components act remain elusive. Because of the high density of PNs in the SOC, the auditory system is an outstanding candidate for studying the relevance of PNs and its unique subcomponents in histology, neuroanatomy and physiology.

REFERENCES

Blosa, M.; Sonntag, M.; Bruckner, G.; Jager, C.; Seeger, G.; Matthews, R. T. et al. (2013): Unique features of extracellular matrix in the mouse medial nucleus of trapezoid body--implications for physiological functions. In: Neuroscience 228, S. 215–234. DOI: 10.1016/j.neuroscience.2012.10.003.

Faissner, Andreas; Pyka, Martin; Geissler, Maren; Sobik, Thomas; Frischknecht, Renato; Gundelfinger, Eckart D.; Seidenbecher, Constanze (2010): Contributions of astrocytes to synapse formation and maturation - Potential functions of the perisynaptic extracellular matrix. In: Brain research reviews 63 (1-2), S. 26–38. DOI: 10.1016/j.brainresrev.2010.01.001.

Frischknecht, Renato; Heine, Martin; Perrais, David; Seidenbecher, Constanze I.; Choquet, Daniel; Gundelfinger, Eckart D. (2009): Brain extracellular matrix affects AMPA receptor lateral mobility and short-term synaptic plasticity. In: Nature neuroscience 12 (7), S. 897–904. DOI: 10.1038/nn.2338.

Maseko, Busisiwe C.; Patzke, Nina; Fuxe, Kjell; Manger, Paul R. (2013): Architectural organization of the african elephant diencephalon and brainstem. In: Brain, behavior and evolution 82 (2), S. 83–128. DOI: 10.1159/000352004.

Matthews, Russell T.; Kelly, Gail M.; Zerillo, Cynthia A.; Gray, Grace; Tiemeyer, Michael; Hockfield, Susan (2002): Aggrecan glycoforms contribute to the molecular heterogeneity of perineuronal nets. In: The Journal of neuroscience : the official journal of the Society for Neuroscience 22 (17), S. 7536–7547.

Morawski, M.; Bruckner, G.; Jager, C.; Seeger, G.; Kunzle, H.; Arendt, T. (2010): Aggrecan-based extracellular matrix shows unique cortical features and conserved subcortical principles of mammalian brain organization in the Madagascan lesser hedgehog tenrec (Echinops telfairi Martin, 1838). In: Neuroscience 165 (3), S. 831–849. DOI: 10.1016/j.neuroscience.2009.08.018.

Morawski, Markus; Alpar, Alan; Bruckner, Gert; Fiedler, Anja; Jager, Carsten; Gati, Georgina et al. (2009): Chondroitin sulfate proteoglycan-based extracellular matrix in chicken (Gallus domesticus) brain. In: Brain research 1275, S. 10–23. DOI: 10.1016/j.brainres.2009.02.046.

Morawski, Markus; Reinert, Tilo; Meyer-Klaucke, Wolfram; Wagner, Friedrich E.; Troger, Wolfgang; Reinert, Anja et al. (2015): Ion exchanger in the brain: Quantitative analysis of perineuronally fixed anionic binding sites suggests diffusion barriers with ion sorting properties. In: Scientific reports 5, S. 16471. DOI: 10.1038/srep16471.

Reinoso- Suárez; E. Merck-AG Darmstadt, 1961

Schwartz, N. B.; Pirok, E. W. 3rd; Mensch, J. R., JR; Domowicz, M. S. (1999): Domain organization, genomic structure, evolution, and regulation of expression of the aggrecan gene family. In: Progress in nucleic acid research and molecular biology 62, S. 177–225.

Sonntag, Mandy; Blosa, Maren; Schmidt, Sophie; Rubsamen, Rudolf; Morawski, Markus (2015): Perineuronal nets in the auditory system. In: Hearing research 329, S. 21–32. DOI: 10.1016/j.heares.2014.12.012.

Suttkus, Anne; Morawski, Markus; Arendt, Thomas (2016): Protective Properties of Neural Extracellular Matrix. In: *Molecular neurobiology* 53 (1), S. 73–82. DOI: 10.1007/s12035-014-8990-4.

Virgintino, Daniela; Perissinotto, Daniela; Girolamo, Francesco; Mucignat, Maria T.; Montanini, Luisa; Errede, Mariella et al. (2009): Differential distribution of aggrecan isoforms in perineuronal nets of the human cerebral cortex. In: *Journal of cellular and molecular medicine* 13 (9B), S. 3151–3173. DOI: 10.1111/j.1582-4934.2009.00694.x.

EVALUATION AND OPTIMIZATION OF EIGHT PRIMARY ANTIBODIES FOR THE DETECTION OF IMMUNE CELLS IN BOVINE LYMPH NOES

Hooshmandabbasi R[1, 2,*], Boos A[1], Klisch K[1]

[1] *Institute of Veterinary Anatomy, Vetsuisse Faculty, University of Zurich, Zurich, Switzerland*
[2] *Department of Basic Sciences, Faculty of Veterinary Medicine, University of Tehran, Tehran, Iran*

INTRODUCTION

Immunohistochemical methods are widely employed for research and diagnostic purposes, enabling the detection of defined antigens in histological sections. To date, several strategies have been designed to optimize the methods. Besides using different antigen retrieval methods [1], assessing different antibodies which bind to different epitopes of a defined antigen, are among these strategies. In the present study, several experiments were conducted to optimize immunohistochemical methods to distinguish immune cells from other cells in bovine lymph node. Regardless of primary antibodies, the dilution of antibodies, the type of tissue preparation, and various protocols of antigen retrieval were variable factors in our different applied methods.

MATERIALS AND METHODS

Immunohistochemical staining was performed using a panel of eight primary antibodies (Anti-CD4 antibody [10B5], Anti-CD8 antibody [SP16], CD45 allotypic variant, Anti-Human CD68 clone PG-M1, Anti - CD163, CD206 Antibody (D-1), MHC Class II antibody, and Anti-Macrophage antibody [MAC387]). Immunogen, sources, clonality, species reactivity, the supplier, and target cell related to each primary antibody are listed in table 1. Table 2 also illustrates the allocated isotype, protein block, secondary antibody, and types of applied sections, antigen retrieval, different tested dilutions, and the summary of results for each experiment.

Tissue processing

Specimens of bovine lymph nodes were routinely fixed in 4% buffered formaldehyde for 24 hours on shaker at room temperature and subsequently embedded in paraffin. A portion of each specimen was also snap-frozen in liquid nitrogen. Paraffin embedded and frozen tissues were sectioned at 2 and 6 µm, respectively. Tissue sections were mounted on positively charged and coated slides.

Antigen retrieval in paraffin sections

In case of paraffin sections, dewaxed and rehydrated sections were subjected to antigen retrieval by three methods as following: (1) microwave oven treatment (600 W) with 10% EDTA (pH=9) for five min three times at 100ºC, (2) microwave oven treatment (600 W) with 2% citrate buffer (pH=6) for five min three times at 100ºC, and (3) treatment with pepsin (0.25% Pepsin in 10mM HCL at 37ºC) for five min and also ten min.

Fixation in cryostat sections

In case of cryostat sections, slides were put in cold acetone (0ºC) for ten min and then dried at room temperature for ten min.

Proceeding of the immunohistochemical staining in all sections

Paraffin and cryostat sections were incubated in 0.3% hydrogen peroxide (H2O2) in methanol for 30 min in order to inactivate endogenous peroxidases. Then the sections were blocked for 20 min (see table 2). This was followed by an incubation with the corresponding primary antibodies and also isotype control with the same type of immunoglobulin and protein concentration as the primary antibodies in a humidified chamber over night at 4ºC. On the next day, the sections were washed in immunohistochemistry (IHC) buffer at pH=7.2 two times for five min and incubated with biotinylated secondary antibodies (from VECTOR laboratory) as shown in table 2 for 30 min at room temperature. The sections were subsequently washed in IHC buffer for five min. Then the secondary antibody was detected with ABC kit for 30 min. After washing in IHC buffer for 5 min, signals were visualized

using DAB reagent. Sections were counterstained with hemalaun i.e. dipping four times, washed in tap water for ten min, dehydrated through graded ethanol, cleared in xylene and mounted.

Table 1. Antibodies used for immunohistochemistry

Primary antibody	*Immunogen*	*Source*	*Clonality*	*Species reactivity*	*Supplier*	*Target Cells*
Anti-CD4 antibody [10B5]	Recombinant full length human CD4 produced in HEK293T cells (NP_000607)	Mouse	monoclonal	Rat, Dog, Human, Monkey	abcam	Helper T cells
Anti-CD8 antibody [SP16]	A synthetic peptide corresponding to the C terminal of alpha chain of Human CD8	Rabbit	monoclonal	Human	abcam	Cytotoxic T cells
CD45 allotypic variant	Porcine peripheral blood lymphocytes	Mouse	monoclonal	Pig	AbD Serotec	T-cell
Anti-Human CD68 *clone PG-M1*	Human mononuclear spleen cell preparation containing more than 80% Gaucher's cells	Mouse	monoclonal	Human	DAKO	pan-macrophage marker
Anti - CD163	Peptide derived from N-terminal sequence of human CD163	Rabbit	clonal	Human	DB BIOTECH	monocytes, macrophages
CD206 Antibody (D-1)	amino acids 1090-1389 mapping within an extracellular domain of CD206 of human origin	Mouse	monoclonal	Human	SANTA CRUZ	macrophages and dentritic cells
MHC Class II antibody	Synthetic peptide derived from the region aa201-296 of UniProt Id P04233.	Rabbit	polyclonal	Human, Mouse, Rat, Rabbit, Dog	biorbyt	Professional antigen-presenting cells
Anti- Macrophage antibody [MAC387]	Human monocytes	Mouse	monoclonal	Mouse, Monkey, Dog, Cow, Rabbit, Human, Pig	abcam	monocytes/ macrophages

RESULTS

Results obtained using different parameters are shown in Table 2. Only with the CD4, CD163, and MAC387 antibodies signals were obtained. The other antibodies seem not to be suitable for usage in bovine tissue. Heated citrate buffer proved to be superior to the other antigen retrieval techniques. Although using citrate buffer resulted in high sensitivity, combined with well-preserved morphology, background staining was also observed (Fig. 1; A and Fig. 2; E). Moreover, microwave treatment was also superior to enzyme digestion (Fig. 2 and 3). The optimal protease treatment time was five min (Fig. 1; C, D and Fig. 2; G, H). Different dilutions (s. table 2) for each antibody did not have noticeable influence on staining intensities. For some antibodies paraffin sections, for others cryostat sections were superior. The CD4-antibody produced strong positive staining only in paraffin sections. CD163 antibody labeled macrophages in both, paraffin and cryostat sections. In the former signal was detected in more cells, but background staining was noticeable. In case of MAC387 a weak signal was detected, which was stronger in cryostat sections, compared to paraffin sections (Fig. 3).

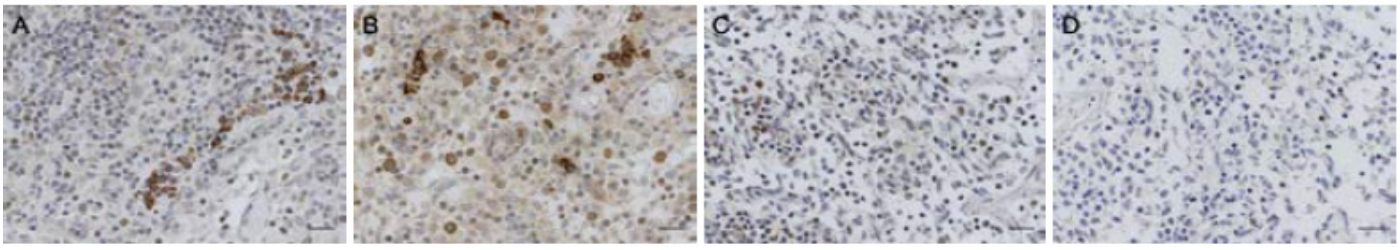

Fig. 1. Immunohistochemical staining of CD4 in bovine lymph node with different antigen retrieval protocols. A: with microwave-citrate buffer; B: with microwave-EDTA; C: with protease digestion for 5 min; D: with protease digestion for 10 min. Bar= 20µm (is tiny)

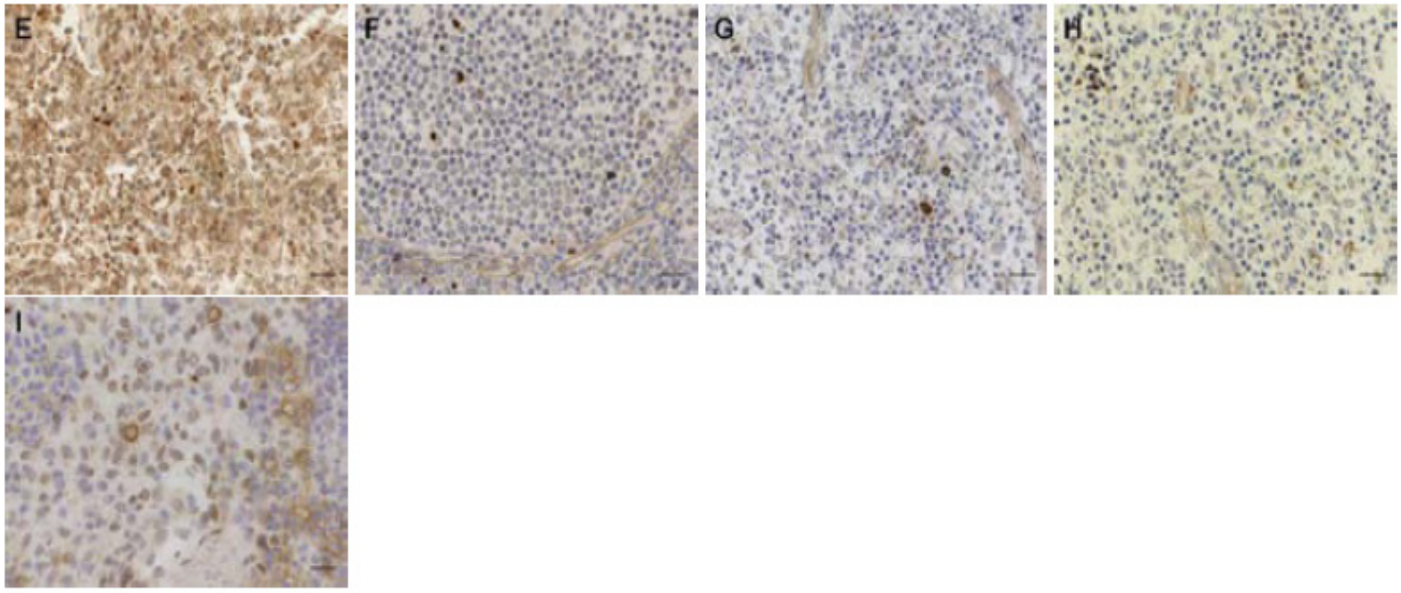

Fig. 2. Immunohistochemical staining of CD163 in bovine lymph node with different antigen retrieval techniques and in cryostat section. E: with microwave-citrate buffer; F: with microwave-EDTA; G: with protease digestion for 5 min; H: with protease digestion for 10 min; I: Cryostat section. Bar= 20μm

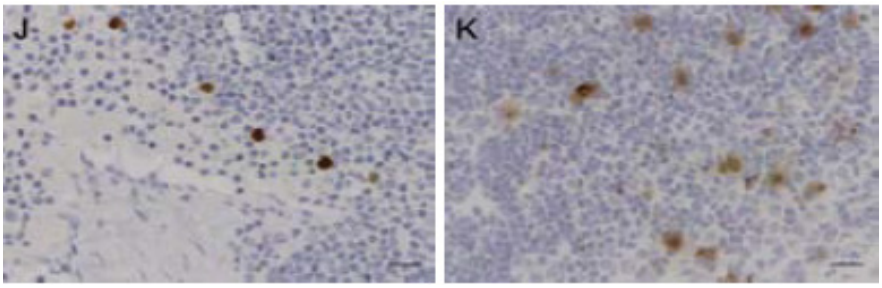

Fig. 3. Immunohistochemical staining of MAC387 in bovine lymph node with J: microwave-EDTA antigen retrieving pretreatment and K: cryostat section. Bar= 20μm

CONCLUSION

In present study we used several antibodies which were previously used as immune cells markers in several species. The initial reason for this study was to validate a primary antibody, as well as an optimized detection method for immune cells in bovine tissues. We employed some variations in several steps, though, the staining was not specific in most cases and no signal was observed in the rest of slides. The most probable reason for this appears to be the lack of cross reactivity of the antibody against bovine epitopes, or it could be due to every single step of the applied protocols. All employed antibodies were not raised against bovine tissue, except MAC387 antibody. In this case we barely detected signals, however, we observed macrophages, identified by highly vacuolated cytoplasm and stained cytoplasmic granules, which were not stained. While Gutierrez et al. (1999) tried different antigen retrieval techniques, such as microwave treatment with EDTA and citrate buffer, for the MAC387 monoclonal antibody, they observed signals in case of EDTA treatment [6]. The working dilution of the primary antibody in that study was 1:50, which is more concentrated than in the present study (1:700). Hence, further studies, which take these variables into account, will need to be undertaken.

REFERENCES

1-Keresztes, G., Takacs, L., Vilmos, P., Kurucz, E., Ando, I., 1996. Monoclonal antibodies detecting components of the bovine immune system in formaldehyde-fixed paraffin-embedded tissue specimens. Vet. Immunol. Immunopathol. 52, 383±392.

2-Gutierrez, M., Forster, F. I., McConnell, S. A., Cassidy, J. P., Pollock, J. M., & Bryson, D. G. (1999). The detection of CD2+, CD4+, CD8+, and WC1+ T lymphocytes, B cells and macrophages in fixed and paraffin embedded bovine tissue using a range of antigen recovery and signal amplification techniques. Veterinary immunology and immunopathology, 71(3), 321-334.

Primary antibody	*Isotype*	*Section*	*Antigen retrieval*	*Dilution of antibody*	*Result*					
					L	M	F	E	T	N
Anti-CD4 antibody [10B5] *1.1 mg/ml*	Mouse IgG1 0.5 mg/ml	Paraffin section	MWC (pH=6)	1:200, 1:400	++++	+	++++	+	-	+++
			MWE (pH=9)	1:200, 1:400	++++	+	++++	+	-	++++
			PD :	1:200, 1:400						
			5 min		+	-	++	++	+	++
			10 min		+	-	-	-	+	+
		Cryostat section	-	1:50, 1:100	-	-	-	-	-	-
Anti-CD8 antibody [SP16] *3.2 mg/ml*	Rabbit IgG 5 mg/ml	Paraffin section	MWC (pH=6)	1:100, 1:200	-	-	-	-	-	-
			MWE (pH=9)	1:100, 1:200						
		Cryostat section	-	1:100, 1:200	-	-	-	-	-	-
CD45 allotypic variant *1 mg/ml*	Mouse IgG2a 1 mg/ml	Cryostat section	-	1:10	-	-	-	-	-	-
Anti-Human CD68 *clone PG-M1* *0.03 mg/ml*	Mouse IgG1 0.5 mg/ml	Paraffin section	MWE (pH=9)	1:10, 1:50	-	-	-	-	-	-
			PD: 5 min	1:10, 1:50	-	-	-	-	-	-
			10 min		-	-	-	-	-	-
		Cryostat section	-	1:10, 1:50	-	-	-	-	-	-
Anti - CD163 *0.1 mg/ml*	Rabbit IgG 5 mg/ml	Paraffin section	MWC (pH=6)	1:200, 1:400	++	++	+++	++	++++	+++
			MWE (pH=9)	1:200, 1:400	++	++	++++	+++	++++	++++
			PD:	1:200, 1:400						
			5 min		++	+	++	+	++++	+
			10 min		++	+	++	+	++++	++
		Cryostat section	-	1:200, 1:400	+	+	++	-	+++	++++
CD206 Antibody (D-1) *0.2 mg/ml*	Mouse IgG1 0.5 mg/ml	Paraffin section	MWC (pH=6)	1:200, 1:400	-	-	-	-	-	-
			MWE (pH=9)	1:200, 1:400						
		Cryostat section	-	1:200, 1:400	-	-	-	-	-	-
MHC Class II antibody *0.5 mg/ml*	Rabbit IgG 5 mg/ml	Cryostat section	-	1:100, 1:200	-	-	-	-	-	-
Anti-Macrophage antibody *[MAC387]*	Mouse IgG1 0.5 mg/ml	Paraffin section	MWE (pH=9)	1:350	++	+	-	-	-	+
				1:700	++	+	-	-	-	-
		Cryostat section	-	1:700	-	++	-	-	-	+++

Table 2. Applied elements in different immunohistochemistry methods and results.

MWC and MWE: Microwave treatment with citrate buffer and EDTA respectively; PD: protease digestion L: Lymphocytes; M: Macrophages; F: Fibroblasts; E: Elongated cells; T: Trabeculae; N: Nonspecific (Background) staining; -: Negative; +: Weak; ++: Moderate; +++: Strong; ++++: Very strong.

* In all cases biotinylated horse Anti-mouse IgG (1: 100) and Horse serum (1:10) was applied as secondary antibody and Protein block respectively with exception of Anti-CD8, Anti-CD163, and MHC Class II antibody in which biotinylated goat Anti-rabbit IgG (1: 100) and goat serum (1:10) were applied.

DISTRIBUTION AND ULTRASTRUCTURE OF EOSINOPHILS IN THE BOVINE CORPUS LUTEUM DURING THE OESTRUS CYCLE AND DURING PREGNANCY

Rodler D, Sinowatz F

Department of Veterinary Sciences, Ludwig-Maximilians-University Munich, Veterinärstrasse 13, D-80539 Munich

INTRODUCTION

Eosinophils (EOS) are able to regulate local immunity and angiogenic processes through their secretion of cytokines and enzymes. So far, no information is available on the distribution and ultrastructure of EOS in bovine CL during defined stages of the oestrus cycle and pregnancy.

MATERIAL AND METHODS

For immunohistochemical studies specimen of ovaries of defined stages of the cycle and pregnancy in Bouin's fluid for 12 h and embedded in paraffin. 5 mm thick section were collected on aminopropyltriethoxysilane (APES)-coated slides . Immunostaining against eosinophil major protein (EMBP), vascular endothelial growth factor (VEGF) and fibroblast growth factor 2 (FGF-2) was performed using the avidin-biotin complex technique. Additionally, small pieces (side length of 1 mm) of ostrich ovary were fixedin Karnovsky's solution (2.5% glutaraldehyde and 2% paraformaldehyde) embedded in Polyembed 812 BDMA. Ultra-thin sections were examined using an EM 902 Zeiss transmission electron microscope.

RESULTS

Using immunostaining of EMBP we could demonstrate that EOS accumulate in the capillaries of the corpus haemorrhagicum and the forming corpus luteum (CL) on day 1 and 2 after ovulation and migrate through the endothelium of newly formed capillaries into the stroma of the developing CL. Ultrastructural investigations of CL of day 1-2 revealed that the eosinophils in the ovary are round cells approximately 9–12 µm in size with a reniform eccentric nucleus and numerous eosinophilic granula. The nucleus of blood eosinophils, in comparison, is lobed and located more in the cell centre. During day 4 and 5 post ovulation the number of EOS in the CL is significantly reduced and remains low until the end of the cycle and in case of pregnancy, until the 6 months of gestation. From then onward, an increase of EOS number can be observed.

DISCUSSION

The CL is formed from an ovulated follicle. It grows rapidly during the first days post ovulation and starts to secrete progesterone (Miyamoto et al.). Additionally to vascular endothelial growth factor and basic fibroblast growth, the migration of EOS from the vascular system into the stroma of the early CL (d1-d2) is an essential stimulus for angiogenesis during early development of the bovine CL.

REFERENCES

Miyamoto A., Shirasanu K., Shimizu T., Matsumi M. (2013). Impact of angiogenic and innate immune systems on the corpus luteum function during its formation and maintenance in ruminants. Reproduction Biology 13,272-278.

THE EFFECTS OF GESTATIONAL NUTRITION ON THE MALE REPRODUCTIVE SYSTEM

Maria Dolores Ruiz-Diaz[1], Nigel Mongan[1], Katrina Copping[2], Aziza Alibhai[1], Matthew Keane[1], Imogen Purvis[1], Viv E. A. Perry[1], Catrin S Rutland[1*].

[1] University of Nottingham, Sutton Bonington Campus, Sutton Bonington, Leicestershire, UK. LE12 5RD.
[2] Robinson Research Institute, University of Adelaide, Frome Rd, S.A. 5005, Australia.
Address for correspondence: catrin.rutland@nottingham.ac.uk. University of Nottingham, Sutton Bonington Campus, Sutton Bonington, Leicestershire, UK. LE12 5RD.

INTRODUCTION

Maturation of the bovine spermatozoa is achieved only after transit through the epididymis. This complex maturation process involves alteration of the membrane lipids, chromatin condensation, migration of the cytoplasmic droplet and changes in the acrosome. These modifications require the interaction of the spermatozoa with proteins synthesised and secreted by the epididymal epithelium. It is widely accepted that environmental perturbations during pregnancy may negatively affect the developing fetus. Numerous studies have focused on reproductive deficiencies produced in offspring following under- or over- nutrition in utero. Dietary protein is an important gestational dietary component in ruminants with its deficiency impacting the quality of the sperm later on in life.

MATERIALS AND METHODS

In this large scale, farm based experiment we studied the impact of either, low or high dietary protein in nulliparous yearling heifers (n=360) during the peri conception (60 days before artificial insemination (AI) to 23 days post conception (dpc)) and/or first trimester of gestation (23dpc to 98dpc) upon the development of the epididymis in their 20 month old male offspring (n=40). Size, number and proportion of the epididymal tubules and blood vessels, as well as the amount of collagen surrounding the tubules were measured. In addition the proteomics of the epididymal fluid were analysed.

RESULTS AND DISCUSSION

The ongoing results will be presented at the meeting and the interesting collagen measurement optimisations discussed. This study provides an insight into the epididymal structural and proteomic alterations in male adult offspring consequent to differing in utero protein environments. The observed effects have the potential to reduce fertility via alterations to the sperm maturational process within the epididymis.

EVALUATING THE EFFECT OF LEPTIN ON BONE DENSITY USING A SEASONAL ANIMAL MODEL OF ADIPOSITY (PHODOPUS SUNGORUS) THROUGH THE USE OF MICROCOMPUTED X-RAY TOMOGRAPHY AND SYSTEMATIC REVIEW

Hollie Cook[1], Catrin S Rutland[2], Craig Sturrock[3], Andrew Mathers[3], Marie Kokolski[1], Francis Ebling[4], Jo Lewis[4], Susan Anderson[1]

[1]Division of Medical Sciences and Graduate Entry Medicine, School of Medicine, University of Nottingham

[2]School of Veterinary Medicine and Science, Faculty of Medicine, University of Nottingham.

[3]Hounsfield facility, Scool of Biosciences, Faculty of Science, University of Nottingham.

[4]School of Life Sciences, University of Nottingham.

INTRODUCTION

Leptin is a 16-kDa adipokine whose role in energy homeostasis regulation in the hypothalamus has been widely investigated. Recently, research has identified additional roles in bone growth and metabolism, where it potentially acts via two distinct mechanisms. Direct binding to marrow stromal cells stimulates proliferation and differentiation of osteoblasts to increase bone density. However, leptin may exert opposing effects by acting centrally; evidence exists that is decreases serotonin synthesis and inhibits serotonin receptor-binding in the ventromedial hypothalamus, resulting in an overall decrease in bone growth through modulation of autonomic and endocrine outputs. As a consequence of these two different putative mechanisms, current literature investigating the effect of leptin on bone density has been conflicting; thus, both high and low bone densities have been associated with leptin deficiency. The overall aim of this project was to investigate the relationship between circulating leptin levels and bone density in the Siberian hamster (Phodopus sungorus), an animal model that shows a profound natural seasonal cycle of body fattening and thus leptin production, and by systematically reviewing current literature. We compared bone density in femurs of Siberian hamsters maintained in long- and short-day photoperiods, to generate either fat hamsters with high serum leptin concentrations or lean hamsters with low leptin concentrations respectively. We tested the hypotheses that leptin increases bone density as measured by microcomputed X-ray tomography (microCT), and that endogenous leptin status influences the response of bone to further leptin supplementation.

MATERIALS AND METHODS

Femurs from Siberian hamsters were dissected and scanned for analysis. Study one consisted of mature male 12-17-week-old long-day (n=6) hamsters and age matched hamsters exposed to short-days (n=7) for 9 weeks. Study two comprised of mature 10-15-week old female hamsters; the short-day photoperiod (n=2) was maintained for 11 weeks and the remaining sample (n=7) was housed in a long-day photoperiod. In both studies, the short-day light exposure ratio was 8:16 hours of light to dark, and long-day hamsters were exposed to a 16:8 hour ratio of light to dark. Femurs were

scanned using a GE v|tome|x m microCT scanner. Each scan consisted of 2160 projections, and the system was set to run at a voltage of 130 kV and a current of 100 μA. The resolution of the scan was 14 μm, and each scan ran for 36 minutes. Two higher-resolution scans were taken using a GE Phoenix Nanotom S scanner, with 2160 projections taken; voltage was set at 80 kV and the current at 120 μA. The resolution of the scan was 2.50μm and each scan ran for 94 minutes. Subsequent to microCT scanning, image analysis allowed quantitative comparisons between samples. The systematic review included literature in which the research was carried out in animal models where two different starting leptin statuses were compared. The search terms 'leptin' and 'bone density' or 'bone mass' were applied to MEDLINE and Web of Science, and generated 442 publications for review; inclusion and exclusion criteria narrowed this down to 18 papers.

RESULTS AND DISCUSSION

MicroCT findings suggested an association between leptin and bone density, as indicated by the positive correlation between body weight and width of bone in male hamsters ($p<0.01$), and negative correlation between body weight and pore size in male short-day hamsters ($p<0.05$). This correlation was not apparent in long-day photoperiod hamsters, suggesting that leptin's effects differ depending on leptin status. A higher-resolution scan identified a network of channels running through the femur, which was structurally different on the dorsal and ventral sides. This novel micro-architectural finding suggests the abundant blood supply required, which appeared to change with photoperiod.

The systematic review revealed a link between starting leptin status and bone density. When wildtype mice with normal-high serum leptin were administered leptin, bone density decreased; the opposite effect was observed in ob/ob leptin-deficient mice. Additionally, it was found that the type of animal model affects response of bone to leptin. Leptin-deficient ob/ob and db/db mice had a lower bone density than wildtype mice. However, the leptin-knockout ($Lep^{\Delta 151/\Delta 151}$) rat had a significantly greater bone density than the wildtype rat. Similarly, the ovariectomised mouse model of obesity (OVX) had a lower bone density than non-ovariectomised mice. As the publications tested different hypotheses to the ones investigated in this research, there was often limited information to interpret including a lack of data concerning serum leptin concentrations prior to supplementation. This may limit the conclusions that can be drawn, although critical appraisal identified that the overall quality of the studies was high. These results, combined with the results from the microCT, indicate that leptin has an anabolic effect on bone density in Siberian hamsters and mice, which is linked to starting leptin status. Both starting leptin status and the type of animal model are factors determining the impact of subsequent leptin treatment on bone growth and density.

ANATOMY AND MICROSTRUCTURE OF THE TONGUE IN THE DOMESTIC TURKEY (MELEAGRIS GALLOPAVO GALLOPAVO VAR. DOMESTICUS)

Skieresz-Szewczyk K, Jackowiak H

Department of Histology and Embryology, Poznań University of Life Sciences, Poznań, Poland

INTRODUCTION

Birds are characterized by wide spectrum of the foraging food and different mechanism of food intake and transport of food into esophagus (Kooloos 1986; Kooloos et al. 1989; Bels and Baussart 2006). These factors influence on the anatomy and microstructure of the mucosa in the oral cavity. Among birds are species foraging on grains, green part of plants, fruits, invertebrates, fishes and mammals. The domestic turkey is classified as the granivorous birds eating mainly grains, plants and small invertebrates by using pecking mechanism of food intake.

The aim of the present study is to investigate the macro- and microstructure of the tongue in the domestic turkey in view of the type of food and mechanism of food intake.

MATERIALS AND METHODS

The study was conducted on the five tongues of the adult domestic turkey (male, average weight 12,5-13,5 kg) collected from the local slaughterhouse. The two tongues after dissection were rinsed in saline and immersed in 4% neutralized formalin and three tongues were immersed in the Bouin solution. After a 24-hour fixation period, macroscopic photographic documentation was made by using digital camera Nicon DS 126311 and stereomicroscope SteREO Discovery v.20 (ZEISS, Germany). Tongues fixated in the Bouin solution was performed to the light microscopy study. Tissue samples were collected from the apex, lingual body, conical papillae and root of the tongue. Tissue samples were dehydrated in a series of increasing concentrations of ethanol (70% - 96%), and routinely embedded in Paraplast ®. Paraplast blocks were cut into sections of 4.5 - 5 μm in thickness. Tissue sections were stained using the Masson-Goldner trichrome histological staining technique and histochemical staining by using PAS, AB and PAS/AB reaction (Romeis, 1989). Observations of the histological sections were performed using an Axioscope2plus light microscope (Zeiss, Germany). On histological section, the measurements of the height of the epithelium and its keratinized layer, using a Multiscan computer morphometric system (ver. 10.2, CSS, Warsaw, Poland). Tongues fixated in the 4% neutralized formalin were studied in the high definition cone beam computed tomography Fidex – Multi Modality X-ray System (Animage, California).

According to the Polish law and the EU directive (no 2010/63/EU) the experiments conducted within the study do not require approval of the Local Ethical Committee for Experiments on the Animals in Poznan.

RESULTS

The tongue in the domestic turkey is build of the apex, body and root of the tongue. The total length of the tongue is 4,7 cm and the width on the apex is 0.5 cm,on the lingual body 1,4 cm and on the root of the tongue 1,1 cm.

The rostral part of the tongue is divided by the median groove into two symmetrical parts. On the ventral surface of the lingual apex the triangle plate of the lingual nail is present. In the caudal part of the body, on the border between the body and root of the tongue, the 14 -15 conical papillae, located in the shape of V-letter are observed. On the lateral surfaces of the lingual body and on the root of the tongue the openings of the lingual glands are seen.

The microscopic observation reveals, that the whole dorsal surface of the apex and body of the tongue is covered with the parakeratinized epithelium, which undergo massive exfoliation. The height of the parakeratinized epithelium on the lingual apex and body is respectively 1486,4 μm and 996,6 μm. The height of the keratinized layer on the apex is 237,2 μm and the body is 159,3 μm.

The ventral surface of the lingual apex and conical papillae of the tongue are covered with the

orthokeratinized epithelium. The height of the epithelium on the ventral surface of the lingual apex is 383,7 μm and its keratinized layer is 129,6 μm height.
On the root of the tongue is cover with the non-keratinized epithelium and its height reaches 382,4 μm.
The complex alveo-tubular lingual glands are located in the lamina propria of the lateral part of the lingual body and on the root of the tongue. The secretory units pass into the wide collecting ducts which open on the lateral surface of the body and root of the tongue. The histochemical staining of secretory cells reveals that the mucous consist of the neutral and acidic mucopolysaccharides. The CT study specifies that internal skeleton of the tongue consists of the paraglossal cartilage, basibranchiale bone, paired ceratobranchiale bone with epibranchiale. The triangle paraglossal cartilage, in the caudal part has indentation in the middle and the caudal edge of the paraglossal cartilage has a shape of V-letter. The basibranchial bone has a shape of rectangle which is narrowed in the rostral part.

DISCUSSION

The macro- and microstructure of the tongue in the domestic turkey reveals the functional adaptation to type of food and the mechanism of food intake. During pecking the bird collects the food by the rostral part of the beak. The food particles are located in the free part of the beak and then the tongue goes under the food and food is transferred on the lingual apex. The lingual nail act a spoon to collect food and also play a role of the external skeleton of the lingual apex. After that, the food particles are transported on the surface of the tongue along the median groove and are located on the conical papillae. Then the laryngeal prominence is closed, the tongue retracts and food is transported over the lingual root and laryngeal prominence to the esophagus. The conical papillae, directed caudally, help to transport the food and also prevent the return of food to the oral cavity.
The dry and hard food can cause the damage of the lingual epithelium, that is why the lingual nail and conical papillae of the tongue, which are directly involved in food intake and transport, are covered with the orthokeratinized epithelium with thick protective, keratinized layer. The dorsal surface of the tongue, where food particles are passively transported is covered with the parakeratinized epithelium. The lingual glands produce the mucous which help to moisturize the oral cavity and also help to create the food bolus which can be easily transported to the esophagus over the nonkeratinized epithelium of the root of the tongue.

REFFERENCES

1. Bels V., Baussart S. 2006. Feeding behaviour and mechanisms in domestic birds. In: Bels V, editor. Feeding in domestic vertebrates. From structure to behavior. CAB International, Wallingford. Oxfordshire, UK: CABI Publishing. Pp. 33-49.
2. Kooloos J.G.M. 1986. A conveyer-belt model for pecking in the mallard (Anas platyrhynchos L.). Neth J Zool 36: 47-87.
3. Kooloos J.G.M, Kraaijeveld A.R., Langenbach G.E.J., Zweers G.A. 1989. Comparative mechanics of filter feeding in Anas platyrhynchos, Anas clypeata and Aythya fuligula (Aves, Anseriformes). Zoomorphol 108: 269-290.

EFFECT OF GINGER ON THYMUS GLAND AND SPLEEN TISSUE IN BROILER CHICKENS

Taghdisi[1*] A, Taghdisi[2] N, Hejazi[3] S

[1] Graduate of Veterinary Medicine, Tabriz Branch, Islamic Azad University, Tabriz, Iran.*

[2] Student of Veterinary Medicine, Babol Branch, Islamic Azad University, Babol, Iran.

[3] Department of Anatomy, Tabriz Branch, Islamic Azad University, Tabriz, Iran.

INTRODUCTION

Beneficial properties of Ginger have been proven as an anti-inflammatory, antioxidant, antibacterial, antiviral, and immune system booster agent. Therefore, in the present study the effects of ginger on spleen and thymus tissues of broiler chickens were investigated; since, the positive effects of ginger on the immune system of birds have a significant value in the economic cycle of the poultry industry.

MATERIALS AND METHODS

In order to conduct the present study 80 one day-old of 308 ROSS broiler chicks were selected and divided into two groups of normal and ginger intervention (treatment) ones. The treatment group received the combination of 1 g/kg ginger powder in the basal diet of the chicks from the beginning of breeding period until the end of the period (42 days-old). The birds were tested randomly to evaluate the antibody titer against Newcastle disease; for this purpose, 1-2 cc blood sample was obtained from each chick and the samples were sent to the Pasteur poultry specialized laboratory in order to measure the hemagglutination (HI) and total immunoglubin. Statistical analysis of blood titer of the test was conducted quite randomly. The obtained results were analyzed statistically using GLM method and SAS statistical software. The means related to the results of the treatment group were evaluated using Duncan‘s multiple range tests and P value was investigated at the level of 5%. At the end of the period the birds were dissected and thymus gland as well as spleen tissue were removed and weighted. Then, they were fixed in the 10% formalin buffer and were sent to the histotechnique laboratory in order to prepare histological samples. Paraffined blocks of samples were cut with a thickness 5µ following histotechnique preparation stages. Then, they were stained using H&E method and finally were investigated under the light microscope (model Eclipse E200 of Nikon made in Japan). Data were expressed as Mean±SE. in order to compare the differences between the two groups the T-test was used via SPSS 13 statistical analysis software. $P<0.05$ was considered in order to determine the meaningfulness level between the two groups.

RESULTS

The mean amount of HI blood titer was different meaningfully between the two groups ($P<0.05$). The mean weights of thymus and spleen were also different meaningfully between the two groups ($P<0.05$). Unlike mammalians, in the present study no marginal zone was observed between white pulp and red pulp. In samples used in the present study the reticular epithelial cells were not seen as Hassall Corpuscle but they were seen as reticular epithelial cells. In comparison the normal group with the treatment group it was evident that the lymphocytic cells density was higher in the latter group. The increased space among lymphocytic cells in the control (normal) group suggested the status of the cells density of the two groups. Central artery of the white pulp in the treatment group has thicker wall thickness compared with that in the control group. Furthermore, increased blood circulation is one of the mechanisms of strengthening the immune system which is resulted of ginger.

DISCUSSION

Spleen and thymus are considered as parts of immune system. The two organs take the attention of scientific researches as indicators of immune system. Considering that the thymus atrophy has a direct relationship with bird's aging, it can be concluded that ginger can have a major role in the consistency of chicks' immune system that feed with diet containing ginger. In the present study it can be concluded based on the results of the Immune titer of the chicks that ginger can demonstrate strengthening of the immune system in a short time such that a significant difference obtained between the two groups during breeding periods (from 14 days-old) until the end of the period. The obtained result s from spleen and thymus weights which were as the main indicator of immune system suggested that the ginger in the chicks' dietary led to their increased body weight. Furthermore, ginger as an antioxidant result in a relative thymus and spleen weight increase. Regarding the results of the present study it can be concluded that the ginger powder can have a positive effect on the chicks' raising as well as the immune system of the broiler chicks due to the antibacterial properties of its ingredients such as gingerol.

GEOMETRIC AND BIOMECHANICAL PROPERTIES OF THE FEMUR IN SHEEP AND RABBIT AS COMMONLY USED ANIMAL MODELS IN EXPERIMENTAL ORTHOPAEDICS

Kara ME[1], Sevil-Kilimci F[1], Turan E[1*], Türker F[1], Çobanoğlu M[2], Theobald P[3], Bozdağ SE[4]

1. Adnan Menderes University, Faculty of Veterinary Medicine, Department of Anatomy, 2. Adnan Menderes University, Faculty of Medicine, Department of Orthopaedic Surgery, 3. Cardiff University, School of Engineering, Mechanical, Manufacturing and Medical Engineering 4. ITU, Faculty of Mechanical Engineering, Biomechanics lab.

INTRODUCTION

Large animal models play a cardinal importance in the understanding and treatment of orthopaedic diseases as well as the testing new surgical procedures and implants in the experimental orthopaedics. Adult sheep offer the advantage of being of a more similar body weight and bones size to human. Besides that, rabbit is the most popular animals because it's small size to easy maintenance during the experiment, early ossification, and larger size than other laboratory animals. How much the bones of these animals can mimic the bones human has still a controversial issue. Femur is the most used bone in experimental orthopaedics. The purpose of this study was to evaluate the morphologic and mechanical properties of the ovine and rabbit femur.

MATERIALS AND METHODS

The femora of the sheep (n=10) and rabbits (n=10) were used. The adult and female animals were used. The sectional images were obtained by computed tomography. The cortical thicknesses and sectional diameters at five levels of the femoral diaphysis were measured on the images. The cortical thickness indices, diaphyseal shape index were also calculated. The three-point bending test were also performed at the left entire bones for the biomechanical evaluation.

RESULTS and DISCUSSION

The cortical thickness index of the sheep and rabbit femoral midshaft were 31.40±2.99 and 35.75±2.53, respectively. The medial and cranial bone cortices were thicker than lateral and caudal side at the all levels of the sheep femoral diaphysis. The cranial and caudal cortical bone were thicker than medial and lateral sides on the rabbit. The diaphyseal shape index of the sheep was greater than 1.0 whereas rabbit the femoral shape ratio less than 1.0 in the all level of the diaphysis. The sheep femora appear to have diaphyseal shape most similar to that of human while rabbit has a closer cortical thickness to that of human than sheep. Rabbit and sheep femur have similar bending strength while rabbit femur has higher Young's modulus of bending than sheep femora. This could be explained by the difference between their geometric features. This study has been prepared regarding the aims of BM1308-SALAAM and it is a part of the continued research "Comparative morphometric and biomechanical studies on the long bones of hind limbs of sheep, goat and rabbit as commonly used large animal models for human orthopaedics, TUBITAK-COST 115-O830". The detailed morphologic and biomechanical data of the femur, tibia and metatarsus will be presented for these animals at the end of this study.

REFERENCES

1. An Y.H, Friedman R.J. (1999) Animal models in orthopaedic research. Boca Raton: CRC Press.
2. Hedgeland M.J., Libruk M.A., Corbiere N.C., Ciani M.J., Kuxhaus L. (2016) The Odocoileus virginianus Femur: Mechanical Behavior and Morphology. PLoS One 12, 1-12.
3. Kieser D.C., Kanade S., Waddell N.J., Kieser J.A., Theis J.C., Swain M.V. (2014) The deer femur a morphological and biomechanical animal model of the human femur. Biomedical Materials Engineering 24, 1693-1703.
4. Pearce A.I., Richards R.G., Milz S., Schneider E., Pearce S.G. (2007) Animal models for implant biomaterial research in bone: a review. European Cells & Materials 13, 1-10.
5. Sevil F., Kara M.E. (2010) The effects of ovariectomy on bone mineral density, geometrical, and biomechanical characteristics in the rabbit femur. Veterinary and Comparative Orthopaedics and Traumatology 23, 31-36.